Industria Textilă

ISSN 1222–5347 (177–232)

4/2013

Revistă **cotată ISI** și inclusă în **Master Journal List** a Institutului pentru Știința Informării din Philadelphia – S.U.A., începând cu vol. 58, nr. 1/2007/
ISI rated *magazine, included in the* ***ISI Master Journal List*** *of the Institute of Science Information, Philadelphia, USA, starting with vol. 58, no. 1/2007*

Editată în 6 nr./an, indexată și recenzată în:
Edited in 6 issues per year, indexed and abstracted in:
Science Citation Index Expanded (SciSearch®), Materials Science Citation Index®, Journal Citation Reports/Science Edition, World Textile Abstracts, Chemical Abstracts, VINITI, Scopus

Recunoscută în România, în domeniul Științelor inginerești, de către
Consiliul Național al Cercetării Științifice din Învățământul Superior
(C.N.C.S.I.S.), în **grupa A** /
Aknowledged in Romania, in the engineering sciences domain,
by the ***National Council of the Scientific Research from the Higher Education***
(CNCSIS), in ***group A***

Sumar

Contents

Referenții articolelor publicate în acest număr al revistei INDUSTRIA TEXTILĂ/
Scientific reviewers for the papers published in this number:

Cerc. şt. gr. I prof. dr. ing./ *Senior researcher prof. dr. eng* CĂRPUŞ EFTALEA
Cerc. şt. gr. I dr. ing./ *Senior researcher dr. eng.* EMILIA VISILEANU
Cerc. şt. gr. III dr. ing./ *Senior researcher dr. eng.* ALINA POPESCU
Cerc. şt. dr. ing./ Senior researcher dr. eng. OLARU SABINA
Cerc. şt. drd. ing. gr. II / *Senior researcher eng.* CLAUDIA NICULESCU *PhD*
Cerc. şt. gr. III ing./ *Senior researcher eng.* DOINA TOMA *PhD*
Cercet. şt. mat./ *Senior researcher mat.* MIHAI STAN
Drd. ing./ *Eng.* GEORGETA POPESCU *PhD*
Biolog/ *Biologist* CLARA RĂDULESCU

Revista „INDUSTRIA TEXTILĂ“, Institutul Național de Cercetare-Dezvoltare pentru Textile și Pielărie – București

Redacția (Editura CERTEX), administrația și casieria: București, str. Lucrețiu Pătrășcanu nr. 16, sector 3, tel.: 021-340.42.00, 021-340.02.50/226, e-mail: certex@ns.certex.ro; Fax: +4021-340.55.15. Pentru abonamente, contactați redacția revistei. Instituțiile pot achita abonamentele în contul nostru de virament: RO25RNCB0074029214420001 B.C.R. sector 3, București.

Lucrare realizată în colaborare cu **Editura AGIR**, Calea Victoriei nr. 118, sector 1, București, tel./fax: 021-316.89.92; 021-316.89.93; e-mail: editura@agir.ro, www.edituraagir.ro

Features and influencing factors of kapok fiber length distribution

HONGYAN WU FUMEI WANG

REZUMAT – ABSTRACT

Caracteristicile și factorii care influențează distribuția lungimii fibrei de capoc

În scopul furnizării unor informații utile pentru procesarea, prelucrarea și filarea fibrelor de capoc, lucrarea s-a axat pe studierea lungimii fibrelor din fructe. S-a analizat structura internă a fructelor de capoc și s-a descoperit faptul că fibrele cu lungime mai mare pot fi separate din fructe cu mai multă ușurință. În urma măsurării lungimii fibrelor, s-au obținut caracteristicile distribuției lungimii fibrelor de capoc. Diagrama aranjamentului este o distribuție continuă, iar distribuția lungime-număr de fibre este una distorsionată, similară cu cea a bumbacului. De asemenea, au fost analizați factorii care influențează lungimea fibrei. Rezultatele au arătat că fructul speciei de capoc de pe insula Hainan este, în mod evident, mai mic decât cel din Java cu aproximativ 5 mm. Lungimea fructelor poate influența lungimea fibrei, pe când perimetrul de mijloc al fructelor și locul de creștere nu afectează lungimea acesteia.

Cuvinte-cheie: fibre de capoc, distribuția lungimii fibrei, specie, mărimea fructelor, locul creșterii

Features and influencing factors of kapok fiber length distribution

In order to supply useful information for kapok fiber planting, processing and spinning, this study focused on length of fibers in fruits. The internal structure of kapok fruit was analyzed to find that fibers with longer length could be separated easily from fruits. By testing fibers length, features of kapok fiber length distribution were obtained. Arrangement diagram is continuous distribution and fiber length-number distribution is all skewed distribution, similar with those of cotton. Moreover, influencing factors of fiber length were analyzed. The results show Hainan Island kapok is obviously shorter than that of Java kapok about 5 mm. Fruit length could impact on fiber length; middle perimeter of fruit and growth site do not affect fiber length.

Key-words: kapok fiber, fiber length distribution, breed, fruit size, growth site

With the depletion of oil resources as well as environmental harm caused by chemical fiber, more people favor natural fibers like cotton, wool, silk and linen. However, increment of the four natural fibers is very limited. Thus, recently, a new natural fiber, namely kapok fiber, is developed and applied.

Kapok is a tropical tree of the family Bombacaceae [1], mainly widespread in Indonesia and Southeast Asia. Currently applied kapok mainly referred to Bombax malabaricum, Gaeritn Bombax insignis and Ceiba Pentandra [2, 3]. Every year, kapoks can bear, as shown in figure 1, green fruits, in which fibers grow, are immature kapok fruits. After fruits are mature, kapok fibers can be extracted to be used in textiles. The high hollowness, about 80 – 90%, is the most significant feature of kapok fibers [4], as shown in figure 2 *a*. From figure 2 *b*, it is seen that both ends of the fiber are closed [4]. So, kapok fibers are often used as a stuffing material, buoyancy material and oil-absorbing material. In recent years, with the development of spinnability, kapok fibers could be blended with other cellulose fibers [5] and a variety of blends are available.

It is known that length is one of the most important parameters of fibers because it has effects on yarn strength, yarn hairiness, the properties of fabrics and the efficiency of the yarn spinning process. Therefore,

Fig. 1. Kapok tree

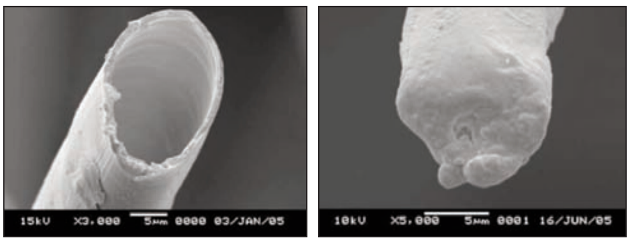

a *b*

Fig. 2. Kapok fiber: ***a*** – hollow structure; ***b*** – end of fiber

in order to apply kapok fiber on textile well, it is necessary to obtain the basic information about kapok fiber length. However, at present, there is little research about features of kapok fiber length-distribution and factors which may affect fiber length. To solve this problem, in this paper, first, structure of kapok fruit was analyzed to provide a method by which longer fibers can be extracted from kapok fruits. Second, kapok fibers, from Java in Indonesia and Hainan Island in China, were tested to get features of fiber length distribution. Third, factors which may affect the fiber length were analyzed. These researches provide useful information for planting, processing and spinning of kapok fibers.

ANALYSIS OF THE STRUCTURE OF KAPOK FRUIT

In order to clarify the fiber distribution in kapok fruit, in this section, the mature kapok fruit was observed. It is slender column in shape (fig. 3 *a*), 150–300 mm in length, about 150 mm of middle perimeter. The pod of the kapok fruit is hard, light brown and had uneven striae in surface.
When the fruit was opened along the central axis, fiber bundles are found, which grow in the inner wall with about 10 mm thickness (fig. 3 *b*) and shaded area of figure 3 *e.* In the middle of pod, there are short staples and seeds divided into five ventricles with same structure by wooden walls (fig. 3 *e*). The wooden wall adheres to short fibers named short staples which enclosed seeds (fig. 3 *c*).
It was observed that fibers in the fruit can be divided into two parts: the first part is the fiber bundle. They tightly folded, densely piled on the inner wall. The fiber bundle extracted from pod is umbrella structure whose one end was orderly and the other is fluffy (fig. 3 *d*). Fiber bundles are mostly 10 – 25 mm in length. Also, they have little adhesion to short staple and seeds. Each fruit can pack about 12 – 15 g fiber

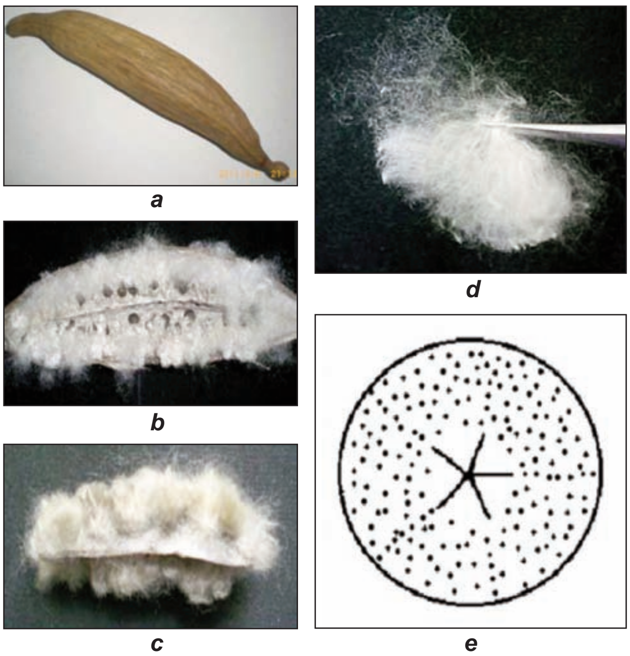

Fig. 3. Structure of kapok fruit

bundles. The second part is short staple in the middle of fruit. They adhere to wooden wall (fig. 3 *c*) and are mostly 6 – 10 mm in length. They also have little adhesion to seeds.
The kapok fiber is different from the cotton fiber. The cotton fiber is seed fiber formed from epidermis cell and adheres to seeds. However, the kapok fiber is fruit fiber. They adhere to the inner wall of fruit, formed from in wall cell and are loosely held to the seed. Cotton fibers are separated from the seed by the ginning process while kapok fibers are separated just by shaking [6]. Also, fiber bundles have little adhesion to short staple, so the two parts can be separated easily. Therefore, processing factory can get only fibers bundles with longer length by separating them from kapok fruits.

FEATURES OF FIBER LENGTH DISTRIBUTION

Sample

Two kapok fruits from Java in Indonesia were marked as 1 # and 2 #, and two fruits of Hainan Island in China were marked as I # and II #. Only fiber bundles in fruits were extracted and measured.

Test method

Single fiber measurement method is the most accurate method for fiber length test, so it was selected to test length of fiber inside kapok fruit. Single fiber measurement method was as follows: pick up single fiber with tweezers, drag it on velvet board to straight it and measure it with a scale reading one decimal. Each experiment tested about 500 fibers [7]. Each of the fruits is zoned in three parts: head, middle and tail. Each part is about one third of the whole fruit, as shown in figure 4. Fiber length of each part was measured, respectively.

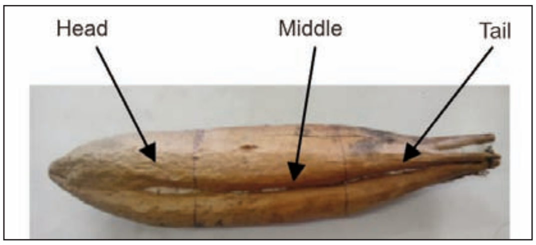

Fig. 4. Zoned three parts of kapok fruit

RESULTS AND DISCUSSIONS

Arrangement diagram

Length of fiber was uneven. Importing the data of fiber length measured by Single fiber measurement method into computer, the fiber length could be arranged from long to short, final arrangement diagram, also called bear diagram, could be obtained (fig. 5).
Figure 5 shows that fiber length arrangement of Java and Hainan Island kapok is continuous distribution from long to short fiber, similar with cotton and having the notable feature of natural fiber distribution.

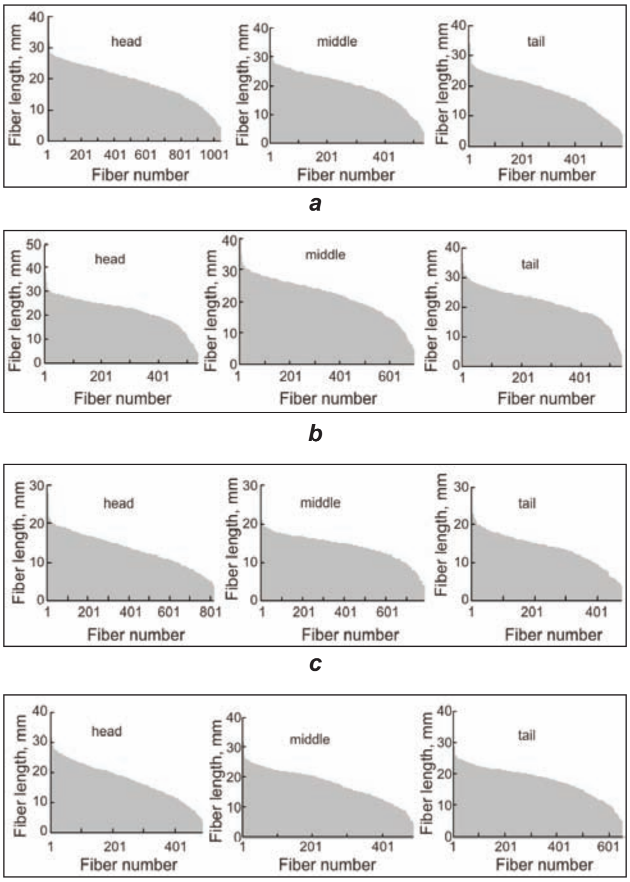

Fig. 5. Arrangement diagram of fiber length: ***a*** – Java kapok 1 #; ***b*** – Java kapok 2 #; ***c*** – Hainan Island kapok I #; ***d*** – Hainan Island kapok II #

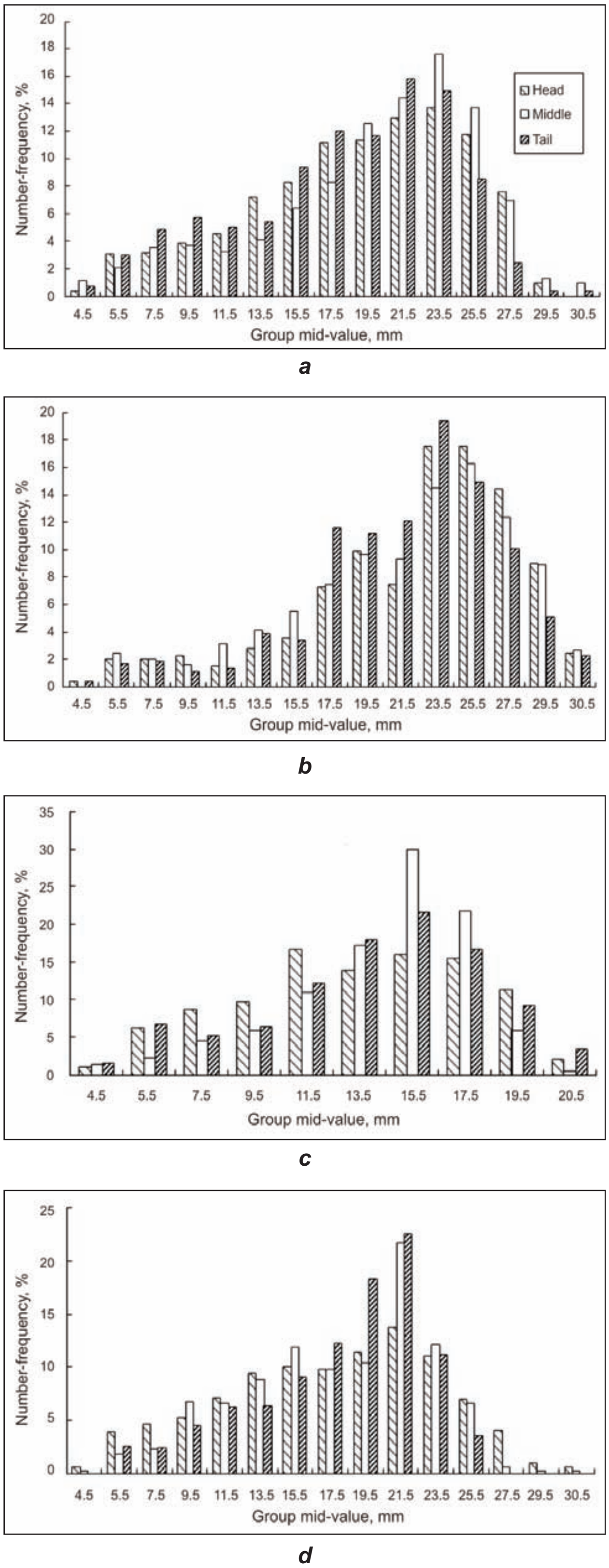

Fig. 6. Histogram of fiber length-number distribution: ***a*** – Java kapok 1 #; ***b*** – Java kapok 2 #; ***c*** – Hainan Island kapok I #; ***d*** – Hainan Island kapok II #

Fiber length-number distribution histogram

The length data above were grouped with interval 2 mm. The length less than 4.5 mm was grouped as the first group. The number of fiber with length more than 30 mm was relatively little, so the length more than 30.5 mm belonged to a group. Finally fiber length-number distribution could be obtained and showed in figure 6.

Figure 6 shows that fiber length-number distributions, in different parts and different breeds of kapok fruit, are all skewed distribution, and similar with those of cotton. From figure 6, it also can be seen that fiber length of Java 1 # and 2 # is mainly ranged from 15.5 to 27.5 mm and 17.5 to 29.5 mm, respectively, and fiber length of Hainan Island I # and II # is mainly ranged from 12 to 20 mm and 16 to 28 mm, respectively. It is readily seen that in different parts and breeds, fiber length is different, so it is necessary to analyze factors which may impact fiber length. Therefore, several possible factors will be analyzed bellow.

ANALYSIS OF THE FACTORS AFFECTING THE FIBER LENGTH

Kapok breeds

Java in Indonesia and Hainan Island in China are main kapok growing area. Java Kapok belongs to Ceiba pentandra and Hainan Island kapok belongs to Panzhihua kapok, which are main kapok breeds. Based on above fiber length measurement, the average length of the two breeds was calculated, as shown in table 1. Also, weight percentage of fibers longer than 16 mm, were calculated, as shown in table 2.

Table 1

AVERAGE LENGTH OF THE TWO BREEDS, mm			
Sample	**Average length**	**Sample**	**Average length**
1 # head	21.0	I # head	14.8
1 # middle	21.7	I # middle	15.2
1 # tail	20.0	I # tail	15.1
2 # head	24.0	II # head	19.7
2 # middle	23.5	II # middle	19.4
2 # tail	23.0	II # tail	19.3

Table 2

WEIGHT PERCENTAGE OF FIBERS LONGER THAN 16 mm, %			
Sample	**Weight percentage**	**Sample**	**Weight percentage**
1 # head	81.4	I # head	39.2
1 # middle	86.4	I # middle	35.2
1 # tail	78.8	I # tail	38.6
2 # head	92.6	II # head	72.5
2 # middle	89.9	II # middle	73.1
2 # tail	92.8	II # tail	78.5

From table 1, it is seen that average length of Java kapok is mainly ranged from 20.0 to 25.0 mm, and that of Hainan Island kapok is mainly ranged from 15.0 to 20.0 mm. So, fiber average length of Hainan Island kapok is shorter than Java kapok fiber's about 5 mm. From table 2, we know that weight percentage of fibers longer than 16 mm of Hainan Island is lower than Java kapok's. Therefore, Java kapok fiber is more useful than Hainan Island kapok fiber in textile application, and Java kapok should be spread in planting industry.

Fruit size

Five kapok fruits from Java in Indonesia were marked as 1 # to 5 #. The fruit size was shown in table 3. These fibers length were tested by Single fiber measurement method, as shown in table 4.

According to the data in table 3 and table 4, figure 7 was drawn to analyze the relationship of fiber length and fruit size. The regression equation is significant by significance test of the linear regression. This indicates the fiber is longer as the fruit is longer. Figure 7 also shows fiber length has no relation with middle perimeter of fruit. So, if you want to get longer fibers, you can choose longer kapok fruits. The relationship has some referential value on purchasing kapok fruits.

Growth size in kapok fruit

Table 4 shows fiber length is different in head, middle and tail. To compare fiber length of the three parts, the data of table 4 were paired for significance test in table 5.

Table 3

KAPOK FRUIT SIZE		
Numbers	**Length of fruit,** mm	**Length of middle perimeter**, mm
1 #	230	165
2 #	204	156
3 #	226	158
4 #	280	156
5 #	188	158

Table 4

FIBER LENGTH, mm				
Numbers	**Fiber length**			
	head	**middle**	**tail**	**average**
1 #	21.60	22.00	20.60	21.40
2 #	20.42	20.36	20.99	20.59
3 #	19.80	21.00	20.20	20.30
4 #	22.50	22.16	22.38	22.35
5 #	19.76	20.22	19.07	19.68

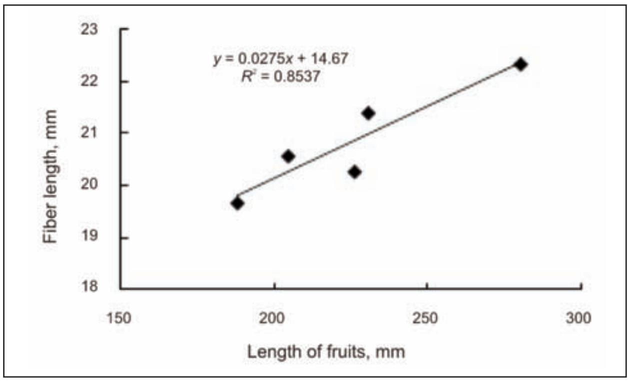

a

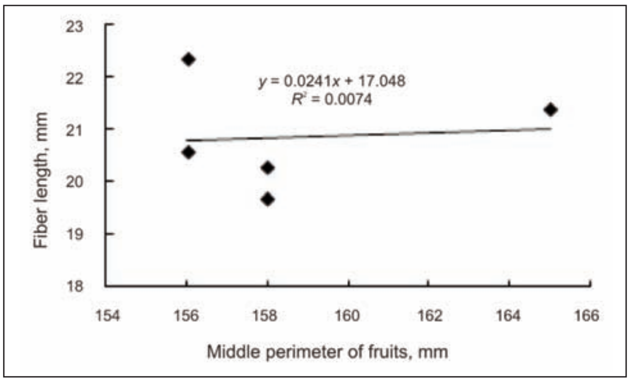

b

Fig. 7. Relationship of fiber length and fruit size

Take significance level: a = 0.05, $t_{1-a/2}(n-1)$ = = $t_{1-0.025}(4)$ = 2.7764, in table 5, three statistics are all less than 2.7764. It shows fiber length of the three parts has no significant difference. So there is no need of taking into account length difference in growth size.

Table 5

SIGNIFICANCE TEST								
Kapok fruits	**1 #**	**2 #**	**3 #**	**4 #**	**5 #**	**Average**	**Sample standard deviation**	**Statistic**
Head-middle	–0.40	0.06	–1.20	0.34	–0.46	–0.33	0.5873	1.2640
Middle-tail	1.40	–0.63	0.80	–0.22	1.15	0.50	0.8829	1.2663
Head-tail	1.00	–0.57	–0.40	0.12	0.69	0.17	0.6772	0.5547
Kapok fruits	1 #	2 #	3 #	4 #	5 #	average	sample standard deviation	statistic

CONCLUSIONS

In order to provide basic information for kapok planting, purchasing and processing, this study focused on kapok fiber length. Main conclusions obtained are following:

- The internal structure of kapok fruit could be divided into two parts: fiber bundle and combination of short staple and seeds, and they had little adhesion. Therefore, it provides a way in which fiber bundle and short staple could be separated easily, and longer fibers could be obtained. It is very useful for factory to process kapok fibers.
- By fiber length measurement, features of kapok fiber length distribution were obtained. Arrangement diagram presents continuous distribution from long to short fiber, and fiber length-number distribution is skewed distribution. So, kapok fiber length has the notable features of natural fiber distribution.
- Factors that may affect fiber length were analyzed. The results show fiber average length of Hainan Island kapok is shorter than Java kapok fiber's about 5 mm, and weight percentage of fibers longer than 16 mm of Hainan Island is lower than Java kapok's; usually the fiber is longer as the fruit is longer; middle perimeter of fruit and grow site do not affect fiber length.

ACKNOWLEDGEMENTS

This work was supported by "the Fundamental Research Funds for the Central Universities" in China.

BIBLIOGRAPHY

[1] Keko, H., Maxima, E. F., Shigenori, K. *Thi bach tuyet lam and Kenji Iiyama*. In: The Japan Wood Research Society, 2000, vol. 46, p. 401

[2] Hong, X., Wei, Y. D., Mei, S. W. *Characters and application prospects of kapok fiber*. In: Journal of Donghua University: Natural Science Edition, 2005, vol. 31, issue 2, p. 121

[3] Chinese Academy of Sciences: China flora Editorial Committee. *Flora of China* (*forty-ninth volumes second fascicule*). Science press, Beijing, 1984, p. 102–111

[4] Wei, L. *Kapok battings and its thermal insulation properties*. Donghua University, 2011, p. 19

[5] Mei, S. W., Hong, X., Wei, Y. D. *The fine structure of the kapok fiber*. In: Textile Research Journal, 2010, vol. 80, issue 2, p. 159

[6] Mwaikambo, L. Y. *Review of the history, properties and application of plant fibers*. In: African Journal of Science and Technology (AJST), Science and Engineering Series, 2006, vol. 7, issue 2, p. 126

[7] GB/T 16257-2008. *Textile fibers – Test method for length and length distribution of staple fibers – Measurement of single fibers*. China Standards Publishing House, Beijing, 2008

Authors:

HONGYAN WU
FUMEI WANG
Donghua University – College of textiles
Room 4007, Bld. G 6, 2999 North Renmin Road
Songjiang District, Shanghai – China
e-mail: hongye419@gmail.com

Corresponding author:

FUMEI WANG
e-mail: wfumei@dhu.edu.cn

Shielding of static magnetic fields by textiles

MARCUS O. WEBER

FARZANA AKTER
ANDREA EHRMANN

REZUMAT – ABSTRACT

Ecranarea câmpurilor magnetice statice cu ajutorul materialelor textile

Câmpurile magnetice statice și de joasă frecvență pot să apară în transformatoarele de rețea, motoare, osciloscoape, magneți puternici de laborator etc. Aceste câmpuri pot fi ecranate doar cu ajutorul unor materiale cu permeabilitate ridicată. În cazul câmpurilor magnetice slabe, μ-metal sau Metglas posedă o permeabilitate foarte mare, ceea ce conduce la factori de ecranare ridicați. Cu toate acestea, niciunul dintre cele două materiale nu este potrivit pentru câmpuri intense, deoarece permeabilitatea magnetică, care este dependentă de intensitatea câmpului magnetic, scade semnificativ în cazul câmpurilor magnetice cu valoarea de aproximativ 1 oersted sau mai mare. În experimentele efectuate, au fost integrate fire metalice fine și fire din diferite materiale magnetice în structuri textile tricotate din urzeală. Aceste materiale au fost înfășurate pe cilindri cu un anumit diametru și s-a măsurat factorul de ecranare în intervalul ± 100 Oe. Indicatorii de protecție s-au dovedit a fi mult mai mici decât valorile unei bare realizate din oțel solid, dar, cu toate acestea, experimentele efectuate arată că, în principiu, ecranarea câmpurilor magnetice statice cu ajutorul materialelor textile magnetice este posibilă.

Cuvinte-cheie: câmpuri magnetice statice, ecranare, textile magnetice, anizotropii magnetice

Shielding of static magnetic fields by textiles

Low-frequency and static magnetic fields occur, e.g., in mains transformers, motors, oscilloscopes, strong laboratory magnets etc. They can be shielded only by materials of high permeability. For weak magnetic fields, μ-metal or Metglas have very high permeabilities leading to large shielding factors. However, both materials are not suited for larger fields, since the field-dependent permeability decreases significantly for magnetic fields of about 1 Oersted (Oe) or higher. In our experiments, we integrated metallic fine yarns fine and yarns from different magnetic materials into warp-knitted fabrics. These fabrics were formed into cylinders of defined diameter. The shielding factor was measured in the field range of ± 100 Oe. Shielding ratios were found to be much lower than values of a solid steel bar; however, these experiments point out that shielding of static magnetic fields with magnetic textiles is possible in principle.

Key-words: static magnetic fields, shielding, magnetic textiles, magnetic anisotropies

People working under high-voltage power lines, at microwave ovens, or in research laboratories can be shielded from high-frequency electro-magnetic fields by protective clothing with conductive parts [1–4]. Low-frequency and static magnetic fields, however, can only be shielded by materials of high permeability. Such fields occur, e.g., in mains transformers, motors, oscilloscopes, strong laboratory magnets etc.

The magnetic permeability (magnetic conductivity) of a material is a measure of the material's ability to support the formation of a magnetic field in it, i.e. the magnetization built up in a material due to an applied magnetic field. Mathematically, this relation can be described as:

$$B = \mu H \qquad (1)$$

where:

B is the magnetic induction, Gauss (G);

H – the magnetic field, Oersted (Oe);

μ – the permeability.

While for diamagnetic and paramagnetic materials, the permeability, μ, can be calculated as:

$$\mu = B/H \qquad (2)$$

The permeability is no longer constant for ferromagnetic or superparamagnetic materials. For these materials, equation (2) has to be changed into the derivation:

$$\mu = \mathrm{d}B/\mathrm{d}H \qquad (3)$$

Equation (3) shows that the permeability of ferromagnetic materials is – for a typical shape of a ferromagnetic hysteresis loop – highest near the coercive field.

The shielding factor is defined as following equation (4):

$$S = B_{without}/B_{with} \qquad (4)$$

where:

$B_{without}$ represents the magnetic induction before the magnetic shielding material is introduced;

B_{with} – the magnetic induction when the shielding is being used.

The shielding factor, as the value of the reduction of the magnetic induction by a shielding material, is larger than 1 for ferromagnetic materials. It can also be expressed in % or in dB. On the other hand, for a long hollow cylinder in a transverse magnetic field, the shielding factor can be calculated as:

$$S = \mu_r d/D \quad (5)$$

where:

d is the material thickness of the cylinder;

D – the cylinder diameter.

For very weak magnetic fields, μ-metal or Metglas [5] have a very high permeability and can thus lead to a high shielding factor. However, both materials are not suited for larger fields, since the field-dependent permeability decreases significantly for magnetizing fields in the order of magnitude of 1 Oe or higher. For shielding of larger magnetic fields, materials need higher coercive fields, i.e. "broader" hysteresis loops.

EXPERIMENTAL PART

Materials used

In our experiments, we integrated fine wires from stainless steal, nickel, and iron into warp and weft knitted fabrics as weft threads or as stitches, respectively (fig. 1). These fabrics have been used to form cylinders of defined diameter. The shielding factor has been measured in the field region of ±100 Oe by measuring $B_{without}$ and B_{with} in the identical setup.

Sample preparation

The knitted fabrics have been used to produce cylinders of diameter 2 cm with the wires perpendicular or parallel to the external field (fig. 2). Depending on the permeability of the wires, the magnetic field lines are more or less strongly drawn into the cylinder material, leading to a reduction of the magnetic field inside the cylinders and a respective deformation of the field lines.

RESULTS AND DISCUSSIONS

While the shielding effect of stainless steel staple fiber yarn has turned out to be too small to be measured accurately, the samples containing different magnetic wires showed significant shielding effects. In order to depict the influence of the field-dependent permeability, measurements for all samples have been performed during a field sweep from *H* = +100 Oe → –100 Oe → +100 Oe.

Figure 3 shows the results of a measurement on sample with nickel wires of diameter 0.08 mm as stitches oriented parallel to the external magnetic field (0°, left panel) or perpendicular to the field lines (90°, right panel). For magnetic fields numerically larger than ~30 Oe, the shielding factor *S* is ~1, which means B_{with} and $B_{without}$ are nearly identical, thus there is no shielding effect. For smaller fields, however, an effect can be seen. Apparently, the direction of the courses does not show much difference in shielding, since both graphs – with the stitches oriented parallel or perpendicular to the field lines – look very similar.

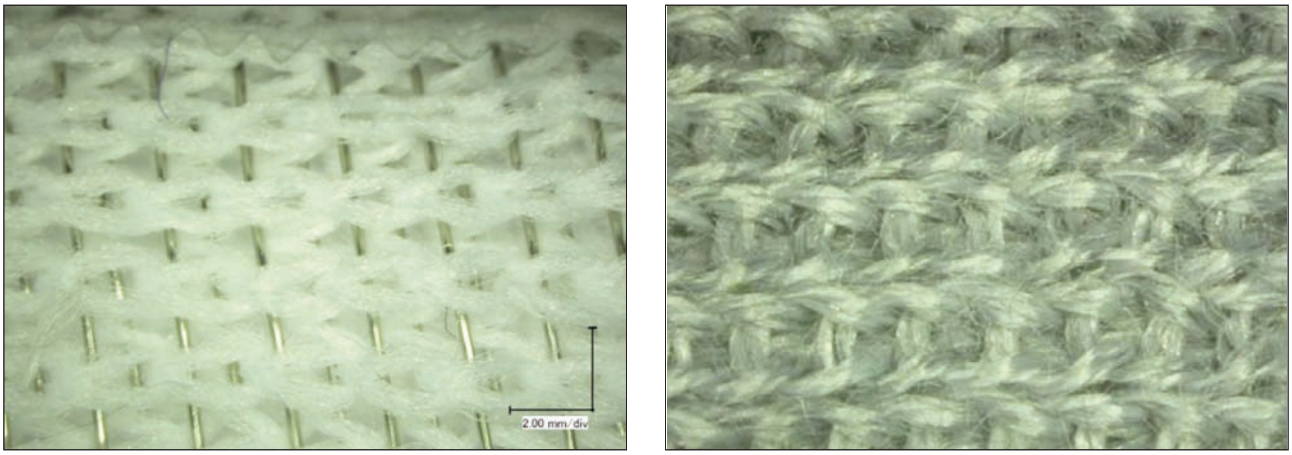

a ***b***

Fig. 1. Weft knitted samples, containing: ***a*** – nickel wires of diameter 0.3 mm as weft threads; ***b*** – produced from stainless steel staple fiber yarn

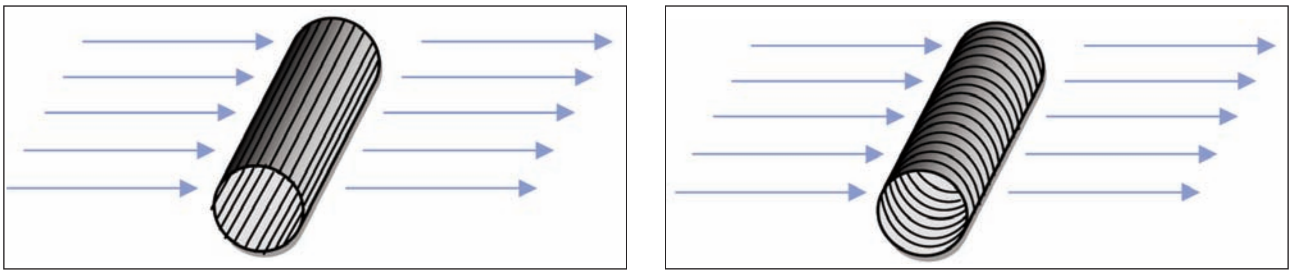

a ***b***

Fig. 2. Cylinders made from knitted samples containing: ***a*** – magnetic wires perpendicular (90°) to the external magnetic field (blue arrows); ***b*** – magnetic wires parallel (0°) to the external magnetic field

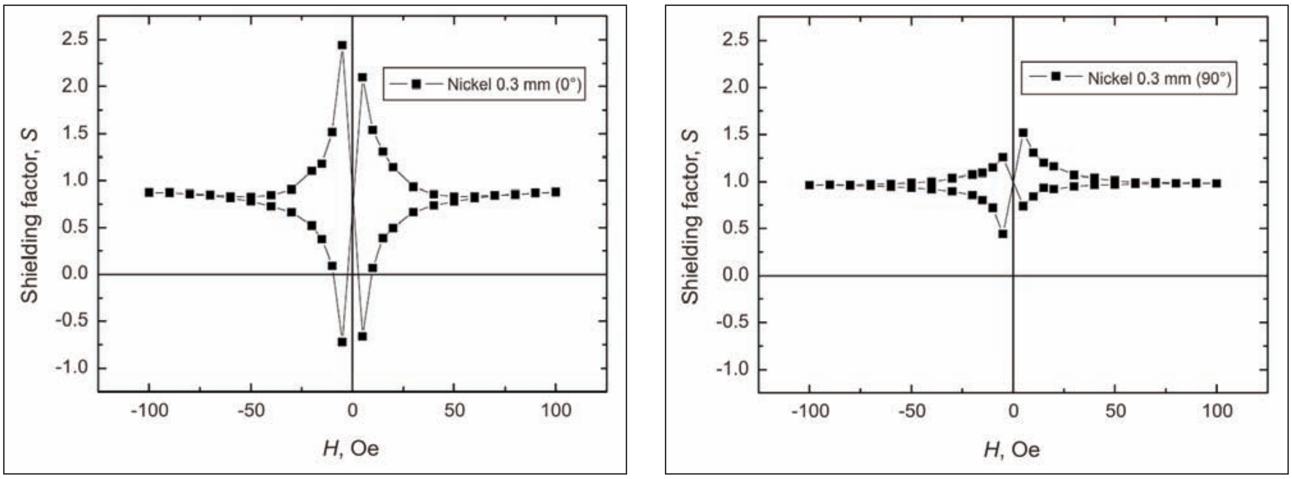

a *b*

Fig. 3. Shielding factors of weft knitted fabrics containing nickel wires of diameter 0.3 mm:
a – weft threads oriented parallel to the external magnetic field (0°);
b – weft threads oriented perpendicular to the field lines (90°)

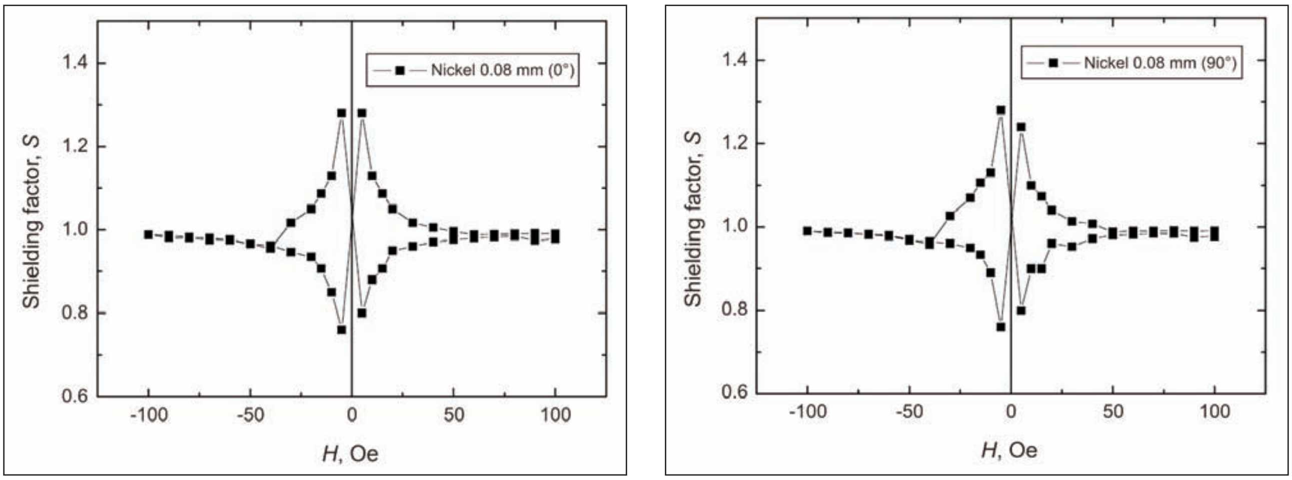

a *b*

Fig. 4. Shielding factors of weft knitted fabrics containing nickel wires of diameter 0.08 mm in stitches:
a – the courses oriented parallel to the external magnetic field (0°);
b – the courses oriented parallel perpendicular to the field lines (90°)

This behavior changes significantly for thicker nickel wires integrated in a non-magnetic knitted fabric as weft threads (fig. 3). On the one hand, the maximum shielding factor *S* is much larger now (~2.5). On the other hand, the difference between a wire orientation parallel to the external magnetic field (fig. 4 *a*) and the orientation perpendicular to it (fig. 4 *b*) is obvious. This finding can be explained as follows: The wires parallel to the external magnetic field can "lead" the magnetic flux along the shielded region, resulting in less magnetic flux B_{with} in the shielded area. If the wires are perpendicular to the magnetic field lines, however, the magnetic flux can only be led along short distances, i.e. inside the wires which have only a small diameter, compared to the distance between neighboring wires. Thus, the shielding efficiency must be smaller in the latter case.

For a comparison of the results of nickel wires with those of other materials, figure 5 shows the shielding factors measured for a knitted fabric containing iron wires of diameter 0.2 mm. Firstly, the maximum shielding factor becomes even larger for iron than for nickel, although the iron wire diameter is smaller than the value for the thicker nickel wire (0.3 mm). This shows that iron has a higher maximum permeability than nickel.

Secondly, the difference between both sample orientations is smaller for the iron wires. Taking into account figure 2 *a* it could be expected that thicker wires would lead the magnetic flux along larger distances (i.e. along their diameters) and thus be more effective for the wires being oriented 90° to the magnetic field lines. However, this idea is only valid for materials with identical form anisotropies, i.e. materials rotating the magnetization in the respective wires in the wire directions in the same way. Higher form anisotropies would decrease the possible ways of the magnetic flux through a wire oriented perpendicular to the field lines. Thus, the finding that iron wires show less difference between both orientations although

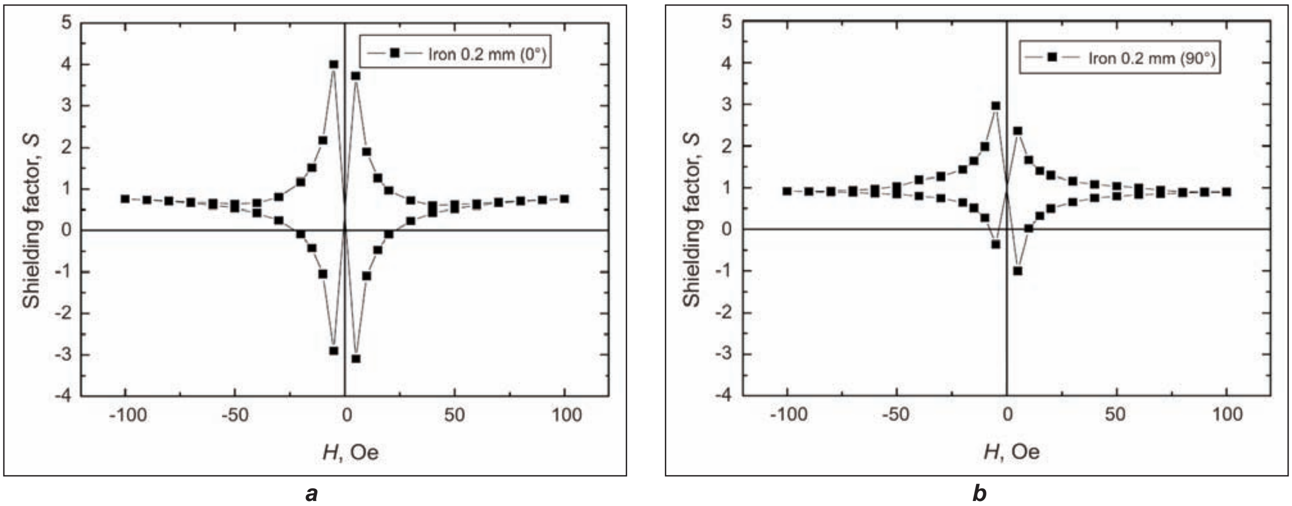

Fig. 5. Shielding factors of weft knitted fabrics containing iron wires of diameter 0.2 mm with:
a – weft threads oriented parallel to the external magnetic field (0°);
b – weft threads oriented perpendicular to the field lines (90°)

they have a smaller diameter points out, that the nickel wires have a stronger form anisotropy which tends to align the magnetization along the wire direction, while in the iron wires, the magnetization orientation is less strongly influenced by the wire orientation, allowing for a better flux conductivity along the wire diameter.

CONCLUSIONS

In conclusion, we integrated fine wires from different materials as well as yarns with metallic fibres into warp-knitted fabrics and formed them into cylinders of defined diameter.

Depending on the wire diameter, the spaces between the wires, their orientation, and the material, we found shielding ratios between 1.3 for fine nickel wires (0.08 mm) and ~4 for thin iron wires (0.2 mm) in the field range of ±100 Oe.

These values are relatively low, compared to, e.g., a solid steel bar reaching values about ten times higher; however, these experiments pointed out that shielding of static magnetic fields with magnetic textiles is possible in principle. Future research will concentrate on experiments with different raw materials for various magnetic fields.

BIBLIOGRAPHY

[1] Brzezinski, S., Rybicki, T., Karbownik, I., Malinowska, G., Rybicki, E., Szugajew, L., Lao, M., Sledzinska, K. *Textile multi-layer systems for protection against electromagnetic radiation.* In: Fibres & Textiles in Eastern Europe, 2009, vol. 17 , issue 73, pp. 66-71

[2] Mac, T., Houis, S., Gries, T. *Faserstoff-Tabellen nach P.-A. Koch.* Metallfasern, 1st edition, Deutscher Fachverlag GmbH, 2004

[3] Sonehara, M., Noguchi, S., Kurashina, T., Sato, T., Yamasawa, K., Miura, Y. *Development of an electromagnetic wave shielding textile by electroless Ni-based alloy plating.* In: IEEE Transactions on magnetics, 2009, vol. 45, issue 10, pp. 4 173-4 175

[4] Sonehara, M., Sato, T., Takasaki, M., Konishi, H., Yamasawa, K., Miura, Y. *Preparation and characterization of nanofiber nonwoven textile for electromagnetic wave shielding.* In: IEEE Transactions on magnetics, 2008, vol. 44, issue 11, pp. 3 107-3 110

[5] Malkowski, S., Adhikari, R., Hona, B., Mattie, C., Woods, D., Yan, H., Plaster, B. *Technique for high axial shielding factor performance of large-scale, thin, open-ended, cylindrical Metglas magnetic shields.* In: Review of Scientific Instruments, 2011, vol. 82, issue 7, p. 075-104

[6] Sasada, I., Yamamoto, T., Yamauchi, T. *Large shielding factor obtained by a multiple-shell magnetic shield having separate magnetic shaking.* In: Journal of Applied Physics, 1996, vol. 79, issue 8, pp. 5 490-5 492

Authors:

MARCUS O. WEBER
FARZANA AKTER
ANDREA EHRMANN
Faculty of Textile and Clothing Technology
Niederrhein University of Applied Sciences
Webschulstr. 31
41065 Mönchengladbach, Germany
e-mail: marc.weber@hsnr.de

Interdependence between anthropometric parameters specific for the age group 7–10 years

ANA VÎRCAN
SAVIN DORIN IONESI
STAN MITU

ALA DABIJA
LAVINIA CAPMARE

REZUMAT – ABSTRACT

Interdependența dintre parametrii antropometrici specifici grupei de vârstă 7–10 ani

Fenomenul de creştere şi dezvoltare este un fenomen neuniform, care se desfăşoară în ritmuri diferite. În lucrare sunt evidenţiate relaţiile necesare unei proiectări constructive, pornind de la datele antropometrice selectate pe un eşantion de 393 de copii (194 de fete şi 199 de băieţi), având la bază algoritmul de stabilire a interdependenţelor cu alte dimensiuni, care au aceeaşi orientare faţă de corp. Datele centralizate în tabele, împreună cu coeficienţii de corelaţie, atestă veridicitatea rezultatelor cercetării teoretice şi experimentale. Scopul lucrării îl constituie determinarea dependenţelor dintre diferite mărimi antropometrice şi elaborarea unor modele matematice, în vederea determinării dimensiunilor secundare, care să caracterizeze cât mai bine forma corpului. Analiza dependenţelor vizează fundamentarea unor modele matematice stabilite pe baza ecuaţiilor de regresie, care sunt utile în proiectarea constructivă a produselor vestimentare pentru copii.

Cuvinte-cheie: corelaţii, interdependenţă, testare, analize comparative

Interdependence between anthropometric parameters specific for the age group 7–10 years

Children's growth and development is an irregular phenomenon that takes place with different rhythms. Based on anthropometric data obtained by measuring a sample of 393 children (194 girls and 199 boys) and taking into consideration the algorithm for establishing the interdependencies' sizes with the same orientation on the body, in the paper are revealed the relationships selected and useful in constructive design. The data summarized in the tables along with the correlation coefficients show the veridical results of theoretical and experimental research. The aim of the paper is to determine the dependencies between different anthropometric sizes and the development of mathematical models in order to determine the secondary dimensions which characterize as well as possible the body shape. The analysis of the dependencies is intended for putting the base of the mathematical models established from the regression equations used in the constructivist design of children' clothing.

Key-words: correlations, interdependency, testing, comparative analysis

The researchers from the field of clothing design show the use of correlations between different anthropometric sizes, noticing a strong connection within the parameters of the same orientation, unlike the dimensions with other orientations [1 – 4].

The aim of the paper is testing the dependencies among different anthropometrical sizes and the development of mathematical models for determining the secondary dimensions of the same orientation, which could better characterize the body shape.

The anthropometric dimensions necessary for this study were taken according to SR 5279/2008 specifications, respectively SR ISO 13402-1/2002, by direct measurement of the body, on a sample of 393 children (194 girls and 199 boys).

Based on the data collected the paper aims to establish interdependency relations between main body dimensions: body height – $Î_c$, chest perimeter – P_b, waist perimeter – P_t, hip perimeter – P_s and secondary dimensions – cervical height point – $Î_{cerv}$, waist height – $Î_{lt}$, hip height – $î_f$, hip fold height – $î_{pl\ sf}$, knee height – $î_g$, corresponding to rectilinear sizes and back waist length taking into account the proeminence of the blade bone – L_T, front waist length – L_{tf}, shoulder length – l_u, shoulder to elbow length – L_{br}, arm length – $L_{m\ sup}$, trouser length – $L_{e.m.inf.}$, waist to floor – $L_{ant.T\text{-}S}$, inside upper leg length – $L_{int.m.inf.}$, cross back width – l_s, chest width – l_b, head perimeter – P_c, neckline perimeter – P_{pg}, upper arm perimeter – P_{br}, wrist perimeter – P_{am}, thigh perimeter – P_{cps}, knee perimeter – P_g, ankle perimeter – P_{gl} corresponding to curved sizes.

The description manner from the body and the positioning of the anthropometric sizes taken into the study are illustrated in figure 1.

In order to obtain the dependencies between the anthropometric sizes studied was used the regression and correlation analysis, which is made in 2 steps:

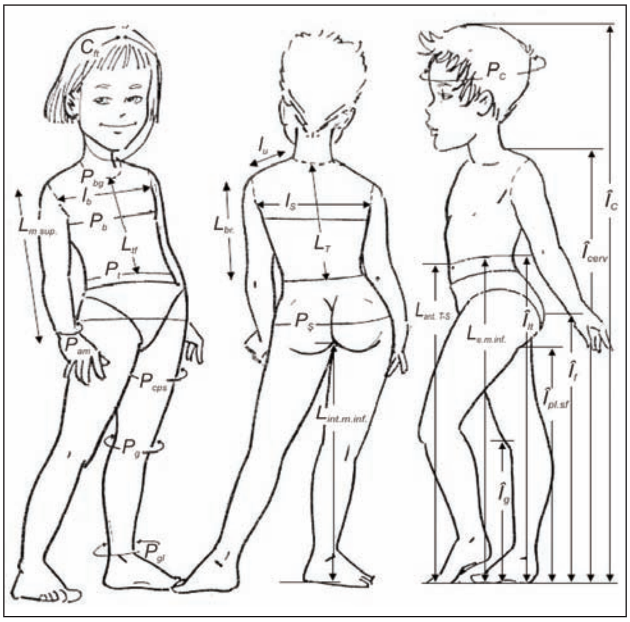

Fig. 1. Body dimensions measurement

– highlighting the existence of the correlation and also its meaning through correlation parameters;
– determining the mathematical model that expresses in the best way the connection between the analysed sizes through regression study.

The algorithm is staggered while applying it and the results obtained are graphically marked, this leading to the centralized and comparative data useful not only for body description but also for constructivist design.

RESULTS AND DISCUSSIONS

The correlation and regression analysis was made using specialized software programs SPSS 18 and Jardel Table Curves 3D, the experimental data base is followed by symbols included in figure 1.

Before establishing simple and multiple regression equations, that can reveal as better as possible the connection between the anthropometric sizes analysed, it is imposed the graphical testing consisting in an axial system of rectangular coordination for the experimental pairs of values intended for correlation. The representation of the points in the graphic is called “points cloud”. The repartition offers information about the existence of the correlation between the analysed sizes, the direction and their intensity.

Afterwards was established the correlation coefficients that could express the dependency of the analysed sizes but also testing these coefficients for the validity of the chosen model.

The signification of the simple correlation coefficients was tested by reporting it to the signification level p, that indicates the measure to which we can go wrong with an affirmation. In practice are often used 2 levels of significations: level 0.01 (1% error) and level 0.05 (5% error). In practice it is considered an important statistical test when the level is ≤ 0.05 [5 – 7].

Another method indicated by the mathematical statistics for coefficient correlation testing is by applying t test and comparing the results obtained with those from the literature according to the selection volume, precision imposed and the number of freedom grade – $t_{(P,f)}$. If $t > (t_{(P,f)})$, according to an imposed probability level, the correlation between the variables is not random.

For the studied group the researchers from the field use for the design of children clothing, both simple but also linear models, and also curved [8, 9]. Choosing the mathematical model to express as better as possible the connection between the analysed sizes differs in the way the unuseful variables are eliminated.

In the paper were used simple and multiple regression calculation for the anthropometrical data. The mathematical models that could better express the body dimensions for this age group are of the type [10]:

$$Y_i = b_0 + b_1x_1 \qquad (1)$$

$$Y_i = b_0 + b_1x_1 + b_2x_2 + \ldots + b_nx_n \qquad (2)$$

$$Y_i = b_0 + b_1x_1 + b_2x_2 + b_3x_2^2 + b_4x_1x_2 + b_5x_1^2 + \ldots + b_nx_n^n \qquad (3)$$

where:

x_i represents the independent variables;

y_i – the value of the dependent variable;

$b_0, b_1 \ldots b_n$ – regression equation coefficients.

The adequacy of mathematical models was calculated through verifying the significance of determination coefficient R^2 and by using Fisher criteria according to the relation:

$$F_{calc} = \frac{R^2}{1 - R^2} \cdot \frac{n - m}{m - 1} \qquad (4)$$

where:

R^2 is the determination coefficient;

m – the number of the parameters from the regression equation;

n – total number of experimental data;

F_{tab} – critical value for a selected trust level (according to Fisher criteria).

Using Jardel Table Curves 3D was determined the value of multiple correlation coefficient for the analyzed types, using the following relation:

$$R_{y,x_1,x_2} = \sqrt{1 - \frac{\sum_{i=1}^{n}(Y_m - Y_c)^2}{\sum_{i=1}^{n}(Y_m - \bar{Y})^2}} \qquad (5)$$

where:

Y_m is dependent measured value;

Y_c – dependent calculated value size;

Y – medium value of the dependent size.

For the secondary dimensions that characterize the body shape were tested the types of correlation with body height, bust perimeter, waist perimeter, hips perimeter as independent variables.

From the analysis of the statistical cloud for all types comes the conclusion that can be accepted the relation of interdependence of the type:

$$y = b_0 + b_1 x \qquad (6)$$

where:

y is the regression line between the 2 variables (in the present case between the pairs of anthropometrical sizes established previously);

b_1, b_0 – the equation coefficients of the regression line.

Before determining the analytical form of the functional dependency it is necessary to verify statistically the supposed linearity of the connection between the variables x_i and y_i. Thus in the beginning it will be calculated the correlation coefficient with the relation:

$$r = \frac{n\sum x_i y_i - \sum x_i \cdot \sum y_i}{\sqrt{\left[n\sum x_i^2 - \left(\sum x_i\right)^2\right]\left[n\sum y_i^2 - \left(\sum y_i\right)^2\right]}} \qquad (7)$$

where:

r is the absolute value of correlation coefficient calculated with relation (1);

n – total number of measurements.

The calculated correlation for the analyzed dimensions is significant on a level of $p = 0.01$.

For all the centralized data in table 1 and table 2, $p < 0.05$ this meaning that the connection between the variables is significant under statistical report.

Beside calculating simple correlation coefficients was made also the calculation of multiple correlations. Multiple correlations coefficient can be defined as

Table 1

SIMPLE CORELATION COEFFICENTS BETWEEN MAIN DIMENSIONS AND SECONDARY DIMENSIONS CORRESPONDING FOR GIRLS SAMPLE

Main dimensions	Secondary dimensions									
	$\hat{I}_c$	$\hat{I}_{cerv}$	$\hat{I}_{lt}$	$\hat{I}_f$	$\hat{I}_{pl.sf}$	$\hat{I}_g$	ARS	L_T	L_{tf}	l_u
$\hat{I}_c$	1	0.998	0.994	0.989	0.985	0.968	0.903	0.917	0.883	0.897
P_b	0.678	0.683	0.663	0.659	0.659	0.644	0.676	0.679	0.671	0.736
$P_ș$	0.716	0.717	0.703	0.700	0.698	0.668	0.697	0.695	0.697	0.738
Main dimensions	$L_{br.}$	$L_{m.sup.}$	$L_{e.m.inf.}$	$L_{ant.T\text{-}S}$	$L_{int.m.inf.}$	l_s	l_b	P_c	P_{ft}	P_{bg}
$\hat{I}_c$	0.930	0.975	0.994	0.994	0.986	0.843	0.826	0.470	0.561	0.647
P_b	0.619	0.682	0.663	0.663	0.658	0.955	0.964	0.616	0.713	0.734
$P_ș$	0.630	0.694	0.703	0.702	0.697	0.080	0.894	0.600	0.751	0.705
Main dimensions	P_b	P_t	$P_ș$	P_{br}	P_{am}	P_{cps}	P_g	P_{gl}	-	
$\hat{I}_c$	0.678	0.613	0.716	0.691	0.698	0.694	0.767	0.677		
P_b	1	0.945	0.896	0.851	0.837	0.874	0.866	0.703		
$P_ș$	0.896	0.870	1	0.848	0.822	0.955	0.932	0.774		

Table 2

SIMPLE CORRELATION COEFFICIENTS BETWEEN MAIN DIMENSIONS AND SECONDARY DIMENSIONS CORRESPONDING FOR BOYS SAMPLE

Main dimensions	Secondary dimensions									
	$\hat{I}_c$	$\hat{I}_{cerv}$	$\hat{I}_{lt}$	$\hat{I}_f$	$\hat{I}_{pl.sf}$	$\hat{I}_g$	ARS	L_T	L_{tf}	l_u
$\hat{I}_c$	1	0.998	0.992	0.987	0.984	0.982	0.880	0.899	0.854	0.837
P_b	0.672	0.674	0.671	0.669	0.665	0.689	0.630	0.643	0.613	0.786
$P_ș$	0.487	0.487	0.496	0.499	0.499	0.532	0.448	0.463	0.429	0.616
Main dimensions	$L_{br.}$	$L_{m.sup.}$	$L_{e.m.inf.}$	$L_{ant.T\text{-}S}$	$L_{int.m.inf.}$	l_s	l_b	P_c	P_{ft}	P_{bg}
$\hat{I}_c$	0.967	0.973	0.992	0.992	0.983	0.868	0.857	0.509	0.636	0.704
P_b	0.627	0.659	0.671	0.672	0.686	0.928	0.937	0.509	0.667	0.723
$P_ș$	0.449	0.492	0.495	0.497	0.526	0.786	0.799	0.509	0.633	0.637
Main dimensions	P_b	P_t	$P_ș$	P_{br}	P_{am}	P_{cps}	P_g	P_{gl}	-	
$\hat{I}_c$	0.672	0.487	0.718	0.543	0.675	0.698	0.707	0.732		
P_b	1	0.910	0.917	0.865	0.743	0.899	0.859	0.587		
$P_ș$	0.910	1	0.857	0.828	0.635	0.858	0.822	0.486		

simple maximum correlation coefficient between the dependent variable y and a combination of independent variable x [16]. A value of R close to 0 shows an insignificant connection from a statistical point of view as while a value close to 1 shows a significant connection. Because the value of R coefficient tends to underestimate the connection between the variables y and x is preferred the coefficient R^2 – the square coefficient of multiple correlation.

As in the case of linear regression analysis with only one independent variable for the multiple regression analysis the main problem is determining the coefficients b_0, b_1, b_2, ..., b_k to minimize the square errors sum of y_i values compared to y_i calculated values [4].

The significance of multiple correlation coefficients for the analysed parameters was determined using t test. As a result of comparing the values of the test taken from the literature with the values calculated, were kept in the relation only the corresponding coefficients for the parameters studied and which have the inequality $t > t_{(P = 0.95,\ v = 4)} = 1.972$.

After applying Fisher test on simple and multiple mathematical models were kept only the models that had the inequality $F_{calc} > F_{tab}$ that expresses the connection between the main sizes and the secondary ones necessary for a complete description of the body, the best concluding ones being in table 3 and table 4 for girls sample and boys sample.

Table 3

MATHEMATICAL MODELS FOR GIRLS SAMPLE					
Tested type	**Mathematical model M_1**	**R^2**	**Mathematical model M_2**	**R^2**	**Propossed model**
Rectilinear sizes					
$\hat{l}_{cerv}$	$Y = 1.040 + 0.827\ x_1$	0.996	$Y = 6.947 + 0.823\ x_1 + (–0.179)\ x_2 + 0.001\ x_2$^2	0.996	M_1
$\hat{l}_{lt}$	$Y = –4.952 + 0.658\ x_1$	0.994	$Y = –4.904 + 0.667\ x_1 + (–0.019)\ x_2$	0.988	M_2
$\hat{l}_f$	$Y = 3.989 + 0.426\ x_1$	0.970	$Y = (–0.753) + 0.498\ x_1 + 65.064/\ x_3$	0.977	M_2
$\hat{l}_{pl.sf}$	$Y = 12.905 + 0.436\ x_1 + 0.300\ x_2 + 0.002\ x_2$^2	0.970	$Y = 2.169 + 0.433\ x_1 + 60.749/\ x_3$	0.970	M_2
$\hat{l}_g$	$Y = –1.181 + 0.298\ x_1 + 53.196/x_2$	0.937	$Y = 0.389 + 0.304\ x_1 + (–0.020)\ x_3$	0.938	M_2
Curved sizes					
ARS	$Y = 1.995 + 0.083\ x_1 + 0.017\ x_2$	0.823	$Y = 2.090 + 0.083\ x_1 + 0.013\ x_3$	0.821	M_1
L_T	$Y = 3.453 + 0.182\ x_1 + 0.033\ x_2$	0.846	$Y = –10.952 + 0.407\ x_1 + (0.0008)\ x_1$^2(0.018) x_3	0.845	M_1
L_{tf}	$Y = 4.627 + 0.167\ x_1$	0.805	$Y = 4.535 + 0.150\ x_1 + 0.036\ x_2$	0.789	M_1
l_u	$Y = –1.738 + 0.081\ x_1$	0.866	$Y = –1.651 + 0.068\ x_1 + 0.022\ x_3$	0.823	M_1
$L_{br.}$	$Y = –4.515 + 0.233\ x_1$	0.951	$Y = –4.605 + 0.246\ x_1 + (–0.024)\ x_3$	0.868	M_1
$L_{m.sup.}$	$Y = –1.985 + 0.363\ x_1$- + 0.012	0.987	$Y = –2 + 0.365\ x_1 + (–0.004)\ x_3$	0.951	M_1
$L_{e.m.inf.}$	$Y = –4.405 + 0.652\ x_1$	0.988	$Y = –4.460 + 0.660\ x_1 + (–0.014)\ x_3$	0.987	M_1
$L_{ant.T\text{-}S}$	$Y = –7.696 + 0.660\ x_1 + 96.683/x_2$	0.988	$Y = 0.056 + 0.661\ x_1 + (–0.161)\ x_{3m} + 0.001\ x_3$^2	0.988	M_1
$L_{int.m.inf.}$	$Y = –0.605 + 0.470\ x_1 + 68.866/x_2$	0.972	$Y = –0.444 + 0.470\ x_1 + 65.786/x_3$	0.972	M_2
Width					
l_s	$Y = 5.003 + 0.345\ x_2$	0.912	$Y = –1.121 + 0.089\ x_1 + 0.256\ x_2$	0.982	M_2
l_b	$Y = 3.853 + 0.332\ x_2$	0.929	$Y = –1.290 + 0.074\ x_1 + 0.257\ x_2$	0.984	M_2
Perimeters					
P_c	$Y = 42.703 + 0.153\ x_2$	0.379	$Y = 41.563 + 0.016\ x_1 + 0.136\ x_2$	0.384	M_2
P_{bg}	$Y = 17.192 + 0.194\ x_2$	0.538	$Y = 13.771 + 0.049\ x_1 + 0.144\ x_2$	0.579	M_2
P_{br}	$Y = 2.302 + 0.293\ x_2$- + 0.006	0.723	$Y = 5.988 + 0.053\ x_1 + 0.012\ x_2 + 0.001\ x_2$^2	0.748	M_2
P_{am}	$Y = 3.906 + 0.155\ x_2$	0.701	$Y = 1.820 + 0.030\ x_1 + 0.125\ x_2$	0.732	M_2
P_{cps}	$Y = –7.280 + 0.655\ x_3$	0.912	$Y = –8.038 + 0.011\ x_1 + 0.644\ x_3$	0.912	M_1
P_g	$Y = 5.959 + 0.341\ x_3$	0.869	$Y = 2.050 + 0.057\ x_1 + 0.287\ x_3$	0.889	M_2
P_{gl}	$Y = 8.073 + 0.174\ x_3$	0.599	$Y = 5.090 + 0.044\ x_1 + 0.132\ x_3$	0.630	M_2

Table 4

MEDIUM VALUE CALCULATED FOR THE MORPHOLOGICAL INDICATORS L_T AND l_s AND THE VALUES OBTAINED FROM THE MODELS			
Tested type	**Medium value measured**	**The value calculated with the model M_1**	**The value calculated with the model M_2**
L_T	29.65	29.63	30.01
l_s	32.75	32.25	32.80

For body description were selected three main dimensions, respectively $\hat{l}_{c(x1)}$, $P_{b(x2)}$ as common ones and the third $P_{ş(x3)}$ for girls and $P_{t(x4)}$ for boys.

The mathematical models proposed for girls and boys clothing design are those that assure the best correspondence between the calculated values and those measured on the body.

After the analysis of the 2 types of mathematical models for the girls sample shown in table 5, choosing the appropriate model was made by taking into account the values of the coefficients of correlation

Table 5

MATHEMATICAL MODELS FOR BOYS SAMPLE					
Tested type	**Mathematical model M_1**	**R^2**	**Mathematical model M_2**	**R^2**	**Proposed model**
Rectilinear sizes					
$\hat{l}_{cerv}$	$Y = -1.036 + 0.842\ x_1$	0.997	$Y = 0.279 + 0.279\ x_1 + (-43.756)/x_2$	0.996	M_1
$\hat{l}_{lt}$	$Y = -7.516 + 0.669\ x_1$	0.985	$Y = -7.546 + 0.665\ x_1 + 0.008\ x_2$	0.985	M_1
$\hat{l}_f$	$Y = -1.807 + 0.506\ x_1$	0.974	$Y = -1.918 + 0.499\ x_1 + 0.015\ x_4$	0.974	M_1
$\hat{l}_{pl.sf}$	$Y = 0.181 + 0.447\ x_1 + (-4.923)/x_2$	0.968	$Y = -0.071 + 0.442\ x_1 + 0.014\ x_4$	0.969	M_2
$\hat{l}_g$	$Y = -1.917 + 0.303\ x_1$	0.967	$Y = -2.477 + 0.296\ x_1 + 0.027\ x_4$	0.967	M_1
Curved sizes					
ARS	$Y = 4.191 + 0.085\ x_1 + (-56.202)/\ x_2$	0.778	$Y = 2.915 + 0.090\ x_1 + (-13.386)/x_4$	0.775	M_1
L_T	$Y = 4.253 + 0.200\ x_1$	0.808	$Y = 4.165 + 0.189\ x_1 + 0.023\ x_2$	0.811	M_2
L_{tf}	$Y = 5.732 + 0.167\ x_1$	0.730	$Y = 5.655 + 0.157\ x_1 + 0.020\ x_2$	0.732	M_2
l_u	$Y = -1.718 + 0.054\ x_1 + 0.058\ x_2$	0.792	$Y = -1.736 + 0.0678\ x_1 + 0.033\ x_4$	0.757	M_1
$L_{br.}$	$Y = -4.188 + 0.232\ x_1$	0.936	$Y = -6.13 + 0.238\ x_1 + 64.632\ /x_2$	0.936	M_1
$L_{m.sup.}$	$Y = -2.922 + 0.371\ x_1 - + 0.001$	0.947	$Y = -2.944 + 0.368\ x_1 + 0.005\ x_2$	0.946	M_1
$L_{e.m.inf.}$	$Y = -7.296 + 0.666\ x_1$	0.985	$Y = -16.086 + 0.790\ x_1 +$ $+ (-0.0004)\ x\text{^}2 + 0.014\ x_4$	0.985	M_1
$L_{ant.T\text{-}S}$	$Y = -7.227 + 0.661\ x_1$	0.985	$Y = -5.730 + 0.655\ x_1 + (-48.500)/x_2$	0.984	M_1
$L_{int.m.inf.}$	$Y = -3.221 + 0.473\ x_1 + 0.035\ x_2$	0.968	$Y = -3.363 + 0.474\ x_1 + 0.038\ x_4$	0.969	M_2
Width					
l_s	$Y = -1.349 + 0.106\ x_1 + 0.224\ x_2$	0.970	$Y = -1.534 + 0.151\ x_1 + 0.143\ x_4$	0.926	M_1
l_b	$Y = 23.104 + (-1636.371)/x_1 +$ $+ 0.224\ x_2$	0.972	$Y = -1.799 + 0.139\ x_1 + 0.142\ x_4$	0.925	M_1
Perimeters					
P_c	$Y = 63.586 + (-0.313)\ x_1 +$ $+ 0.001\ x_1\text{^}2 + 0.087\ x_2$	0.315	$Y = 53.494 + (-0.159)\ x_1 +$ $+ 0.0008\ x_1\text{^}2 + 0.083\ x_4$	0.350	M_2
P_{bg}	$Y = 12.053 + 0.073\ x_1 + 0.125\ x_2$	0.609	$Y = 11.884 + 0.095\ x_1 + 0.089\ x_4$	0.608	M_1
P_{br}	$Y = -3.777 + 0.\ 386\ x_2$	0.749	$Y = 22.094 + (-0.016)\ x_1 +$ $+ (-0.353)y\ x_2 + (0.005)y\text{^}\ x_2$	0.750	M_2
P_{am}	$Y = -1.342 + 0.052\ x_1 + 0.130\ x_2$	0.608	$Y = -1.452 + 0.079\ x_1 + 0.083\ x_4$	0.578	M_2
P_{cps}	$Y = -8.039 + (-0.137)\ x_1 +$ $+ 0.0009\ x_1\text{^}2 + 0.739\ x_2$	0.824	$Y = -25.522 + 0.232\ x_1 + 0.542\ x_4$	0.838	M_2
P_g	$Y = 23.670 + 0.090\ x_1 +$ $+ (-0.518)\ x_2 + 0.006\ x_2\text{^}2$	0.777	$Y = -45.588 + 0.741\ x_1 +$ $+ (-0.002)\ x_1\text{^}2 + 0.290\ x_4$	0.802	M_2
P_{gl}	$Y = -3.951 + 0.154\ x_1 + 0.064\ x_2$	0.552	$Y = -4.089 + 0.162\ x_1 + 0.053\ x_4$	0.557	M_2

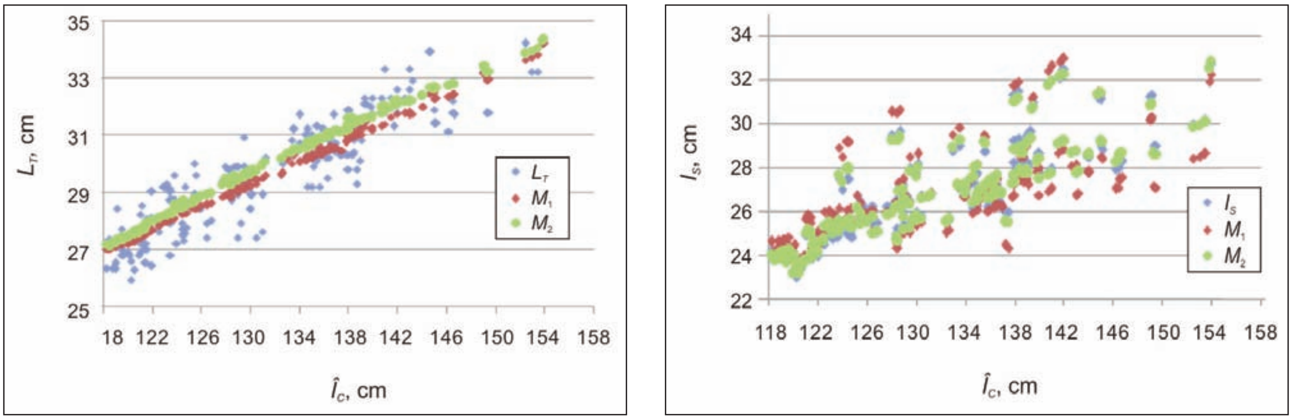

a ***b***

Fig. 2. The distribution of calculated values with the measured values for L_T and l_s based on the models obtained

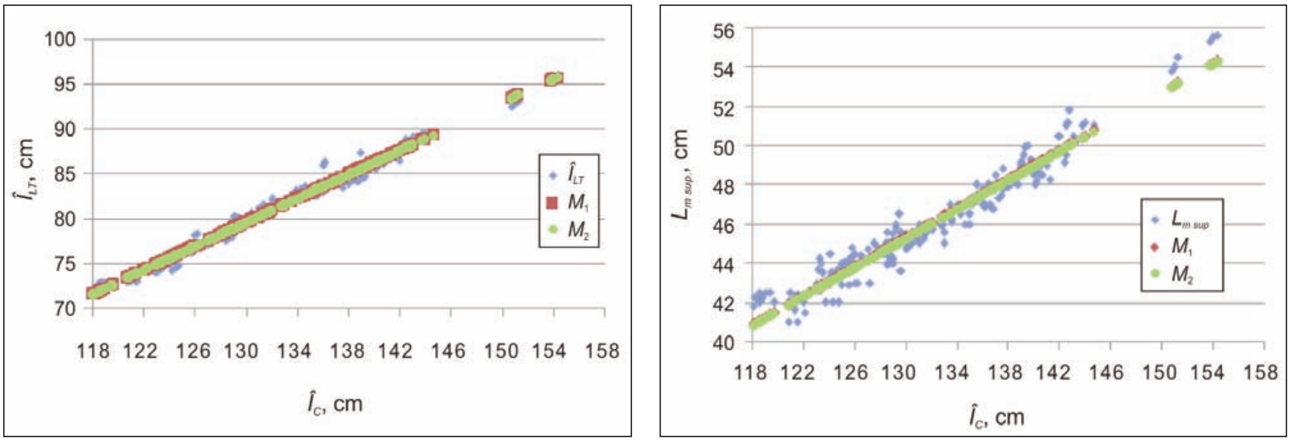

a ***b***

Fig. 3. The distribution of calculated values with those measured for $Î_{lt}$ and $L_{m.sup}$ based on the obtained models

and the distribution of calculated values through the 2 methods of direct body measurement, in figure 2 being presented the testing examples for the 2 secondary dimensions – the back length to the waist and the back width.

Choosing the models for boys sample was made from the same principle as girls selection, figure 3 and table 6 being concluding in this way for secondary dimensions respectively waist line height and arm length.

The mathematical models obtained can be used for determining secondary dimensions if the main ones are known, thus becoming primary relations for the pattern segments in which can be added different specific things(the type of product to be crested, the material used, the wearers group).

Both the mathematical models obtained through simple regression analysis and also those obtained through curved multiple regression can represent work instruments in the revision activity for the rules applied for constructivist design on children' clothing.

Table 6

THE CALCULATED MEDIUM VALUE FOR MORPHOLOGICAL INDICATORS $Î_{lt}$ AND $L_{m.sup}$ AND THE VALUES OBTAINED FROM THE MODELS

Tested type	Medium value measured	The value calculated with the model M_1	The value calculated with the model M_2
$Î_{lt}$	80.65	80.58	80.53
$L_{m.sup.}$	45.96	45.93	45.83

CONCLUSIONS

Based on the experimental results presented in the paper and also based on the bibliographical materials consulted can be presented the following conclusions:

– using the statistical modelling programs SPSS 18 and Jardel Table Curves 3D were obtained the mathematical models of 2 types, represented graphically and afterwards centralized in tables;

– was imposed testing those models, the results being compared with the values obtained by anthropometrical measurements, selecting in these conditions the mathematical model that can be used in constructivist design for base patterns for products with shoulder support and products with waist support;

– based on regression equations can be established medium values for secondary parameters but following main anthropometrical parameters;
– the values obtained from the statistical work can be included in the existent design relations;
– establishing the optimal number of subjects, the regression relation obtained for the studied group can become the base for new rules and anthropometrical standards, the existent ones having the need for corrections because of the phenomenon called "secular growth";
– for obtaining interdependence relations between the anthropometric dimensions with the same orientation it is necessary making a experimental data base specific for the studied age group and also based on the specifications of the anthropometric standards.

BIBLIOGRAPHY

[1] Bălan, S., Mitu, S. *Prelucrarea statistică unidimensională a parametrilor antropometrici principali pentru femei, grupa de vârstă 18-29 ani.* Al II-lea Simpozion Internaţional Universitar, Editura Tehnică a Moldovei, Chişinău, 1997, p. 32, ISBN 9975-910-18-1

[2] Niculescu, C., Săliștean, A., Olaru, S. *Anthropometric parameters of children in Romania, result of the anthropometric survey carried out in 2010-2011*. In: Industria Textilă, 2012, vol. 63, nr. 1, p. 176-182

[3] Ciocoiu, M. *Bazele statistico – matematice ale analizei şi controlului calităţii în industria textilă*. Editura Performantica, Iaşi, 2002, ISBN 973-8075-31-9

[4] Dabija, A. *Cercetări privind particularităţile constructiv tehnologice ale echipamentelor de protecţie destinate operatorilor care deservesc utilităţi publice din Republica Moldova.* Teză de doctorat, 2011

[5] Clocotici, V. *Introducere în statistică multivariată*. Universitatea „Al. I. Cuza", 2007

[6] Landau, S., Everit, B. S. *A handbook of statistical analzses using SPSS.* Chapman & Hall/CRC Press LLC, 2004, ISBN 1-58488-369-3

[7] Griffith, A. *SPSS for Dummies*. Published 2007, ISBN: 978-0-470-11344-8

[8] Vouyouka, A. A. *Comprehensive pattern making guide book suitable for use with any pattern making method.* Publications AB, 2001, ISBN 960-8430-34-8

[9] Winifred, Aldrich. *Metric pattern cutting for children's wear and babywear*. Published 2009, ISBN-13: 978-1405182928

[10] Avădanei, M. *Contribuţii teoretice şi experimentale privind utilizarea datelor antropometrice în proiectarea produselor vestimentare.* Teză de doctorat, Universitatea Tehnică „Gheorghe Asachi" – Iași, 2001

Authors:

Drd. ing. ANA VÎRCAN
Drd. ing. SAVIN DORIN IONESI
Prof. dr. ing. STAN MITU
Drd. ing. ALA DABIJA
Drd. ing. LAVINIA CAPMARE
Universitatea Tehnică "Gheorghe Asachi" Iași
Facultatea de Textile, Pielărie și Management Industrial
Bd. D. Mangeron nr. 53, Iaşi
e-mail: avircan@tex.tuiasi.ro

Auto-generation color image for fabric based on FFT

HONGXIA JIANG
JIHONG LIU
RURU PAN
WEIDONG GAO
HONGFU WANG

REZUMAT – ABSTRACT

Autogenerarea unei imagini color pe materiale textile, cu ajutorul FFT

A fost studiată o metodă de autogenerare a unei imagini color, folosind transformata Fourier rapidă (FFT). În acest scop, s-a elaborat un program de autogenerare a unor imagini color rafinate, într-un număr foarte mare de variante. Au fost proiectate probe ale imaginilor analizate, prin generarea de modele digitale din puncte. Procesul de autogenerare a culorilor s-a realizat în patru etape: dimensionarea imaginii, crearea șablonului de bază, alegerea culorii modelului și conversia imaginii la modelul de culoare dorit. Au fost analizate trei dintre cele mai simple modele de bază, precum și combinații ale acestora. În cadrul acestei cercetări, a fost adoptat modelul de culoare HSV. Pentru proiectarea imaginii, în cadrul acestui studiu, au fost luați în considerare trei parametri importanți, inclusiv H, S și V. Rezultatele au arătat că imaginile reprezintă o combinație a patru proprietăți. Dimensiunea și culoarea imaginii pot fi controlate în funcție de cerința designerului. În cadrul acestui studiu, imaginile au fost transferate pe materialele textile, folosind un program ce conține imaginea virtuală a unui mobilier. Rezultatele au arătat că designerul textil are acces direct la imaginile create. Aceste imagini pot fi folosite pentru proiectarea imaginii pe elemente textile, de exemplu pe mobilierul textil.

Cuvinte-cheie: elemente de design, textile digitale, creare de modele, imagini color, mobilier virtual

Auto-generation color image for fabric based on FFT

An auto-generation method of color image was researched based on the fast Fourier transform theory. We developed a program to auto-generate abundant exquisite color images. Samples of images, using patterns of points, were designed. The auto-generation color processing can be divided into the four steps: giving the image size, drawing basic pattern, giving the color pattern and transforming color image. The simplest basic patterns and their combinations were analyzed. HSV color model was adapted in the research. Three important parameters, including H, S and V, were considered in this research for image design. The results showed that the images have the properties of alliance quartet. The size and color of image element can be controlled according to requirement of designer. In the present research the images were transformed to textiles by virtual furniture software. The results also showed that the images can be used for textile designer directly. The application of the images was also discussed for the elements for textile image design such as furniture textile.

Key-words: design elements, digital textile, pattern design, color image, virtual furniture

Image making is a kind of artwork, it is time-consuming and difficult for engineering. To solve the problem, an image making method by dots of monochrome was researched. As a result of conducting factor analysis about the product of original images, the relation between the design condition and the image of the design can be clarified and the basic data of the image making for the textile designer were able to be obtained [1]. The application of moiré patterns to clothes was examined. The patterns were made by pilling up the same two figures of color dots arranged at points of intersection of square fretwork. The number of patterns became innumerable by changing a rotation angle between the two figures [2]. Bye briefly introduced some of the history and main concepts of the design discipline and design research. He presents a framework for design scholarship to initiate a discussion about research, and suggested ways to contribute to the larger academic dialogue on forming a design discipline [3]. The effects of indirect training, provided by apparel design and product development courses on spatial visualization skills, were examined [4]. The images were introduced into CAD systems and its adjustment to the technical and aesthetic limitations of the printing industry. Gray-scale image analysis was applied to the characterization of textural patterns of 29 kinds of lace.

Factor analysis showed beauty to be related to the entropy and fractal dimension, transparency and light sensation to the angular second moment, contrast, thickness and weight, as well as lacunarity to the number of voids and mean void size [5].

Recently many art works based on mathematics, were studied [6]. The generation of an image originating from the mapping has been proposed [7]. A complete design process, beginning with a design from the mathematical perception of fractal geometry, was introduced [8]. A parameterized program to generate various uniform stochastic web images was developed based on a kind of nonlinear scientific technology-weak chaos. It is in favor of perfecting digital textile technology. Methods of transforming mapping function to obtain abundant colorful digital images for ink-jet printing were proposed [9]. Image processing has been used in analyzing the textile widely [10–13]. With the development of computer science and technology, nonlinear science, including fractal geometry, chaos and other important branches, provides us with a new resource of pattern design [5].

In this paper, an auto-generation method of color image was researched. Because of the color sense with a sense of expansion and contraction, we use the HSV model to illustrate algorithm in the research in order to show the real Fourier transform automatically generated patterns internal fine structure. Based on the fast Fourier transform (FFT) theory, we developed a program to auto-generate abundant exquisite color images. Samples of images, using patterns of points and their combinations, were designed. Using the techniques of computer-aided textile design, an artwork is created on a pure mathematical basis as a result.

THEORY OF GENERATING IMAGES BY FFT

Basic theory of FFT

FFT was used to design virtual woven fabric [14]. Express the gray level of an image of width $X \cdot$ height Y as a two dimensional function $f(x, y)$, where $x = 0, 1, 2, \ldots, X-1$, and $y = 0, 1, 2, \ldots, Y-1$, are the sampled points in the spatial coordinates. The discrete Fourier transform (DFT) of $f(x, y)$ is written as following equation (1):

$$F(k,l) = \sum_{x=0}^{X-1} \sum_{y=0}^{Y-1} f(x,y)\, e^{-j2\pi\left(\frac{xk}{X} + \frac{yl}{Y}\right)} \qquad (1)$$

where:

$k = 0, 1, 2, \ldots, X-1$, and $l = 0, 1, 2, \ldots, Y-1$, are the sampled points in the frequency coordinates.

In turn, the relationship of inverse discrete Fourier transform (IDFT) allows us to recover the image from the frequency. In practice, FFT algorithm is used to substitute the DFT for increasing the speed of calculation. FFT returns the DFT of pattern. In the same way, inverse fast Fourier transform (IFFT) algorithm is used to substitute the IDFT for increasing the speed of calculation. IFFT returns the IDFT of pattern.

DFT and IDFT are powerful computational tools for performing frequency analysis of image processing. The DFT transforms time- or space-based data into frequency-based data. DFT has been widely used in assessing and monitoring weaving density, detecting defect of non-woven fabric, acquisition parameters of fabric, and so on. When using the FFT to generate the color image, one can draw points, lines or geometrical shapes on a picture accurately. The pictures are called as basic pattern. Then a new geometrical pattern can be generated by discrete Fourier transform (DFT) or inverse DFT (IDFT). The patterns are called as color image, which are the result of design.

HSV model

The RGB coordinate system reproduces a color by combining the three primary colors, including red, green and blue as shown in figure 1. HSV model was developed in the 1970s for computer graphics applications, and is used for color pickers, in color-modification tools in image editing software. HSV stands for hue, saturation, and value, respectively. HSV model is the most common cylindrical-coordinate representations of points in an RGB color model, which rearrange the geometry of RGB in an attempt to be more intuitive and perceptually relevant than the cartesian (cube) representation [15–16].

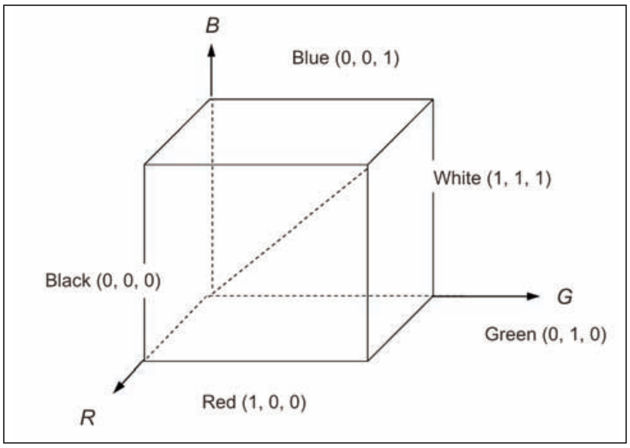

Fig. 1. RGB coordinate system

In HSV cylinder, the angle around the central vertical axis corresponds to “hue”, the distance from the axis corresponds to “saturation”, and the distance along the axis corresponds to value. Note that hue $H \in [0°, 360°]$, saturation $S \in [0.0, 1.0]$, and value $V \in [0.0, 1.0]$ [17]. Each unique RGB device has unique HSV spaces to accompany it, and numerical HSV values describe a different color for each basis RGB space. The color spaces are related to human’s concept of tint, shade and tone [18, 19]. The space in which hue, saturation and value are represented can be described with a cone as shown in figure 2.

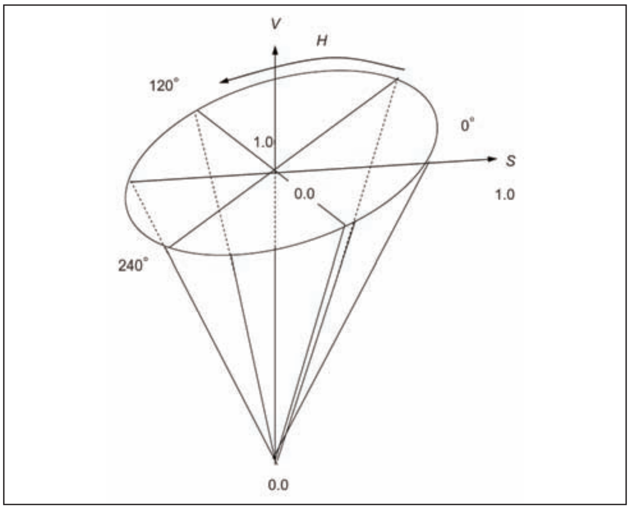

Fig. 2. HSV coordinate system

Converting to RGB

The transformation from HSV to RGB is a non-linear operation. Figure 3 gives a graphical representation of RGB coordinates transforming from HSV coordinates. According to the figure, the transformation from HSV to RGB color space is accomplished through the following steps.

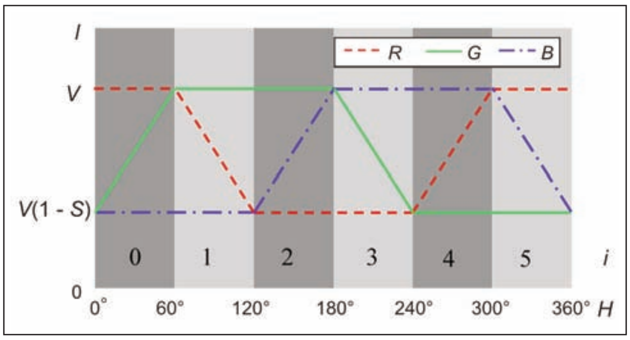

Fig. 3. Relationship of RGB and HSV coordinates

First, the H value in HSV model was divided into six segments and calculated the integral part i and factorial part f by:

$$i = \text{integral}\left(\frac{H}{60}\right) \tag{2}$$

$$f = \frac{H}{60} - \text{integral}\left(\frac{H}{60}\right) \tag{3}$$

In the equations (2) and (3), integral means to get the integral part from the result of algebraic division. Therefore, i is belong to a integer set {0, 1, 2, 3, 4, 5}, $f \in [0, 1)$. Next the intermediate value t, n, p were introduced:

$$t = 1 - S \tag{4}$$

$$n = 1 - S \cdot f \tag{5}$$

$$p = 1 - S \cdot (1 - f) \tag{6}$$

Then, R_1, G_1, and B_1 can be calculated by matching value:

$$(R_1, G_1, B_1) = \begin{cases} (1, p, t) & \text{if } i = 0; \\ (n, 1, t) & \text{if } i = 1; \\ (t, 1, p) & \text{if } i = 2; \\ (t, n, 1) & \text{if } i = 3; \\ (p, t, 1) & \text{if } i = 4; \\ (1, t, n) & \text{if } i = 5. \end{cases} \tag{7}$$

Finally, R, G, and B can be calculated by multiplying value by a given value:

$$(R, G, B) = (V \cdot R_1, V \cdot G_1, V \cdot B_1) \tag{8}$$

Auto-generation steps

To describe the auto-generation color image process for textile products, figure 4 gives main procedure flow chart of auto-generation system. The auto-generation process can be divided into the four steps: defining the image size, drawing basic pattern, giving color pattern and calculating color image. The designer will design from the first step to the third step. The fourth step is calculated by FFT. After these steps, the application software can be used for the color image.

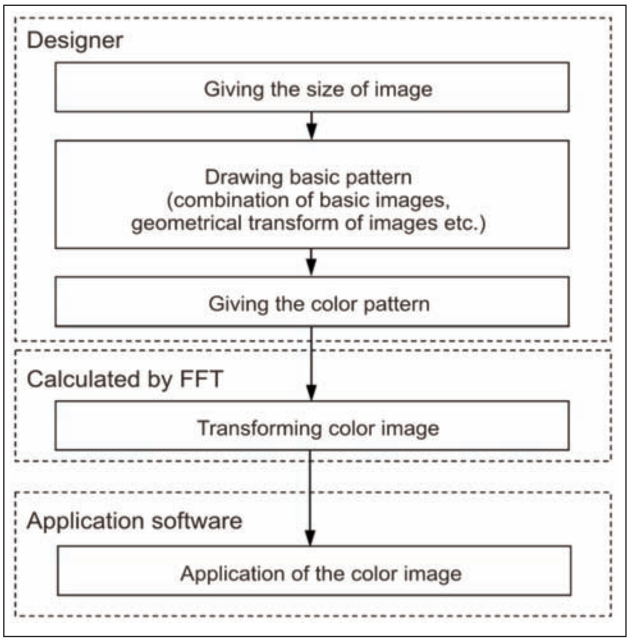

Fig. 4. Flow chart of auto-generation system

Giving the size of image

The image size for design, including width *ww* and height *hh*, was defined at first. In our examples of design, both *ww* and *hh* of the pattern were set simply to 256 pixels. All of the elements in the image construct a matrix. Then the data in all of the elements were set to zero and the matrix became a kind of zero matrixes. If the matrix element is 0, the pixel is black, if the matrix element is 1, the pixel is white. Therefore, all of pixels in the pattern were initialized as black dots and the image became a black image.

Drawing basic pattern

In order to construct a fully and balanced demonstrate the patterns; the center of the picture must be the drawing center according to the theory of FFT. Coordinates of center (*cw*, *ch*) can be determined and the coordinates were equal to (*ww*/2, *hh*/2). The designers paint a few simple points, lines signal in the first quadrant.

Giving the color pattern

First, the number of color is defined according to requirement of designer. Next, the data of HSV color pattern are designed to human's concept of tint, shade and tone. Then the HSV color pattern is converted to RGB color pattern. For an example, figure 5 shows a result of color pattern. There are eight kinds of color. A black rectangle was drawn around each color in the color pattern for distinguishing the color easily. The color pattern is designed by designer. The designer can select the number of color and each color in color pattern. The corresponding data for

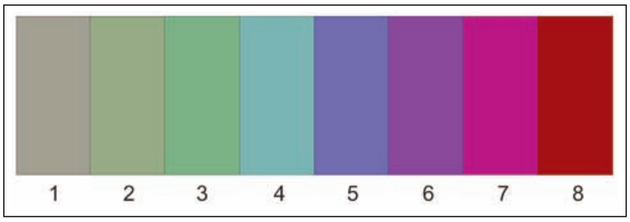

Fig. 5. Color pattern

Table 1

PHSV DATA OF COLOR PATTERN IN FIGURE 5			
No.	***H***	***S***	***V***
1	32	0.125	0.525
2	64	0.250	0.550
3	96	0.375	0.575
4	128	0.500	0.600
5	160	0.625	0.625
6	192	0.750	0.650
7	224	0.875	0.675
8	255	1.000	0.700

Table 2

RGB DATA OF COLOR PATTERN IN FIGURE 5			
No.	***R***	***G***	***B***
1	0.525	0.507	0.460
2	0.481	0.550	0.413
3	0.359	0.575	0.413
4	0.300	0.600	0.600
5	0.234	0.332	0.625
6	0.406	0.163	0.650
7	0.675	0.084	0.527
8	0.700	0.000	0.000

calculation can be acquired. The data of HSV color pattern in figure 5 are listed in table 1. The data of RGB color pattern, calculated by equations (7) and (8), from table 1, are listed in table 2.

Transforming color image by FFT

The software, designed for generating FFT images, recognizes the patterns as an image data, then converts the image data to a matrix and each matrix element represents an image pixel. By the algorithm of FFT, the point of the pattern is transformed into additive sinusoidal signal. The signal is transformed according to the position and gray of the point. The period cycle is decided by the position and the amplitude is decided by the gray of the point. After that the result was made from logarithmic transformation, and re-defined as a matrix. At this step, the type of data is double type. That means infinite number of grades for the data. Then each HSV is corresponding to a range of the result for reducing the number of grade of the result as shown in figure 6. The result of FFT has

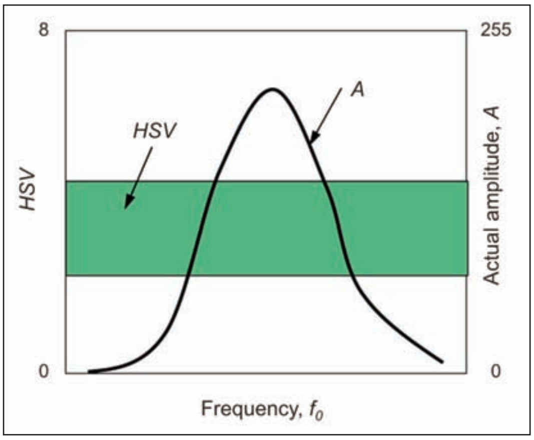

Fig. 6. Effective grayed amplitude width

256 gray grades. In fact, the designer wants to get lesser grades, e.g. eight kinds of grades. Since the gray grades can not satisfy the demand of designer, a cluster algorithm must be applied to generate an optimal threshold value of HSV color pattern. As results, eight kinds of colors are produced in the color pattern. These colors are corresponding to color pattern in figure 5. At last a restored pattern was produced as shown in figure 7.

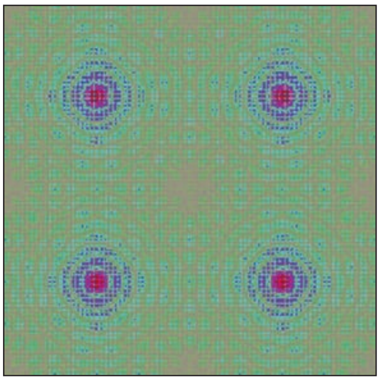

Fig. 7. Restored pattern

EXPERIMENTAL SETUP

The Matlab 2009 was used as the software tool to develop the system of auto-generation color image for textile products, and the CPU of the computer used in the experiment is P8600 3.00GHz and 2G DDRIII memory.

EXPERIMENTAL RESULTS OF BASIC IMAGE

Transform from circle

Figure 8 shows a circle and transformed result. The pattern can be produced as following. First, a zero matrix was defined. Both of the column (*ww*) and row (*hh*) of the pattern are set to 256 pixels. Because the coordinates of center (*cw*, *ch*) is equal to (*ww*/2, *hh*/2), *cw* can be calculated and is equal to 128, and *ch* can also be calculated and is equal to 128. Secondly, a circle was drawn in the center of the picture as shown in figure 8 *a*. Center of the circle overlapped the coordinates of center of the matrix. The

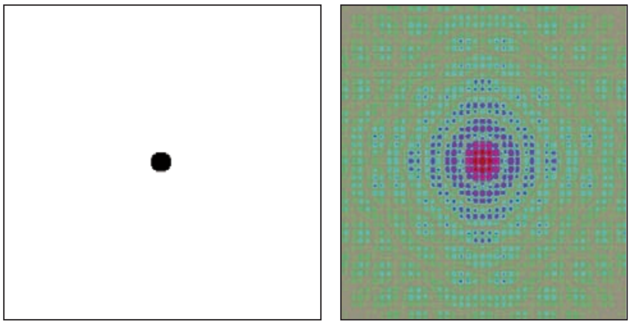

a *b*

Fig. 8. Circle and transformed result:
a – circle; ***b*** – transformed result

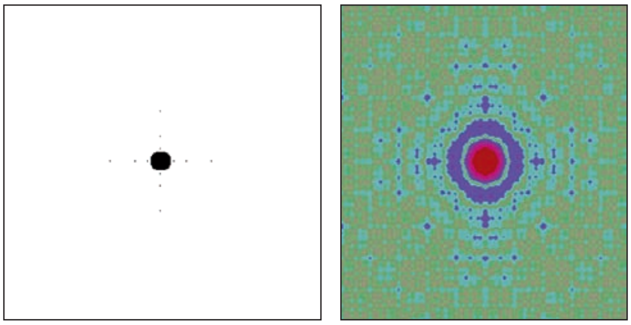

a *b*

Fig. 10. Combination of basic patterns:
a – combination of circle and points; ***b*** – mirror image of *a*

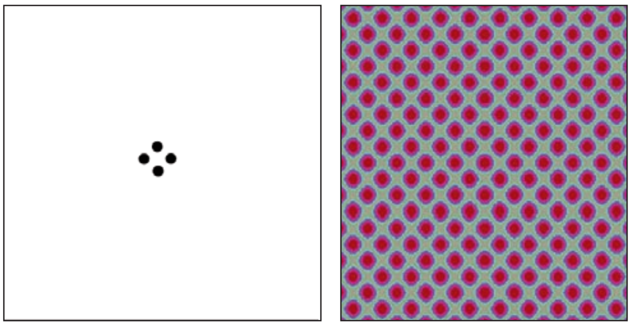

a *b*

Fig. 9. Geometrical patterns transformed from four points:
a – circle; ***b*** – basic pattern with *d* = 2 and mirror image of *a*

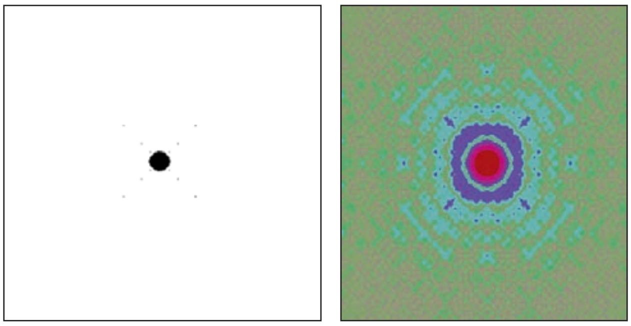

a *b*

Fig. 11. Geometrical transform of basic images:
a – geometrical transform of circle and points;
b – mirror image of *a*

radius *r* was set to be 10. That means if the distance between the center of matrix and the element was less than or equal to the radius 10, then the element of the matrix was set to be 1. Otherwise, if the distance between the center of matrix and the element was more than the radius 10, then the element was set to be 0. Third, a gray pattern was generated by FFT as shown in figure 8 *b*.

Transform from point

A basic patterns transformed from four points, based on FFT as shown in figure 9, was designed. The distance *d* between the point and the center of matrix was 10. In the figure 9, the sizes of the points were enlarged for viewing easily. According to the design size of pattern, *ww* and *hh* were set as 256 × 256 pixels, respectively. The color pattern as shown in figure 5 was selected. Figure 9 *b* was FFT results of figure 9 *a*.

DISCUSSIONS

Auto-generation for complex color image

Combination of basic images

The complex pattern can be produced by combination of basic images. A combination pattern of circle and points as shown in figure 10 *a* can be generated the mirror image as shown in figure 10 *b*. The radius of the circle *r* was 10. And there were four points in the basic pattern. The distances *d* between the point and the center of matrix were 10, 20 and 40. The color pattern as shown in figure 5 was selected. After FFT, a color image was generated as shown in figure 10 *b*.

Geometrical transform of images

The complex pattern can also be produced by geometrical transform of basic images. A geometrical transform of circle and points as shown in figure 11 *a* can be generated a color image as shown in figure 11 *b*. The parameters of figure 11 *a* and figure 10 *a* were the same. The radius of the circle was 10. The distances *d* between the point and the center of matrix were 10, 20 and 40. The pattern rotates 45 degrees anti-clockwise based on the basic pattern. After FFT, a color image was generated as shown in figure 11 *b*. From the figure 11, we can find that the result also rotates at a corresponding angle.

Features of auto-generation color images

Auto-generation color images for textile products based on FFT are different from the traditional design works that are made from computer graphics software such as Photoshop, CorelDraw, CAD and other design software. The auto-generation color images are new kinds of graphics which can not be replaced by other software. The auto-generation color images are based on rigorous science in a number of internal information according to certain rules and methods, transforming data involved or the mathematical model into visible graphics. The method demonstrated fully the complex structure of the digital science in

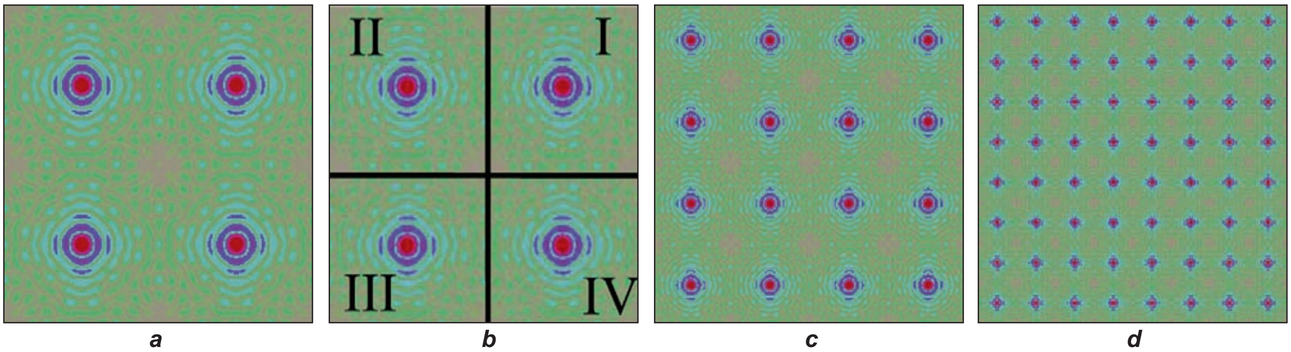

Fig. 12. Larger images constructed by basic images

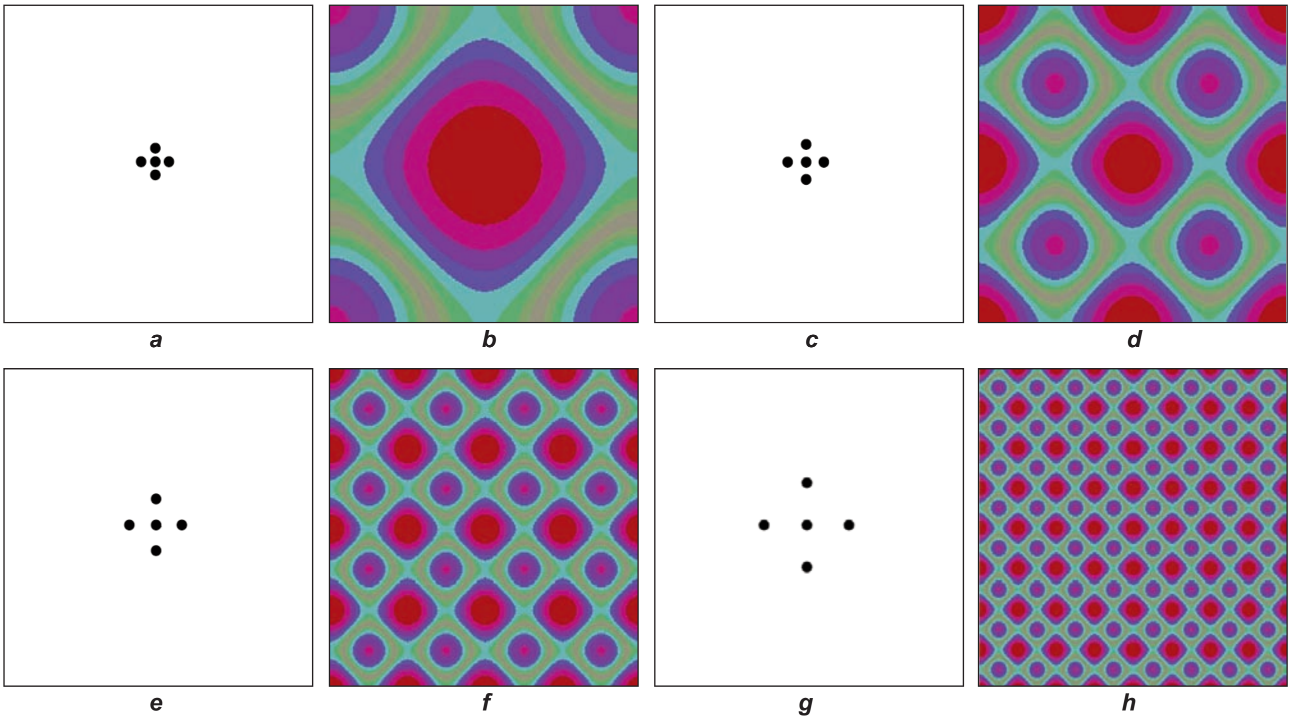

Fig. 13. Geometrical transform of basic images:
a, c, e, g – geometrical transform of points; ***b, d, f, h*** – mirror image of *a, c, e, g;*
a, b – distance 1; ***c, d*** – distance 2; ***e, f*** – distance 3; ***f***, ***h*** – distance 4

its own way. The method also digs out the deep beauty which the human can not see before and from the "invisible" world. The generated images of this research have the following characteristics.

Patterns associated with alliance quartet features

Alliance quartet features are based on units of patterns starting continuously around left and right (horizontal), up and down (vertical) and all other directions.

Design of the product for textile with alliance quartet features can be extended freely from the four sides of the pattern, and the symbols are continuous. The balance, harmony and rhythm of the formal beauty of the patterns can be reflected by using the methods of alliance quartet. Patterns associated with the quartet characteristic have a strong regularity. The four mirror images can construct in advanced larger images as shown in figure 12 *a*. The images in figures 12 *c* and *d* were minified 1/4 and 1/8, respectively for easy comparison. The main feature of the images was using unit image for composition through continuous order in effect. The image gave a regular and consistent feel. The images had the properties of balance and unity. The image can also be divided into four regions as shown in figures 12 *b*, *c* and *d*.

The change effects of the four consecutive images are extremely rich. They are common image art works for people on the clothing and textile.

The size of pattern element can be controlled

The size of pattern element is inversely proportional to the mid-point line of the original lattice. According to the needs of design, it is quite easy to adjust the pattern primitives. Through the scientific visualization methods, FFT automatically generated images. The images display the information of the nature which cannot be described with the traditional language in a more intuitive way. Compared with traditional patterns, FFT automatically generates pattern structure which is extremely complex, because it has unlimited fine graphic details. With sets of image layers, numerous and varied, both in small-scale and multi-perspective, they are more subtle than the structure of traditional human hand-drawn by the hard, and they look very attractive visually. Point, line, surface of right and wrong change, thickness contrast, the relationship among the density of the composition factors have great impact on the pattern-style. As long as one or more parameters were adjusted in the pattern, the different styles of the image will be generated.

Figures 13 *b, d, f* and *h* are color images of points in figure 13 *a, c, e, g*. The color images were transformed from source patterns by FFT. The variable is the number and position of points around the center of pattern. These points built a cross-shaped. There are 2 points in four directions including left, right, above or below the center of pattern as shown in figure 13 *a*, respectively. There are five points in figure 13 *c, e, g* in turn and the distance between points and the center is changed 1, 2, 4 and 8. These points also constructed a cross-shaped. Although there were significantly different structures and styles in four patterns, we can find the value of number of points increased in source patterns, and the size of grain of mirror images decreased accordingly.

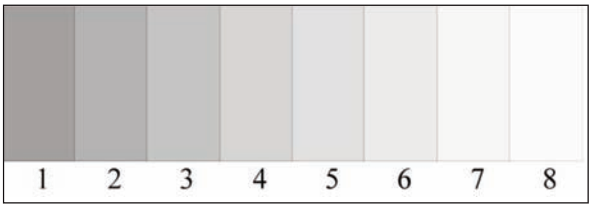

Fig. 14. Gray pattern

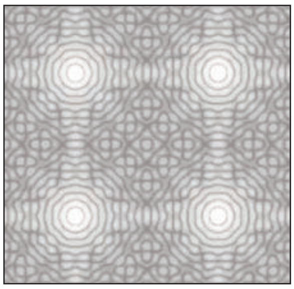

Fig. 15. Color image from gray pattern

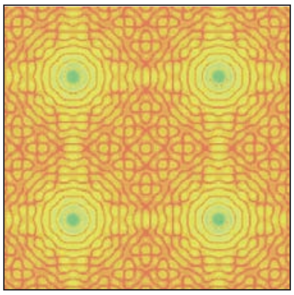

Fig. 16. Color image (*H* is parameter)

Pattern with color control

Generated patterns can be controlled freely using the HSV model. The patterns can be divided into gray and color image. The gray image can be generated by setting the *S* be zero and setting different value for *V* in the in the HSV model. For an example, figure 14 shows a result of gray pattern. There are eight kinds of gray. A black rectangle was drawn around each gray in the pattern for easy distinguishing of the gray. After that the result was made logarithmic transformation, and re-defined as a matrix. Then an effective HSV was applied for reducing the grade of the result as shown in figure 15. The color image can be generated by selecting different *H* and same value for *S* and *V* and in the in the HSV model. For an example, figure 16 shows a result of color image. There are eight *H* values in the image including 10, 19, 29, 38, 48, 57, 67 and 77, respectively. The *S* is set to 0.5 and the *V* is set to 0.8.

In figure 17, *S* is set to be 0.125, 0.250, 0.375, 0.500, 0.625, 0.750, 0.875 and 1, respectively. The *V* is 0.8. In figures 17 *a* to *d*, the *H* is changed, and they are 0.2, 0.4, 0.6 and 0.8, respectively.

Application of the pattern

The pattern in the specific culture conveys a special meaning. Meanwhile, there were solo properties

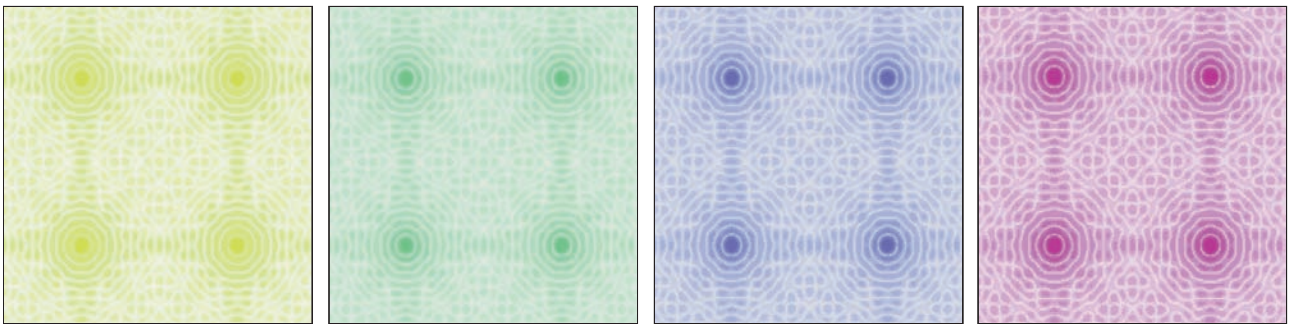

a *b* *c* *d*

Fig. 17. Color pattern for different *H* (*S* is parameter)

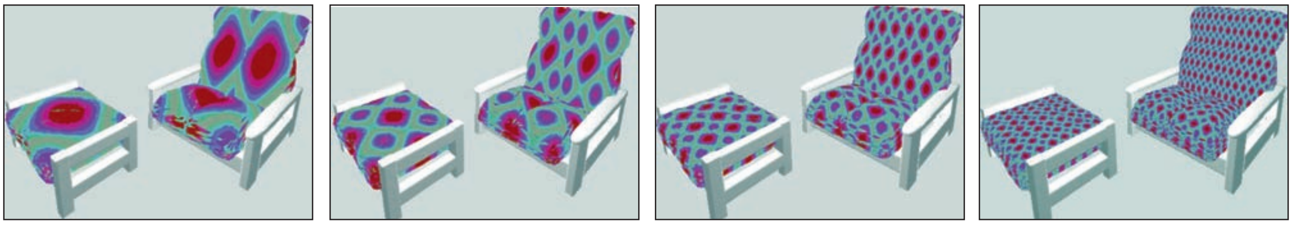

a *b* *c* *d*

Fig. 18. Virtual textile products of auto-generation monochrome image

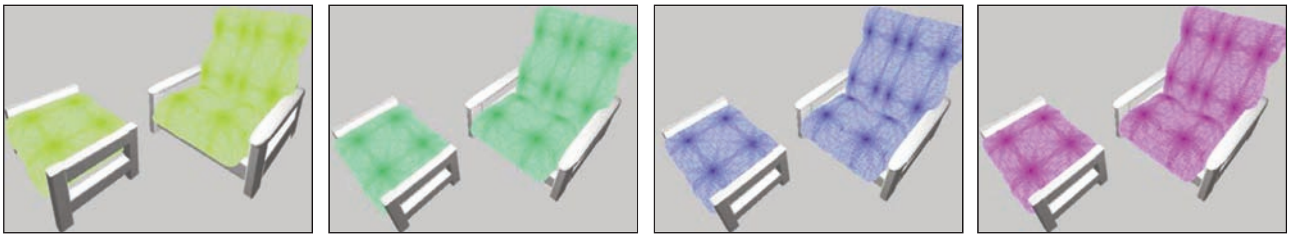

a *b* *c* *d*

Fig. 19. Virtual textile products of auto-generation monochrome image

when the auto-generation color images by FFT theory were applied in textiles. There were many kinds of ways to experience the color images in textile, such as printing by digital ink-jet printers, weaving by electronic jacquard machines, and so on. In the present work, we transfer the patterns of design to fabrics by virtual furniture software. After the patterns are designed, they are transferred to textiles products, thanks to the development virtual furniture software by Jiangnan University. Figures 18 *a* to *d*, show the samples of virtual furniture textiles with the patterns shown in figure 13 *b*, *d, f* and *h*, respectively. Figures 19 *a* to *d*, show the samples of virtual furniture textiles with the patterns shown in figures 17 *a* to *d*, respectively. From the figures, we can feel the preliminary effect of design. Although the images were new kinds of art forms, in terms of the visual level, there were no clear boundaries between the auto-generation color images by FFT and traditional geometric images. They can also be used in all kinds of textile as art work. The auto-generation color images by FFT reflect only different modern sense of beauty from traditional geometric images.

CONCLUSIONS

A program was developed to auto-generate abundant exquisite color images using the FFT theory in the research. Samples of images, using simplest patterns and their combinations, were designed. The auto-generation color process can be divided into the four steps: giving the image size, drawing basic pattern, giving the color pattern and transforming color image. HSV color model was adapted in the research. Three important parameters, including *H, S* and V, were considered in this research for image design. The results showed that the images have the properties of alliance quartet. The size and color of image element can be controlled according to requirement of designer. In the present research the images were transformed to textiles by virtual furniture software. The results also showed that the images can be used by textile designer directly. The application of the images for textile image design was also discussed for the elements for textile image design such as furniture textile. The results also showed that the images can also be used in all kinds of textile as art work. The auto-generation color images by FFT just reflect different modern sense of beauty from traditional geometric images.

ACKNOWLEDGEMENTS

The authors were grateful for the financial support by the Fundamental Research Funds for the Central Universities of Jiangnan University (JUSRP211A51), the open project progran of key laboratory of ECO-Textiles (Jiangnan University), ministry of education, China (NO. KLET 1113, NO. KLET 1114).

BIBLIOGRAPHY

[1] Nishikawa, S., Yoshizumi, M., Miyake, H. *Pattern making method and evaluation by dots of monochrome*. In: Seni Gakkaishi, 2008, vol. 64, issue 10, pp. 284-288

[2] Nishikawa, S., Yoshizumi, M., Miyake, H. *A pattern making method and evaluation by color dots*. In: Seni Gakkaishi, 2008, vol. 64, issue 12, pp. 345-351

[3] Bye, E. *A direction for clothing and textile design research*. In: Clothing and Textiles Research Journal, 2010, vol. 28, issue 3, pp. 205-217

[4] Jane, E. W, Lark, F. C. *Effects of training in apparel design and product development on spatial visualization skills*. In: Clothing and Textiles Research Journal, 2007, vol. 25, issue 1, pp. 42-57

[5] Mori, T., Endou, Y. *Evaluation of the visual texture and aesthetic appearance of lace patterns*. In: Journal of Textile Institute, 1999, vol. 90, issue 1, pp. 100-112

[6] Frantz, M., Crannell, A. *Three-point perspective and plane geometry*. In: Journal of Mathematics and the arts, 2007, vol. 1, issue 4, pp. 213-223

[7] Zaslavsky, G. M., Sagdeev, R. Z., Usikov, D. A., Chernikov, A. A. *Weak chaos and quasi-regular patterns*. Cambridge University Press, Cambridge, 1991

[8] Neves, J., Neves, M., Janssens, K. *Fractal geometry – A new tool for textile design development applications in printing*. In: International Journal of Clothing Science & Technology, 1994, vol. 6, issue 1, pp. 28-36

[9] Yang, X., Sui, J., Meng, B., Zhang, X. *Auto-generating uniform stochastic web images for ink-jet printing textiles*. In: Textile Research Journal, 2010, vol. 80, issue 18, pp. 1 942-1 948

[10] Adel, G., Faten, F., Radhia, A. *Assessing cotton fiber maturity and fineness by image analysis*. In: Journal of Engineered Fibers and Fabrics, 2011, vol. 6, issue 2, pp. 50-60

[11] Liu, J., Xie, Z., Gao, W., Jiang, H. *Automatic determination of slub yarn geometrical parameters based on an amended similarity-based clustering method*. In: Textile Research Journal, 2010, vol. 80, issue 11, pp. 1 075-1 082

[12] Gao, W., Liu, J., Pan, R., Wang, S. *Construction of pilling grade evaluation system based on image processing*. In: Industria Textilă, 2011, vol. 62, issue 4, pp. 192-197

[13] Zhang, X., Liu, J., Pan, R., Gao, W., Xu, B. *Design gabor filters in the frequency domain for unsupervised fabric defect detection*. In: Industria Textilă, 2011, vol. 62, issue 4, pp. 174-182

[14] Liu, J., Pan, R., Gao, W., Jiang, H. *A virtual woven fabric of plain using real float*. In: Applied Mechanics and Materials, 2011, vol. 43, pp. 760-763

[15] Chen, C., Wu, W. *Color pattern recognition with the multi-channel non-zero-order joint transform correlator based on the HSV color space*. In: Optics Communications, 2005, vol. 244, pp. 51-59

[16] Chan, T. F., Kang, S. H., Shen, J. *Total variation denoising and enhancement of color images based on the CB and HSV color models*. In: Journal of Visual Communication and Image Representation, 2001, vol. 12, pp. 422-435

[17] Lu, Y., Gao, W., Liu, J. *Color separation for colored fiber blends based on the Fuzzy c-means cluster*. In: Color research and application, DOI 10.1002/col.20662

[18] Russ, J. C. *The image processing handbook*, CRC Press, Boca Raton, FL, 1994

[19] Gonzales, R. C., Woods, R. E, Eddins, S. L. *Digital image processing using Matlab®*, Pearson Prentice-Hall, Upper Saddle River, NJ, 2004

Authors:

Chief of works dr. eng. HONGXIA JIANG
Conf. dr. eng. JIHONG LIU
Conf. dr. eng. RURU PAN
Conf. dr. eng. WEIDONG GAO
Conf. dr. eng. HONGFU WANG
Jiangnan University
1800 LiHu Road, Wuxi, 214122 China
e-mail: jianghongxiatex@hotmail.com; liujihongtex@hotmail.co

Improving cotton textile materials properties by treating with chitosan and metallic salts

ABRAMIUC DANKO
CRIȘAN POPESCU
SIMONA DUNCA
AUGUSTIN MUREȘAN

REZUMAT – ABSTRACT

Îmbunătățirea proprietăților materialelor textile din bumbac, prin tratarea cu chitosan și săruri metalice

Lucrarea analizează posibilitatea îmbunătăţirii caracteristicilor de rezistență a vopsirii materialelor textile din bumbac, imprimate cu coloranţi reactivi. În urma folosirii mai multor variante de tratare, s-a constatat că utilizarea chitosanului şi a sulfatului de cupru posedă un potenţial crescut de funcționalizare a materialelor și mărește absorbția colorantului reactiv în fibră, astfel că apele uzate rezultate sunt mai puțin colorate. Rezultatele finale au arătat că, datorită prezenţei ionilor de cupru şi chitosanului, odată cu îmbunătăţirea capacităţii de vopsire s-au obţinut şi efecte antibacteriene.

Cuvinte-cheie: bumbac, coloranţi reactivi, chitosan, sulfat de cupru, parametri cromatici, efect antimicrobian

Improving cotton textile materials properties by treating with chitosan and metallic salts

The paper investigates the possibility to enhance the dyeing characteristics of cotton fabrics dyed with reactive dyes. Several variants have been tried and the results indicate that the treatment with both chitosan and copper sulphate present the most potential for functionalizing the fabrics, enhancing the dye absorption into the fabric, thus resulting less coloured waste water. The final results suggests that together with the enhancement of the dyeing capacity it was also obtained antibacterial effect due to the presence of copper ions and chitosan.

Key-words: cotton, reactive dyes, chitosan, copper sulphate, chromatic parameters, antimicrobial effect

Cellulosic fibres are widely used for apparel industry and the most demanded class of dyes required for colouring them is those of reactive dyes. As a consequence numerous studies are concerned with the improvement of the dyeing performances achievable with this class of dyes. Reactive dyes are largely used because of their bright shades and high fastness to wet treatments. There are, however, many drawbacks which need addressed for improving further the dyeing process. Among them there are problems raised by the large amount of electrolytes required for dyeing, and sometime by the low yield of the reaction of dye with the fibre, which leads to the loss of unfixed dye from the fabric in effluents and produces a waste of resources [1–7].

Micro-organisms are often found on natural polymer fibres like cellulose because due to their natural retention of water, oxygen and other nutrient sources (salts, amino acids, carboxylic acids from sweat, skin fat and dead cells) that provide the medium for cells growing. The consequences of contamination of textile materials with microorganisms are: the bad odour (from essential metabolic processes of bacteria), the colour fading, the mould spots and the loss of functional proprieties. The degradation action of fungi and bacteria for cellulosic fabrics is a major inconvenient for using these fibres in products like: camping articles, canvas, filters, textiles for fishing industry, furniture fabrics, textiles for decoration etc.

Chitosan has been found as a promising natural alternative to overcome the problems of micro-organism growing. It is not yet well documented how chitosan attacks the bacteria cell, but there are presumptions that positive charged primary amino groups interact with negative charged residues found on the surface of the bacteria cell. This interaction changes the surface of the organism cell by blocking air permeability and leads in cell death. The antimicrobial effects together with the non-toxicity, biodegradation, and biocompatibility grant chitosan to be used in different fields like agriculture, medicine, pharmacy, and textile industry.

The use of chitosan has been studied for improving both the dyeing capacity and the antimicrobial activity against microorganism and fungi found on textile materials. Some heavy metal salts are also known for having antimicrobial properties against a large spectrum of gram positive and gram negative bacteria, as well as against some fungi (mould and yeast) [8–12].

The aim of this paper is to look after a treatment combining chitosan and heavy metal salts for improving the dyeing capacity, increasing the crease recovery and providing antimicrobial properties to cellulosic based textile materials.

EXPERIMENTAL PART

Treatment variants

Clean and bleached samples of cotton fabrics were treated with solutions of $CuSO_4$ and chitosan, respectively, then dyed using reactive dye C.I. Reactive Violet 5R (1), in different variants.

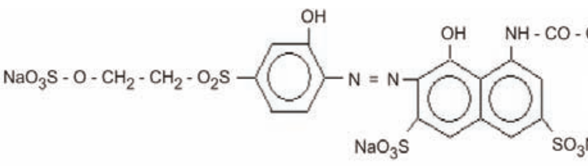

(1)

Variant 1. Samples were dyed with C.I. Reactive Violet 5R dye in the following conditions: 2.5% dye, 5 g/L Na_2CO_3, 50 g/L Na_2SO_4, 1 mL/L NaOH of 38°Be, *LR* = 30:1 for 60 minutes at 70°C. After dyeing, samples were washed in cold water and dried at 60°C. One set of dyed fabrics were impregnated with $CuSO_4$ solution of 10, 20, 30, 40 g/L, respectively, padded with a squeeze out degree of 100%, rolled and stored covered in a protective foil for 24 hours at room temperature. After storage the samples were dried for 20 minutes at 60°C.

Variant 2. Another sample set dyed according to variant *1* was impregnated with chitosan solution of 6, 8 and, respectively, 10 g/L padded with squeeze out degree of 100%, dried, and thermally treated at 150°C for 4 minutes.

Variant 3. Samples were impregnated with $CuSO_4$ solution of 10, 20, 30 and, respectively, 40 g/L padded with squeeze out degree of 100%, dried for 20 minutes at 60°C, thoroughly washed in distilled water and then dyed under the following conditions: impregnation in solution containing 8 g/L dye, 50 g/L urea and 20 g/L Na_2CO_3, padded with squeeze out degree of 100%, impregnation in 10 g/L chitosan solution, dried and thermal treatment at 150°C for 4 minutes. All samples treated according to any of the 3 variants were washed for 20 minutes at 90°C in 0.5 g/L Cotoblanc NSR solution, rinsed in warm, then in cold water.

Measurements

For treated and untreated samples the following properties were measured: chromatic parameters, dyeing intensity *K/S*, colour difference Δ*E CIELAB*, dyeing fastness to washing and rubbing, material handle, crease recovery angle and the antimicrobial effect.

Colour intensity *K/S* and colour difference Δ*E* were calculated by using Micromatch 2000® software after measuring chromatic parameters with the Spectroflash 300 Datacolor device [13]. Dyeing fastness to washing, rubbing and perspiration were determined according to standards [14, 15].

The treatment modifies the handle, therefore we measured the stiffness of the treated and untreated samples. The method consists in measuring the free bending length (cm) of the fabric under its own weight, in an 45° angle [16].

A SEM Quanta 200 3D Dual Beam electron microscope equipped with an EDAX analysis system Edax-Ametek Holland was used to analyse the surface of the treated materials. Characterization was performed in Low Vacuum mode, electron acceleration 10 kV, Secondary electrons imaging (SE) mode.

Evaluation of antibacterial activity for the treated samples was tested in vitro, using Kirby-Bauer method [17, 18].

RESULTS AND DISCUSSIONS

The results on the chromatic parameters are shown in the figures 1 – 3. The results show that the colour

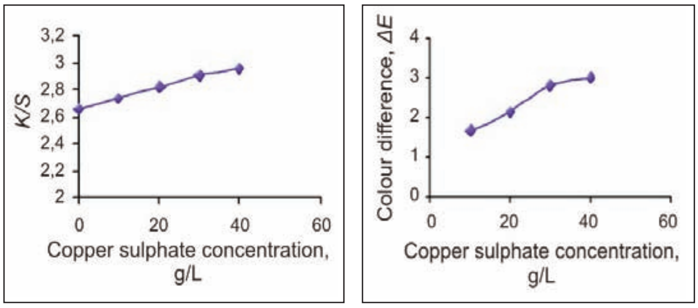

a ***b***

Fig. 1. Influence of copper sulphate concentration on:
a – colour strength, *K/S*; ***b*** – colour difference, Δ*E*

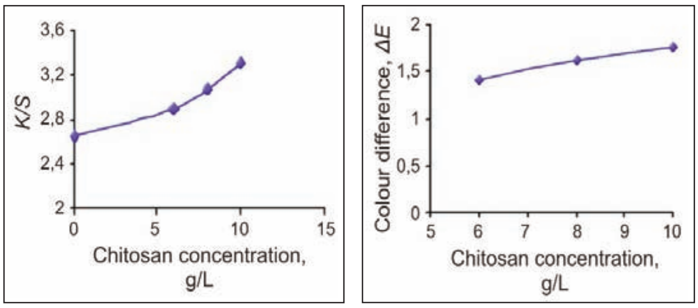

a ***b***

Fig. 2. Influence of chitosan concentration on:
a – colour strength, *K/S*; ***b*** – colour difference, Δ*E*

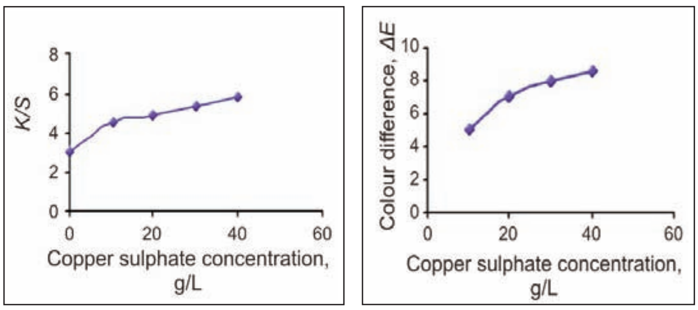

a ***b***

Fig. 3. Influence of copper sulphate and chitosan (10 g/L) concentrations on:
a – colour strength, *K/S*; ***b*** – colour difference, Δ*E*

intensity increases for the samples treated with copper sulphate and chitosan. Significant changes in colour intensity between the treated and untreated samples can be seen for the treatment variant *3.*

The results measured for dyeing fastness to washing and rubbing are shown in the tables 1 – 3 below. One may notice from these results that the fastness to washing and the fastness to dry rubbing keep the same value at treated and at the reference (only dyed fabric) samples. Fastness to wet rubbing decreases when cotton is treated with $CuSO_4$ and chitosan. Best results to perspiration fastness were obtained for treatment variant *3* followed by variant *1* and then variant *2*. For all fastness the lowest values has been obtained for the treatment variant *3.* A possible explanation of this could be the formation of a dye – $CuSO_4$ – chitosan complex on the fibre surface.

Fabric handle

The results of measuring the fabric handle are presented in figure 4. Figure 4 *c* indicates that the highest stiffness is reached for the treatment variant *3* – maximum chitosan and copper sulphate concentration.

SEM characterization of the prepared samples as presented is shown in figure 5. On samples surface a number of deposits is observed smaller and less for reference sample which is only dyed where to find dye. These deposits become enlarged for samples it prepared for variants *1 – 3* where beside dye there are copper sulphate and chitosan.

The EDAX analysis of cotton fabrics was performed. Due to the fact that high energy electron beam damage fast the fibres, this analysis has only qualitative value in our case. The supplementary results confirm the presence of the treated samples of elements such as copper, and increased nitrogen content which derives from dye and chitosan (table 4).

Evaluating the antibacterial activity for the treated samples the experiments proved that the samples treated with $CuSO_4$ and chitosan have an antimicrobial effect on a large spectrum of microorganisms (gram positive and gram negative), also confirmed by literature. The antibacterial results are shown in figure 6 and table 5.

Table 1

THE VALUES RECORDED FOR FASTNESS TO WASHING, RUBBING AND PERSPIRATION (Variant *1*)

$CuSO_4$ concentration, g/L	Fastness to washing	Fastness to rubbing		Perspiration	
		Wet	***Dry***	***Acid***	***Alkaline***
10	5/5/5	5	4-5	4/5/4-5	4-5/5/4-5
20	5/5/5	5	4-5		
30	5/5/5	5	4-5		
40	5/5/5	5	4-5		
0	5/5/5	5	5		

Table 2

THE VALUES RECORDED FOR FASTNESS TO WASHING, RUBBING AND PERSPIRATION (Variant *2*)

$CuSO_4$ concentration, g/L	Fastness to washing	Fastness to rubbing		Perspiration	
		Wet	***Dry***	***Acid***	***Alkaline***
6	5/5/5	5	4-5	3-4/5/4-5	3-4/5/4
8	5/5/5	5	4-5		
10	5/5/5	5	4-5		

Table 3

THE VALUES RECORDED FOR FASTNESS TO WASHING, RUBBING AND PERSPIRATION (Variant *3*)

$CuSO_4$ concentration, g/L	Chitosan concentration, g/L	Fastness to washing	Fastness to rubbing		Perspiration	
			Wet	***Dry***	***Acid***	***Alkaline***
10	10	5/5/5	5	4	4-5/5/5	4/5/5
20		5/5/5	5	4		
30		5/5/5	5	4		
40		5/5/5	5	4		

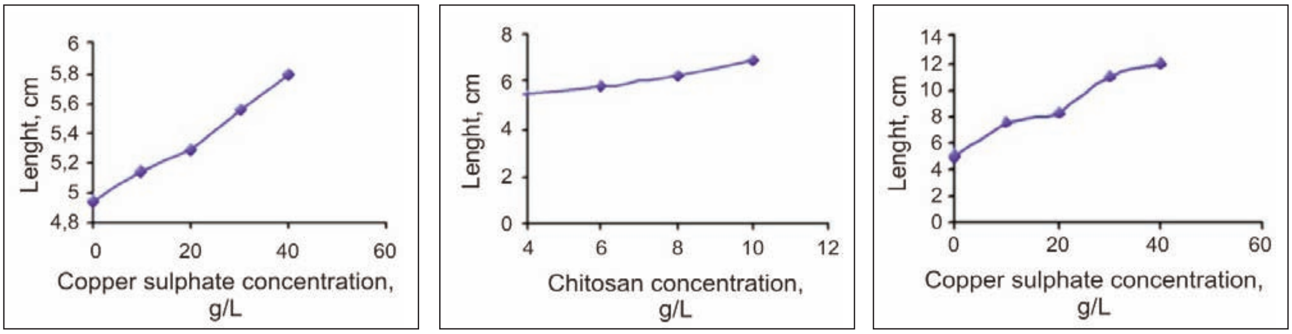

a *b* *c*

Fig. 4. Influence of copper sulphate and chitosan on fabric stiffness:
a – variant *1*; ***b*** – variant *2*; ***c*** – variant *3*

Table 4

MEDAX COMPONENT ANALYSIS							
References		**Variant *1***		**Variant *2***		**Variant *3***	
Element	***Wt,*** %	***Element***	***Wt,*** %	***Element***	***Wt,*** %	***Element***	***Wt,*** %
CK	45.42	CK	35,75	CK	28.23	CK	29.09
NK	02.16	NK	02.17	NK	09.27	NK	09.03
OK	51.61	OK	60.15	OK	61.70	OK	60.26
SK	00.81	SK	01.14	SK	00.80	SK	00.69
-	-	CuK	00.79	-	-	CuK	00.93

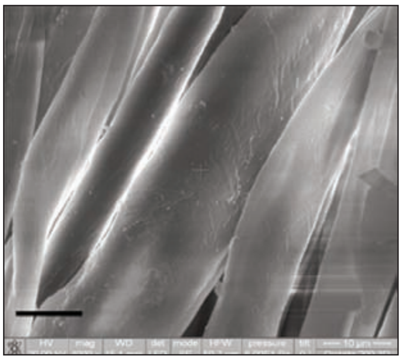
a
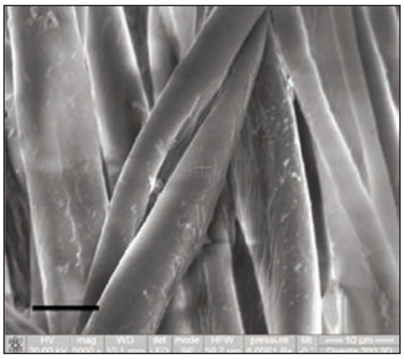
b
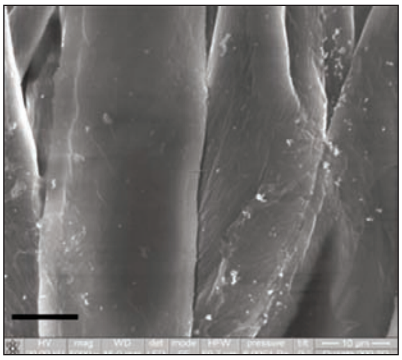
c
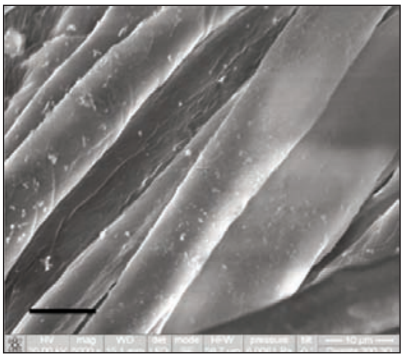
d

Fig. 5. SEM images of cotton fabrics samples:
a – reference; ***b*** – variant *1*; ***c*** – variant *2*; ***d*** – variant 3; scale bar – 10 μm

The results given in table 5 show that the treatments lead to a good inhibition of bacteria growth measured for Escherichia coli followed by Staphylococcus aureus and Pseudomonas aeruginosa.

Antimicrobial activity improves with the increasing concentration of copper sulphate.

For the reference sample no inhibition of bacteria growth was noticed.

Table 5

ANTIMICROBIAL ACTIVITY OF CHITOSAN AND $CuSO_4$ TREATMENT				
$CuSO_4$, g/L	**Chitosan,** g/L	**Microorganism test**		
		Staphylococcus aureus	***Escherichia coli***	***Pseudomonas aeruginosa***
10	10	+	+	+
20	10	+	+	+
30	10	++	++	+
40	10	++	++	+
Reference	-	-	-	-

Note: **+** is weak inhibition of bacteria growth; **++** is good inhibition of bacteria growth;
- is no inhibition of bacteria growth

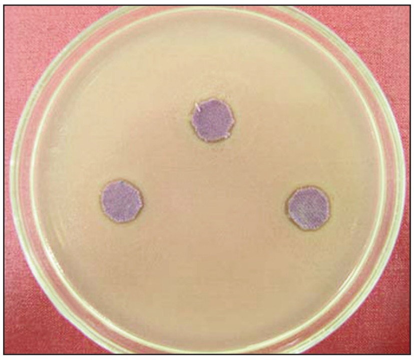

a

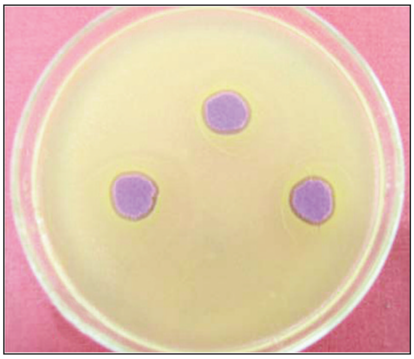

b

Fig. 6. Highlighting diameters of inhibition zones for antibacterial testing of samples treated with $CuSO_4$ and chitosan:
a – 30 g/L $CuSO_4$; ***b*** – 40 g/L $CuSO_4$

CONCLUSIONS

The use of chitosan and copper sulphate for treating cotton materials dyed with reactive dye adds a significant improvement for the functionality of the cotton fabrics.
The antibacterial effects have been enhanced as the experiments show. The dye intensity improves when the fabric is treated with both $CuSO_4$ and chitosan therefore increasing the efficiency of the dyeing process.

ACKNOWLEDGEMENT

This paper was realised with the financial support of the project POSDRU CUANTUMDOC “Doctoral studies for European performances in research and innovation” ID79407, project financed by the European Social Fund and the Romania Government.

BIBLIOGRAPHY

[1] Lei, X. P., Lewis, D. M. *The dyeing behaviour of cotton modified with Chloropropionyl Chloride and related compounds.* In: Dyes and Pigments, 1991, vol. 16, p. 273

[2] Wu, T. S., Chen, K. M. *New cationic agents for improving the dyeability of cellulose fibres.* Part 1 – *Pretreating cotton with Polyepichlorohydrin-amine polymers for improving dyeability with direct dyes.* In: J.S.D.C., 1992, vol. 108, p. 388

[3] Kamel, M. *The addition of reactive compounds to nonreactive dyebaths*. Part 5 – *Procedure for obtaining reactive dyeings on cotton*. In: J.S.D.C., 1992, vol. 108, p. 450

[4] Wu, T. S., Chen, K. M. *New cationic agents for improving the dyeability of cellulose fibres.* Part 2 – *Pretreating cotton with Polyepichlorhydrin-amino polymers for improving dyeability with reactive dyes.* In: J.S.D.C., 1993, vol. 109, p. 153

[5] Atav, R., Yurdakul, A., Akçakoca, E. *Effect of hardness arises from salts used by dye houses on color yield in reactive dyeing.* In: Industria Textilă, 2011, vol. 62, issue 3, p. 115

[6] Lewis, D. M., Gillingham, E. L. *Fixation of Aspartyl-Triazine dyes*. In: Textile Chemists and Colorists, 1996, vol. 28, p. 76

[7] Mureșan, R. *Coloranți și auxiliari utilizați în industria textilă.* Editura CERMI, 1998

[8] Chun, D. T. W., Gamble, G. R. *Using the reactive dye method to covalently attach antibacterial compounds to cotton*. In: The Journal of Cotton Science, 2007, vol. 11, p. 154

[9] Hui, Z., Zhu, L. *Treatment of cotton fabric with SnO_2 nanoparticle and chitosan*. In: Industria Textilă, 2012, vol. 63, issue 5, p. 260

[10] Bhuvana, G., Raghunathan, S. *Studies on frictional. Behaviour of chitosan – coated fabrics*. In: AUTEX Research Journal, 2006, vol. 6, issue 4, p. 216

[11] Grace, M., Chand, M. N., Bajpai, S. K. *Copper alginate-cotton cellulose (CACC) fibers with excellent antibacterial properties*. In: Journal of Engineered Fibers and Fabric, 2009, vol. 4, issue 3, p. 24

[12] Anita, S., Ramachandran, T., Rajendran, R., Mahalakshmi, M. *A study of the antimicrobial property of encapsulated copper oxide nanoparticles on cotton fabric.* In: Textile Research Journal, 2011, vol. 81, issue 10, p. 1 081

[13] Puşcaş, E. L., Radu, D. C. *Introducere în cunoaşterea şi măsurarea culorii*. Editura Dosoftei, Iaşi, 1997

[14] * * * SR ISO 105 – A02:1995

[15] * * * SR EN 22313/1997

[16] Bucur, M. *Metode obiective de apreciere a tuşeului*. In: Industria Textilă, 2001, vol. 32, issue 1, p. 39

[17] Lau, L., Fan, J., Siu, T. *Garments with Wrinkle-free treatment*. In: Textile Research Journal, 2002, vol. 72, p. 931

[18] Mukhopadhyay, A., Kothari, V. K. *Crease recovery of fabrics with air-jet textured weft yarns*. In: Indian Journal of Fibre & Textile Research, 2002, vol. 27, issue 4, p. 393

Authors:

Crd. ing. ABRAMIUC DANKO
Prof. dr. ing. AUGUSTIN MUREȘAN
Universitatea Tehnică Gheorghe Asachi
Facultatea de Textile-Pielărie şi Management Industrial
Bd. D. Mangeron nr. 53, 700050 Iaşi
e-mail: dabramiuc@tex.tuiasi.ro

Prof. dr. ing. CRIȘAN POPESCU
DWI at RWTH Aachen University, Germany
e-mail: popescu@dwi.rwth-aachen.de

Conf. dr. SIMONA DUNCA
Universitatea "Alexandru Ioan Cuza"
Bd. Carol nr. I20 A, 700506 Iași
e-mail: sdunca@uaic.ro

Corresponding author:

AUGUSTIN MUREŞAN
e-mail: amuresan@tex.tuiasi.ro

The relationship between model types and related parameters

OKSAN ORAL
M. CETIN ERDOGAN
ESRA DIRGAR

REZUMAT – ABSTRACT

Relația dintre tipurile de modele și parametrii conecși

În articol este analizată influența diferitelor caracteristici ale modelelor articolelor de îmbrăcăminte asupra tăierii și coaserii. În urma studiilor efectuate, a fost elaborată o metodă de determinare a timpilor de tăiere și de coasere pentru categoriile de produse folosite ca eșantioane, respectiv fustă și sacou bărbătesc. Au fost studiate opt modele diferite de fuste și 7 modele diferite de sacouri bărbătești. Folosind relația Pearson, s-a calculat numărul total de piese, perimetrul pieselor, timpul de tăiere și timpul de coasere. Pentru a stabili care sunt efectele altor factori asupra acestor procese, s-a efectuat o analiză de regresie. În urma analizării tuturor factorilor și gradelor de afectare, s-a constatat că anumite caracteristici ale unui model pot influența productivitatea și timpul în producția de confecții. Lucrarea evidențiază importanța caracteristicilor diferitelor modele de articole de îmbrăcăminte pentru scurtarea timpilor de tăiere și de coasere.

Cuvinte-cheie: model, caracteristici, timp de tăiere, timp de coasere, perimetrul pieselor

The relationship between model types and related parameters

In the study, the effects of different model characteristics of garments on cutting and sewing times have been investigated. Following the experiment, a method for determining cutting and sewing times for sample product groups has been created. Product groups subject to the study are skirt and men's coat. In the study, 8 different models to the chosen skirt group and 7 different models to the men's coat group were applied. Total number of pieces, perimeter of pieces, cutting time, and sewing time were investigated. Pearson correlation was used in the study. Regression analysis was conducted to investigate the effects of other happenings on the observed process. Following the investigations of all factors and their degrees of effect, it was observed that a characteristic of a model is one of the important factors that affect the productivity and time in apparel company. The paper provides that different model characteristics of garments is very important for cutting and sewing times.

Key-words: model, characteristics, cutting time, sewing time, perimeter of pieces

One of the most important key factors of increasing compatibility in textiles is being able to reduce the costs towards the global averages. The compatibility of apparel manufacturers depends on product standardization, technology, how advanced they are and whether they have the mental work-power to deal with the technology. The technology development is not limited only with automation of the machinery on the production line but also includes processes before and after the production [1, 2].

In companies, technology improvements are towards increasing productivity and reducing costs [3]. Production is vitally important for the companies. Improvement of productivity is not only increasing profit but also the improvement in the way of production. Material and work-power are the basic subjects of the efforts on improving productivity. The benefits depending on the structures of the products models, will affect directly the productivity of the company [4].

In companies, cost determination is the primary issue, on which most attention and care is paid. Since all savings without sacrificing from the quality affect the costs in a positive manner, savings from the materials and production time should be the primary target. One of the main factors that affect the cost of a product is the characteristics of the model [5]. It should be taken into consideration that model's being in fewer numbers of pieces will affect the amount of fabric to be used; its cutting and sewing times.

It is obvious that customer demands directed the manufacturer to work with different models. Various models can be formed for garment types. Forming a model on a garment may be defined as cutting the garment into desired pieces, changing the form of the garment by dividing it into pieces. When forming a model, it is important to consider all phases of the production line and doing it economically with existing resources [6, 7].

In the study, the effects of different model characteristics of garments on cutting and sewing times have been investigated. Following the experiment, a method for determining cutting and sewing times for sample product groups has been created.

In apparel companies, after the model is formed, this method will be useful in estimating cutting and sewing times, calculating the productivity, production planning and estimating delivery date.

METHODOLOGY USED

The material of the study consisted of clothing product groups made of woven fabric and garment models, CAD (computer aided design) machine used in model pattern department and CAM (computer aided manufacturing) cutting machine used in cutting department.

Product groups subject to the study are skirts and men's coats. In forming the models to be applied to each product group, some criteria were taken into consideration. In order to be able to compare different modeling within each group, various dividing were made and the criteria for models were determined. These are classic, horizontally cut, vertically cut and both vertically and horizontally cut types of models. In cutting of models some drawing bases were benefited from. Since investigation of the relationship of the number of pieces with cutting and sewing time was one of the aims of the study, preparing models with higher number of pieces was a priority [8].

In this study, evaluation research method includes an analytic evaluation suitable for the aim of the study, conduction of the study, experiments and data analyses.

Analysis of production process and production flow

The production line comprising:

Step 1 – preparations of the patterns of the chosen models using Muller pattern system according to CAD system;

Step 2 – grading of patterns according to determined sizes;

Step 3 – preparation of marker plans for models;

Step 4 – cutting of marker plans using CAM;

Step 5 – determination of sewing times for the models using the method MTM – pre-accepted properties of the study.

Fabric used

The woven fabric used in the study is single colored, has no nap and available for placing the patterns in both directions. The 148 cm wide fabric (the most common one in the market) was used and all pattern placements were practiced on 148 cm width.

Sizes

Since there is no size table adapted to Turkish men and women sizes and since the nationality of the size table was not effective on the aims of the study, normal German size table for men and women were used in preparing the patterns.

Assortment of sizes

Before the patterns were prepared, sizes to be used in the experiment and their numbers together with their assortment numbers have to be determined. In this study, sizes and the assortments used for the women group are shown below:

$$\frac{36}{1} \qquad \frac{38}{1} \qquad \frac{40}{1} \qquad \frac{42}{1}$$

The following sizes and assortments are for the men group:

$$\frac{46}{1} \qquad \frac{48}{1} \qquad \frac{50}{1} \qquad \frac{52}{1}$$

Determination of number of samplings

In the study, 8 different models to the chosen skirt group and 7 different models to the men's coat group were applied. Skirt group is given in figure 1 and men's coat group is given in figure 2.

THE EXPERIMENTAL PATTERN OF THE STUDY

In the study the following parameters were investigated:

Total number of pieces – total numbers of pieces on the cutting plan belonging to sizes were taken into account;

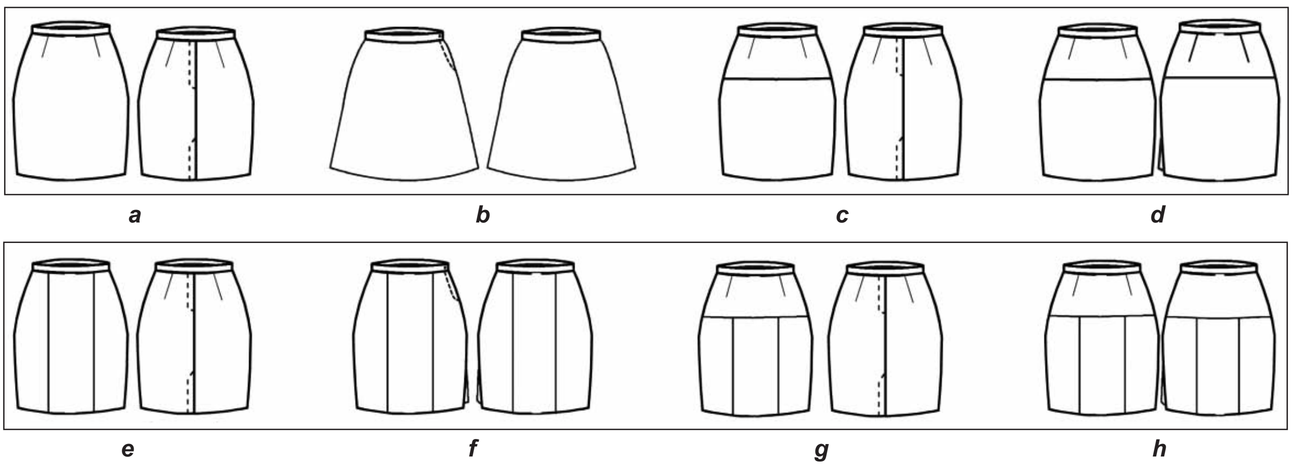

Fig. 1. Skirt groups:
a – clasic; ***b*** – flared; ***c*** – horizontally cut, model *1*; ***d*** – horizontally cut, model *2*; ***e*** – vertically cut, model *1*; ***f*** – vertically cut, model *2*; ***g*** – both vertically and horizontally cut, model *1*; ***h*** – both vertically and horizontally cut, model *2*

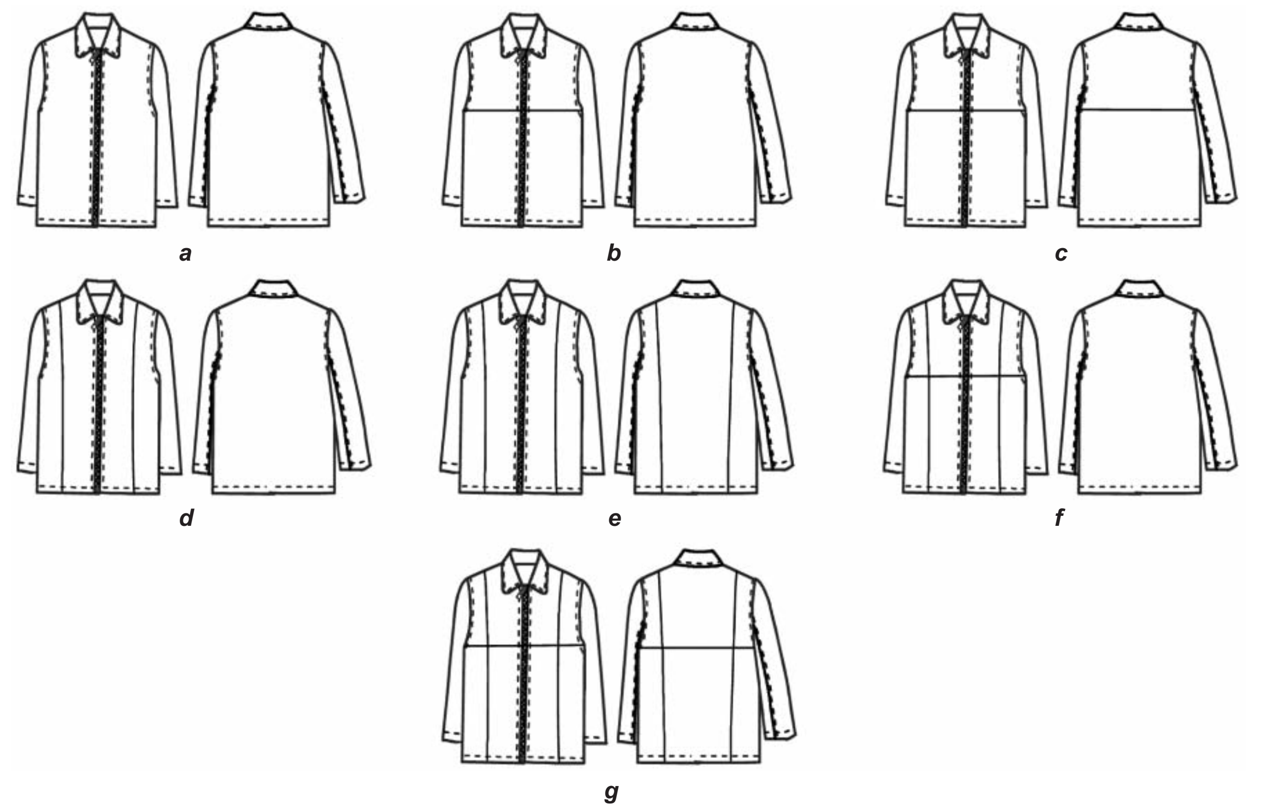

Fig. 2. Men's coat groups:
a **–** classic; ***b*** **–** horizontally cut, model *1*; ***c*** **–** horizontally cut, model *2*; ***d*** **–** vertically cut, model *1*;
e **–** vertically cut, model *2*; **f –** both vertically and horizontally cut, model *1*;
g **–** both vertically and horizontally cut, model *2*

Perimeter of the pieces – total length of the perimeters of the sizes on the cutting plan was taken in meters;
Cutting time – the duration of the CAM operated cutting process of a single layer of the cutting plan was taken in minutes;
Sewing time – taking the production diagrams of the models into consideration, operation unit times were taken in minutes according to MTM (method's time measurement).
The results of the trials were evaluated using SPSS (statistical packet software). Pearson correlation was used in the study. If p the significance value is smaller than 0.05 (probability) the linear relation (positive correlation) ($p < 0.05$) between variables is significant. And if $p > 0.05$, there is no positive correlation, therefore, insignificant.
Regression analysis was conducted to investigate the effects of other happenings on the observed process [8].

FINDINGS

Finding for number of pieces and the perimeter of the pieces

Correlation analyses of the results of trials conducted as 7 trials for men's coat models and 8 for skirt models were investigated using the software SPSS. Values obtained as a result of correlation are given in table 1.

Table 1

CORRELATION FOR THE TOTAL NUMBER OF PIECES AND THE PERIMETER OF PIECES ON THE MARKER BOTH FOR THE SKIRT GROUP AND MEN'S COAT GROUP

Factors	*r*	*p*	*n*
Skirt – total number of pieces – perimeter of pieces	0.972	0	8
Men's coat – total number of pieces – perimeter of pieces	0.914	0.004	7

When the results in table 1 is examined:
- In the relation of the perimeter of the pieces and number of pieces in the skirt group, $p = 0$, therefore, the linear relationship between these variables is statistically significant;
- In the relation of the perimeter of the pieces and number of pieces in the men's coat group, $p = 0.004$, therefore, the linear relationship between these variables is statistically significant.

Findings regarding number of pieces, cutting time and sewing time

Skirt models

Correlation analyses of the results of trials conducted as 8 trials for skirt models were investigated using the software SPSS. Values obtained as a result of correlation are given in table 2.

Table 2

THE CORRELATION OF NUMBER OF PIECES, CUTTING TIME AND SEWING TIME IN SKIRT GROUPS			
Factors	***r***	***p***	***n***
Number of pieces – cutting time	0.549	0.159	8
Number of pieces – sewing time	0.968	0	8

When the results in table 2 are examined:

- since the relationship between number of pieces and cutting time is p = 0.159, the linear relationship between these variables is statistically insignificant;
- since the relationship between the number of pieces and sewing time is p = 0, the linear relationship between these variables is statistically significant.

Figure 3 shows the changing in the sewing time depending on the number of pieces.

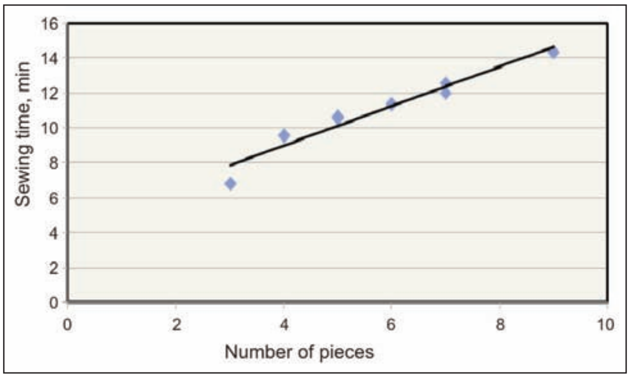

Fig. 3. Changes in the sewing time depending on the number of pieces in skirt models

Men's coat models

Correlation analyses of the results of trials conducted as 7 trials for men's coat models were investigated using the software SPSS. Values obtained as a result of correlation are given in table 3.

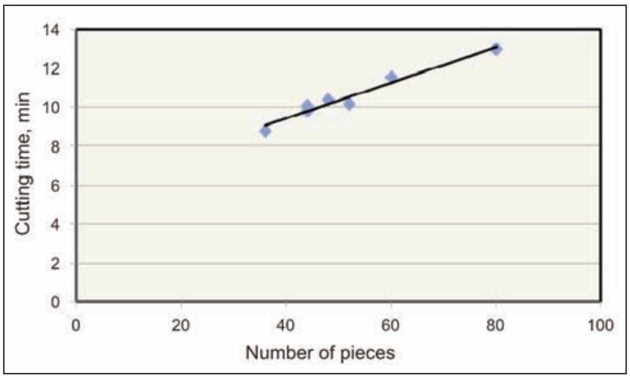

Fig. 4. Changes in the cutting time depending on the number of pieces in men's coat models

Table 3

THE CORRELATION OF NUMBER OF PIECES, CUTTING TIME AND SEWING TIME IN MEN'S COAT GROUPS			
Factors	***r***	***p***	***n***
Number of pieces – cutting time	0.981	0	7
Number of pieces – sewing time	0.942	0.002	7

When the results in table 3 are examined:

- since the relationship between number of pieces and cutting time is p = 0, the linear relationship between these variables is statistically significant;
- since the relationship between the number of pieces and sewing time is p = 0.002, the linear relationship between these variables is statistically significant.

Figure 4 shows the changing in the cutting time depending on the number of pieces, and figure 5 shows the changing in the sewing time depending on the number of pieces.

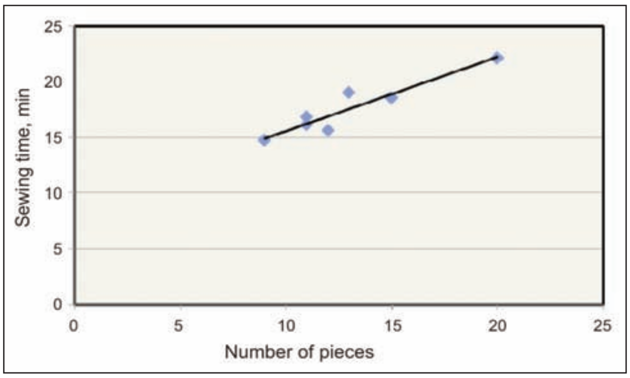

Fig. 5. Changes in the sewing time depending on the number of pieces in men's coat models

Findings regarding perimeter of pieces, cutting time and sewing time

Skirt models

Correlation analyses of the results of trials conducted as 8 trials for skirt models were investigated using the software SPSS. Values obtained as a result of correlation are given in table 4.

When the results in table 4 are examined:

- since the relationship between perimeter of pieces and cutting time is p = 0.137, the linear relationship between these variables is statistically insignificant;
- since the relationship between the perimeter of pieces and sewing time is p = 0.001, the linear relationship between these variables is statistically significant.

Table 4

THE CORRELATION OF PERIMETER OF PIECES, CUTTING TIME AND SEWING TIME IN MEN'S COAT GROUPS			
Factors	***r***	***p***	***n***
Perimeter of pieces – cutting time	0.573	0.137	8
Perimeter of pieces – sewing time	0.929	0.001	8

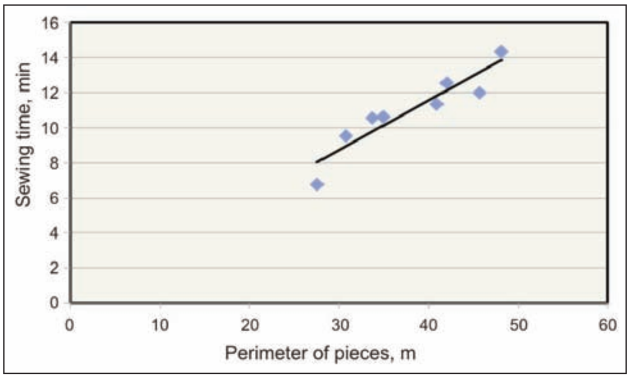

Fig. 6. Changes in the sewing time depending on the perimeter of pieces in skirt models

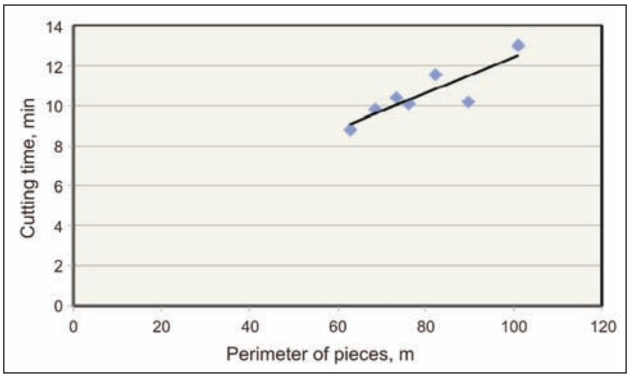

Fig. 7. Changes in the cutting time depending on the perimeter of pieces in men's coat models

Figure 6 shows the changing in the sewing time depending on the perimeter of pieces.

Men's coat models

Correlation analyses of the results of trials conducted as 7 trials for men's coat models were investigated using the software SPSS. Values obtained as a result of correlation are given in table 5.

Table 5

THE CORRELATION OF PERIMETER OF PIECES, CUTTING TIME AND SEWING TIME IN SKIRT GROUPS

Factors	*r*	*p*	*n*
Perimeter of pieces – cutting time	0.866	0.012	7
Perimeter of pieces – sewing time	0.977	0	7

When the results in table 5 are examined:

– since the relationship between perimeter of pieces and cutting time is p = 0.012, the linear relationship between these variables is statistically significant;

– since the relationship between the perimeter of pieces and sewing time is p = 0, the linear relationship between these variables is statistically significant.

Figure 7 shows the changing in the cutting time depending on the perimeter of pieces and figure 8 shows the changing in the sewing time depending on the perimeter of pieces

RESULTS

Results regarding total number of pieces and perimeter of pieces

In both product groups of the study, it was observed that an increase in the number of pieces increases the perimeter of pieces. If the model is divided into higher number of pieces, lines to be attached are prolonged. And this causes the perimeter of pieces that form the model to prolong. According to the results of the study, it was proven that vertically cut models have longer perimeters than horizontally cut models. If the perimeter length is desired to be prolonged, the model has to be divided into higher number of pieces. This increases the number of pieces.

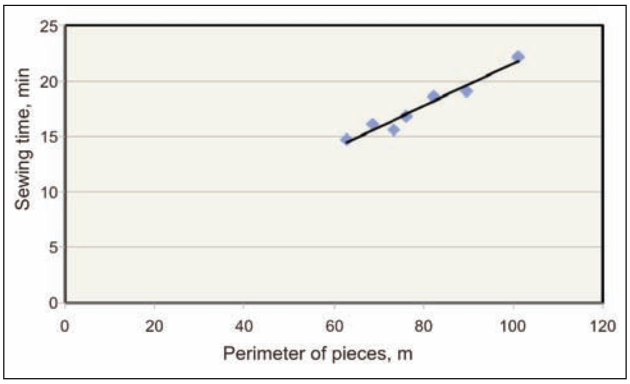

Fig. 8. Changes in the sewing time depending on the perimeter of pieces in men's coat models

Results regarding number of pieces, cutting time and sewing time

When number of pieces and cutting times were examined while the increase in the number of pieces had no effect on cutting time in skirt models, higher number of pieces increased cutting time in men's coat models, while when number of pieces and sewing times are examined, an increase in the number of pieces in all product groups prolonged the sewing time. In both cutting and sewing processes another factor related to the number of pieces is the perimeter of pieces. Therefore, it was found more appropriate to evaluate cutting and sewing time data in comparison with the data for number of pieces and perimeter of pieces. Data for number of pieces and cutting time is given in table 6. Data for number of pieces and sewing time is given in table 7.

Results regarding the perimeter of pieces, cutting time and sewing time

In the previous evaluations, a positive correlation was found, namely an increment in the number of pieces increased the perimeter of pieces and cutting and sewing processes depend completely on the lengths of perimeters. Higher numbers of pattern pieces on the model will certainly increase the total perimeter lengths and therefore, changes will occur

Table 6

RESEARCH FİNDİNGS ACCORDİNG TO THE NUMBER OF PİECES AND CUTTİNG TİME İN MARKER PLAN		
Skirt models	**Cutting time,** min.	**Number of pieces**
Classic	6.66	16
Flared	3.83	12
Horizontally cut, model *1*	6.96	20
Horizontally cut, model *2*	5.19	20
Vertically cut, model *1*	7.64	24
Vertically cut, model *2*	6.18	28
Both vertically and horizontally cut, model *1*	7.35	28
Both vertically and horizontally cut, model *2*	6.66	36
Men's coat models		
Classic	8.81	36
Horizontally cut, model *1*	9.82	44
Horizontally cut, model *2*	10.4	48
Vertically cut, model *1*	10.09	44
Vertically cut, model *2*	10.19	52
Both vertically and horizontally cut, model *1*	11.55	60
Both vertically and horizontally cut, model *2*	13	80

Table 7

RESEARCH FİNDİNGS ACCORDİNG TO THE NUMBER OF PİECES AND SEWİNG TİME		
Skirt models	**Cutting time,** min.	**Number of pieces**
Classic	9.539	4
Flared	6.792	3
Horizontally cut, model *1*	10.628	5
Horizontally cut, model *2*	10.567	5
Vertically cut, model *1*	11.351	6
Vertically cut, model *2*	11.991	7
Both vertically and horizontally cut, model *1*	12.545	7
Both vertically and horizontally cut, model *2*	14.333	9
Men's coat models		
Classic	14.733	9
Horizontally cut, model *1*	16.141	11
Horizontally cut, model *2*	15.619	12
Vertically cut, model *1*	16.849	11
Vertically cut, model *2*	19.061	13
Both vertically and horizontally cut, model *1*	18.585	15
Both vertically and horizontally cut, model *2*	22.174	20

in cutting and sewing times depending on the properties of the systems used in the production.

When number of pieces, perimeter of pieces and cutting times were examined, it was observed that increments in number of pieces and perimeter of pieces had no effect on cutting time in skirt models whereas in men's coat models the increments in these elements prolonged the cutting time.

In computer aided cutting machines, cutting times and characteristics are affected by a number of factors such as: height of layers, type of the fabric and characteristics of the model – corners in the model, number of rounds and stops, number of markings and notches, numbers and characteristics of inner lines to be cut, cutting distance and number of patterns. All these factors affect cutting speed and determine cutting times in these computer aided cutting machines used in the study.

When cutting times of a circle and a square with same perimeter are examined, cutting time of the square is longer than the circle because the knife has to be taken out of the fabric layer three times due to the need for turnings at right angels. But there is no need for taking the knife out of the layer because there is no corner turning in cutting the circle shape and once cutting is started it continues without any pause, therefore, the speed will be higher and cutting time will be shorter. If number of marks, notches and hole marks is high, this will also slow down the system and prolong cutting time. When skirt models are examined with same concerns, number of stops will increase due to the number of darts, therefore, although the perimeter length is short cutting speed will slow down and cutting time will prolong.

The skirt product group is different from the men's coat group in terms of structure. Taking the applied model criteria for the skirt groups into consideration, when horizontally cut models are examined; secondary models are observed to have shorter perimeter of pieces. They are also cut in shorter cutting periods. The cutting time is closely related to not only the model but also to the structure and working characteristics of the computer aided cutting system used. Factors such as measurement of the marker, length of the cut, corner turnings, notches, holes and bents closely affect the cutting time.

In models with less pattern functions compared to skirts such as, men's coat, increment in the number of pieces and the perimeter of pieces prolong the cutting time.

Regression equalities for cutting time in men's coat models are given below:

$$\textit{men's coat cutting time}\ [\text{min.}] = 3.438 + 8.99 \cdot 10^{2} \cdot \textit{perimeter of pieces}\ [\text{m}] \quad (1)$$

When number of pieces and sewing time is examined, in all models subject to the study, increment in the number of pieces and the perimeter of pieces affect the sewing time. The increment in the number

Table 8

RESEARCH FİNDİNGS ACCORDİNG TO THE NUMBER OF PİECES AND SEWİNG TİME			
Skirt models	**Cutting time,** min.	**Sewing time,** min.	**Number of pieces**
Classic	6.66	9.539	30.7
Flared	3.83	6.792	27.5
Horizontally cut, model *1*	6.96	10.628	34.9
Horizontally cut, model *2*	5.19	10.567	33.7
Vertically cut, model *1*	7.64	11.351	40.9
Vertically cut, model *2*	6.18	11.991	45.7
Both vertically and horizontally cut, model *1*	7.35	12.545	42
Both vertically and horizontally cut, model *2*	6.66	14.333	48.1
Men's coat models			
Classic	8.81	14.733	62.9
Horizontally cut, model *1*	9.82	16.141	68.6
Horizontally cut, model *2*	10.4	15.619	73.4
Vertically cut, model *1*	10.09	16.849	76.2
Vertically cut, model *2*	10.19	19.061	89.6
Both vertically and horizontally cut, model *1*	11.55	18.585	82.3
Both vertically and horizontally cut, model *2*	13	22.174	101

of pieces prolongs the length of the lines to be sewed. More lines to be sewed, means longer sewing time. Regression equalities for sewing times for skirt and men's coat models are given below:

$$\textit{skirt sewing time}\ [\text{min.}] =$$

$$= 0.276 + 0.282 \cdot \text{perimeter of pieces [m]} \qquad (2)$$

$$\textit{men's coat sewing time}\ [\text{min.}]\ 0.020 =$$

$$= 2.456 + 0.191 \cdot \textit{perimeter of pieces}\ [\text{m}] \qquad (3)$$

Data for perimeter of pieces, cutting time and sewing time are given in table 8.

CONCLUSIONS

Following the investigations of all factors and their degrees of effect, it was observed that a characteristic of a model is one of the important factors that affect the productivity and time.

Time and productivity take the cost factor under its influence and divert it. Cost and profit calculations that only take into account the cost efficiency of the fabric are inappropriate.

Labor, a very important factor that affects the cost must be taken into consideration. The main factor affecting the labor cost is the time. In this respect, apparel manufacturers should handle both fabric and labor costs as a whole in cost calculations.

BIBLIOGRAPHY

[1] Denno, P. *Aspects of a product model supporting apparel virtual enterprises.* In: International Journal of Clothing Science and Technology, 1997, vol. 9, no. 1, pp. 62-74

[2] Olaru, S., Mocenco, A., Teodorescu, M., Niculescu, C. Săliștean, A. *Shape categories for the Romanian female population and specific clothing recommendations*. In: Industria Textilă, 2011, vol. 62, nr. 3, pp. 155 -160

[3] Jerrigen, M. H., Easterling, C. R. *Fashion merchandising and marketing*. Amazon Publishing, 1997

[4] Jones, R. M. *The apparel industry*. Blackwell Publishing, 2006, p. 328, ISBN 1405135999

[5] Chase, R., Aquiland, H. J. *Production and operations management.* Richard D. Irwing Inc., 1993, p. 194

[6] Erdogan, M. C. *Erkek takim elbisesi üretiminde ekose boyutlarinin kumaş giderine etkisi*. In: Tekstil ve Konfeksiyon, 1992, vol. 3, pp. 241-246

[7] Sieling, M. S., Curtin, D. *Patterns of productivity change in men's and boys' suits and coats*. Questia, Montly Labour Rewiev, 1988, vol. 11

[8] Kansoy, O. *The effects of model properties on fabric usage amount and costs on labour*. Unpublished doctoral theses, Ege University, 2003

Authors:

Dr. OKSAN ORAL
Prof. Dr. CETIN M. ERDOGAN
Dr. ESRA DİRGAR
Ege University
Bergama Technical and Business College
Textile Department
35700 Bergama – İzmir, Turkey
e-mail: oksan.kansoy@ege.edu.tr; esra.dirgar@ege.edu.tr

The influence of traditional art in the current fashion design

MIHAELA CARP AUREL POPP

REZUMAT – ABSTRACT

Influenţa artei tradiţionale în creaţia vestimentară actuală

Arta tradiţională reprezintă ansamblul de activităţi artistice care sunt transmise de la o generaţie la alta, prin intermediul experienţei directe, prin mediul familial sau prin instrumentele comunitare. Tehnicile şi formele artelor tradiţionale evoluează însă foarte lent, de aceea se impune fructificarea efortului creator al designerilor vestimentari în ceea ce priveşte creaţia, pentru a promova originalitatea şi diversitatea vestimentaţiei, elemente care sunt necesare în industria modei, pentru care arta este o sursă importantă şi inestimabilă. Lucrarea evidenţiază unele aspecte privind relaţia dintre arta tradiţională şi creaţia tehnică în vestimentaţie.

Cuvinte-cheie: artă tradiţională, design vestimentar, creaţie tehnică, industria modei

The influence of traditional art in the current fashion design

Traditional art represents the body of artistic activities that are transmitted from one generation to another by means of direct experience, family or community tools. The techniques and the forms of traditional arts evolve very slowly, so it is necessary to enrich the creative effort of fashion designers in terms of creativity, in order to promote originality and diversity of clothing, which are necessary elements in the fashion industry, for which art is an important and invaluable source. This paper highlights some aspects regarding the relationship between traditional art and technical creativity in fashion design.

Key-words: traditional art, fashion design, technical creativity, fashion industry

Through traditional arts, each generation adds the gift of creativity to tradition, the sense of what is beautiful, symbolic and well done. This specific value is defined by the community rather than the creative approach of a specific individual, therefore the valorification of the creative ideas of fashion designers is required in this respect. In order to keep the tradition of true folk art, the hand stitching points were underlined in this paper, together with those performed mechanically, and successfully used in the creation of clothing, so popular even today.

This is the way the transition from technology to art was made by textile expressions, but also by means of a new approach and performance of the old ennoblement manual techniques. The wool blades were embroidered since the Middle Ages, with cross-shaped points, while the women learned to write letters even during those activities (fig. 1). These symbols (spiral, circle, tangent to circle, diamond or triangle and cross, symbolizing the sun and moon) were taken also in decorating clothing during Cucuteni period, becoming a source of inspiration even in the present stage.

The elements specified originally were part of the ornamentation of Neolithic clothing, a theory supported also by the discovery of same symbols in artistic traditions, belonging to other nations in Europe, including the Romanian tradition of costumes decoration (except for clothing, they were used to decorate household objects, amulets, ceramic, wood, stone or in building houses) [1].

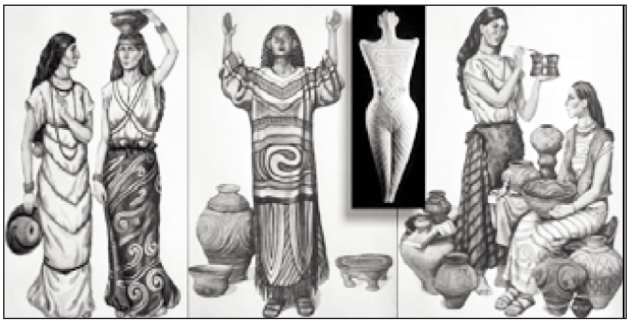

Fig. 1. Clothing in Cucuteni – Trypillia culture (5500 BC – 2750 BC)
Source: Vladimir Dumitrescu – Bucharest, 1979; graphic Zinayda Văşină

STAGES, RESEARCHES AND MODELS' SUGGESTIONS

Some traditional motifs in our country and other countries with common tradition (fig. 2 *a, b, c*), are a constant source of creation for fashion designers, finding successfully a place both in modern clothing ornamentation, and in the hearts of the potential customer, who will wear them. Preserved until today, the tradition of enrichment of the textile surfaces but also of clothing appeared in noble circles from Paris and Versailles.

Current fashion promotes vividly natural trends. Great designers have announced that they return to nature, which will mean that the natural tendencies are under the sign of normality, with predominant

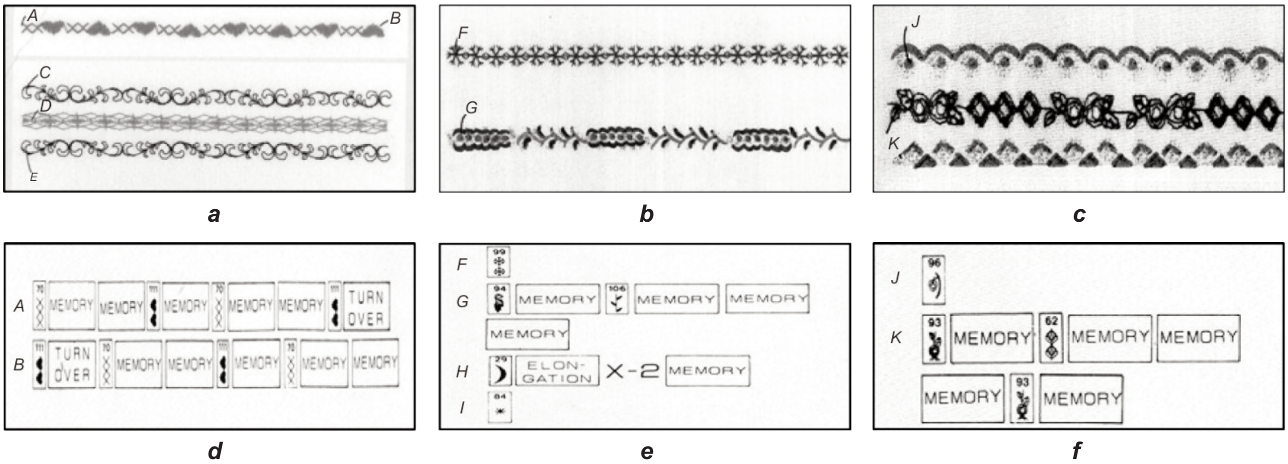

Fig. 2. Types of embroideries performed with special mechanical embroidery machines:
a **–** zigzag embroideries; ***b*** **–** double zigzag embroideries; ***c*** **–** decorative satinated embroideries;
d, e, f – automatic specific programs, in the software of sewing and embroidery machines, that perform those embroideries

colors reminiscent of nature. Fashion will be placed under the tactile and special visual impressions sign due to models and contexts, used for the most interesting clothes. By making decorations with modern techniques, one imprints certain art prints and stylistic features to compositions and the report of the chosen motifs give the fabrics and clothing a special look; the examples in the following figures 2 *d, e, f* indicate the possibilities of implementing them with the help of mechanical embroidery [2, 3].

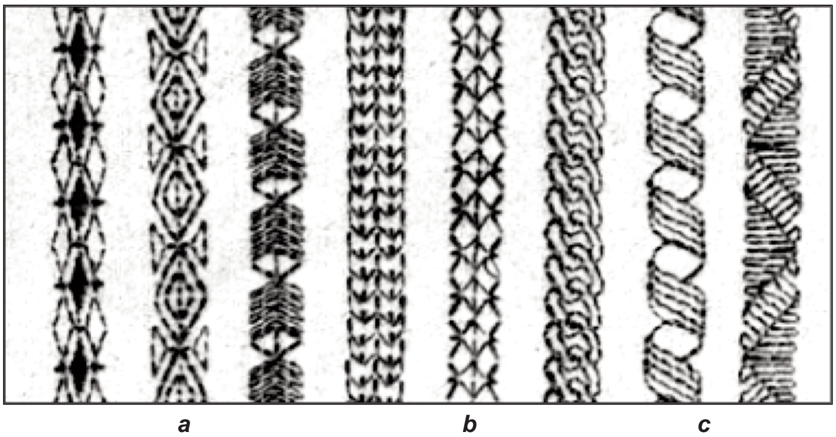

Fig. 3. Stiches and embroideries samples, performed with semiautomatic embroidery machines (automatic specific programs, in the software of sewing and embroidery machines):
a – the sewing of different decorative traditional models included in the basic programs; ***b*** – mixing the models, the mirror image of *a* model;
c – decorative sewing

The modern sewing and embroidery machines have multiple possibilities for achieving these ornaments and similar seams of those of folk art.

The technology has progressed in time, bringing forward the current computerized embroidery together with the special techniques and little secrets that from the most appreciated method of embroidery and enrichment of textile products. Embroidery is valuable and because it has a great visual impact, it brings light and brightness to these products (especially when using high quality embroidery thread), but the most important thing is that embroidery has a long life, it does not deteriorate in time due to the repeated washings or other external factors.

Embroidery is an art by which one decorates or personalizes a variety of clothing products and other textile items with different uses. Years ago this art was done manually, women were involved in this "job" of ancient tradition that was taught from an early age. After a while they started using a simple sewing machine embroidery but the frame movement in which the material for embroidery was tied up, was also done manually, following the designs drawn on the fabric [4, 5]. This can be achieved today mechanically with the help of sewing and embroidery machine (fig. 3 *a, b*).

The analysis of the traditional seam by the multiple actual technological possibilities facilitates bringing the folk art, the modes of composition and the ennoblement of textile surfaces in foreground. It should be noted however that any mechanical seam can have beside the role of proper assembly also a role in decoration.

Ethnic-inspired clothing is worn and appreciated in most countries with tradition, these trends are coming back strong in the current fashion, with decorative accents, using all types of stiches and embroideries, performed today by modern technologies, advanced in time.

Based on these technologies, the present research was carried out with suggestions for modern outfits for women, having in this case as inspiration the Romanian traditional costume in Muscel area (fig. 4 *a, b*) and will be characterized by unique features of

a

b

Fig. 4. Traditional costume from Muscel decorated with geometrical embroideries, inspiration source in modern clothing: ***a*** – assembly; ***b*** – detail

the folkloric garments, specific to this area, carried out with great craftsmanship.

The shirt is made of cotton cloth, richly decorated with handmade embroideries, and over this dress is worn, made of silk fabric, wool or cotton, in which silver or gold threads are integrated. At holiday costumes, the peasant blouses and waist cords are decorated with sequins or beads applied manually. The peasant blouses are made of thin cloth, woven at home (twisted cotton with rustic trend), preserving the cut and the structure of Romanian traditional shirts, ennobled with counted thread embroideries, decorative compositions being placed on the sleeves and chest, made with wire cotton [6].

The dominant chromatic is white-black, blue-purple and the eternal gold or silver thread. It is known that the Muscel head dress has unique motifs as women create on their own and never repeat it, representing an element of female folkloric garments in this area, being an indispensable accessory for headwear, on holidays and it is made of fine silk threads woven in the house, decorated with geometric or floral motifs, embroidered with lace technique, like the whole folkloric costume in that region. The head dress is pinned on the head with a black velvet headband with beads applications, arranged in geometric and floral combinations.

The example shown in the previous figure is analyzed and a proper variant is elaborated, based on the classic pattern of a dress with shoulder and waist darts (fig. 5).

For this purpose, one can study examples from the history of the costume or of the traditional costume of other people [7].

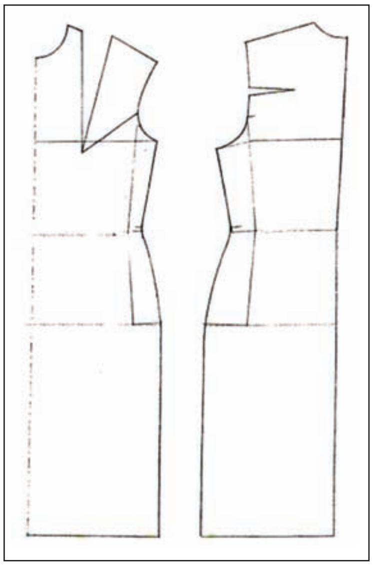

Fig. 5. Clasic dress–basic pattern

The designer has the role of taking the products' details, according to their structure, to achieve their enrichment by different methods and to apply assembling and proper finishing technologies, for example the detailed study of design methods, combining the traditional methods with those of the specific automatic devices, which can be extended depending on the production capacity of a unit. It is envisaged that, regardless of the achieving method of the traditional motifs, cannot be isolated by these modalities regarding the presentation method of the materials used in creating products [8]. These aspects are associated with the characteristics regarding the definition of the drapery, flexibility, rigidity and friction coefficient etc., characteristics which define the feel of the material. The elaborated analysis of the relation between the fineness and the thread color as well as the fineness and the structure characteristics of the materials is not excluded. By means of the technique and of the materials (fig. 6, *a, b, c, d, e, f*) the originality of the newly created clothing assembly was underlined, imprinting new trends of the feminine fashion.

It concerns the classic pattern dress with bust and waist darts (table 1) no sleeves, the total length of 191,6 cm. The top part of the dress is individually tailored and it is inspired by the traditional Russian sleeveless jacket (therefore two independent dresses will be assembled together in lateral seams. The lower parts will be completed independently of each other.

The face and the back of the above dress are identical therefore two superposed dressed, from which the above one will be cut according to the pattern. The zip will be on the left side of the dress, with a length of cca 36 cm. It is mentioned that for the design, one used the program Gemini Pattern Editor, with the stages given in figures 7 and 8.

Following the presentations of the main stages of design it is noted that the program allows the creation of multiple models, if one starts from the basic pattern shown in figure 5. This enables the creation of new models by designing sleeves, pockets or collars, according some custom designs. The enrichment by means of embroideries or other decorative stitches can be the produced on details or parts of the product, before assembling them.

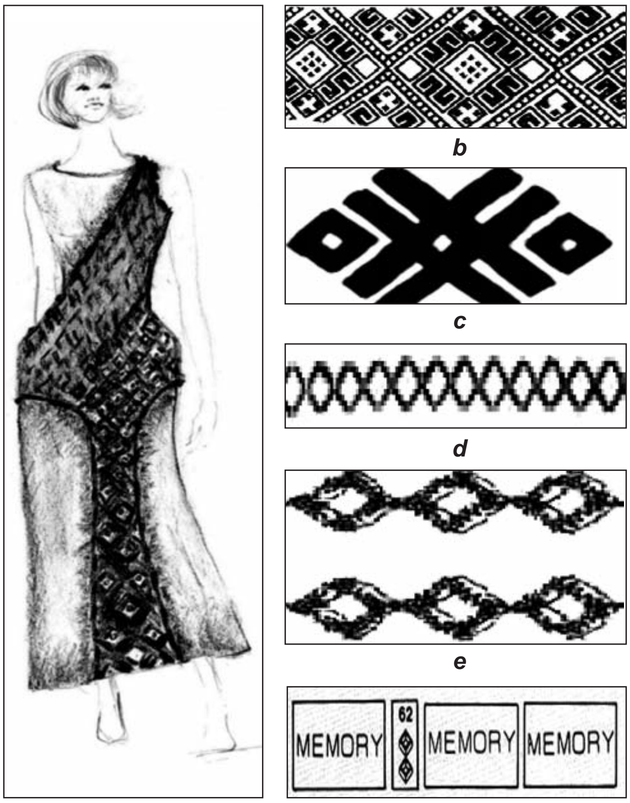

a f

Fig. 6. The taking-over of the traditional decorative details in the suggested garments:
a – dress model decorated with embroideries inspired by traditional costume; ***b*** – traditional geometric motif from Mușcel area; ***c*** – styling of the traditional motif *d* representation of mechanical embroidery;
d, e – the modality of mechanical execution of embroidery done on automatic embroidery machine;
f – selection of the program especially for performing mechanical embroidery

Table 1

TDESIGN DIMENSIONS – TABLE OF SIZES		
Ref.	**Size**, cm	**38 I**
1	Body height	168
2	Bust (chest) circumference	84
3	Hip circumference	94
4	Waist circumference	68
5	Product length	191,6
6	Back length to the waist line	41.4
8	Length of the shoulder	12.1
9	Bust addition	4
10	Waist addition	2.5
11	Hip addition	2

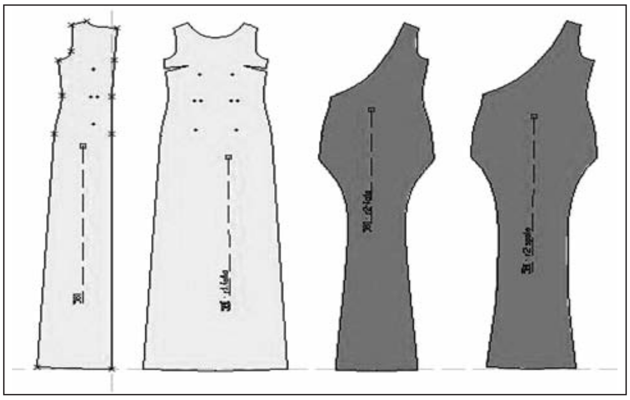

Fig. 7. Technical chart dress model face and back (2nd stage)

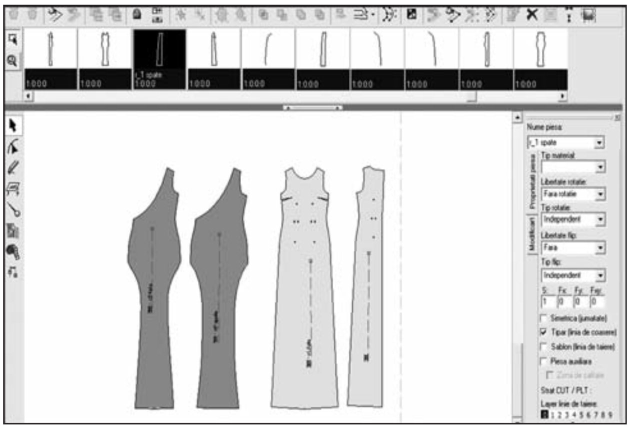

Fig. 8. Working stages in designing the model

CONCLUSIONS

This paper aims to promote cultural heritage, the development of respect for the beauty of folk art, the stimulation of curiosity for everything that means tradition and Romanian traditions and customs, creating opportunities that help textile designers present their creative work products.
The perception of beauty and harmony of Romanian folkloric textiles and the identification of some phytomorphic, zoomorphic, anthropomorphic, skeomorphic motifs etc., our generations and the future ones will always have access to the inexhaustible source of beauty and authentic aesthetic experience, which is our cultural heritage.
The study of figurative language of Romanian folk art, the artistic representations of an ornament as interesting in the stylistic expression as it is full of meaning, reveals a unity in diversity that marks the originality of some cultural values, sources of adequate systems of the artistic expression.
The individual research on the similarities of the traditional motifs with techniques to automatically achieve the ornaments, have allowed the expansion of the use of appropriate equipment for applications in technical creation, customed to personalised products.
The embroidery and decorative stitching applications on product details and landmarks, have an important role in terms of product quality and clothing ensembles.

BIBLIOGRAPHY

[1] Haşegan, M. *Imprimeurile industriale – artă şi tehnologie*. Editura Artes, Iaşi, 1998

[2] Mitu, S., Mitu, M. *Bazele tehnologiei confecţiilor textile*, vol. 1, 2. Editura Performantica, Iaşi, 2005

[3] Necef, O. K., Ondogan, Z. *A study about garment collection preparation steps and quality control methods.* In: Industria Textilă, 2013, vol. 64, issue 3, pp. 163-167

[4] Popp, A., Babcineţchi, V., Carp, M. *Modern processes of ennoblement for garment.* In: Industria Textilă, 2012, vol. 63, issue 2, pp. 79-84

[5] Papaghiuc, V., Creţu, M. *Tehnici de înnobilare a suprafeţelor textile prin coasere*. Editura Performantica, Iaşi, 2007

[6] Ion, O. *Istorie şi cultură în Lereşti - Muscel*. Editura Ars Docendi, 2004

[7] Carp, M., Mitu, S. *Similitudini între arta tradiţională şi tehnologiile mecanice textile*. Simpozionul anual al specialiştilor din industria de tricotaje – confecţii, Iaşi, 4-5 decembrie 2009

[8] Carp, M. *Broderiile industriale şi fuziunea între artă şi tehnologie*. Simpozionul anual al specialiştilor din industria de tricotaje – confecţii, Iaşi, 4-5 decembrie 2009

Authors:

Drd. ing. MIHAELA CARP
Drd. ing. AUREL POPP
Universitatea Tehnică Gheorghe Asachi
Facultatea de Textile-Pielărie şi Management Industrial
Bd. D. Mangeron nr. 53, 700050 Iaşi
e-mail: mcarp@tex.tuiasi.ro; e-mail: apopp@tex.tuiasi.ro

DOCUMENTARE

Nanotehnologii

POLIMERI RANFORSAȚI CU NANOPARTICULE PENTRU DISPOZITIVE MEDICALE

Compania ***Foster Corporation,*** cu sediul în Putnam, Connecticut/S.U.A., în colaborare cu unul dintre liderii de piață în producerea compușilor polimerici pentru dispozitive medicale, au lansat compozitele ranforsate cu nanoparticule destinate dispozitivelor medicale minim invazive, de tipul cateterelor, având o greutate suplimentară de până la 30%.

Compușii ranforsați cu nanoparticule, cu o mare capacitate de umplere, oferă un avantaj substanțial în optimizarea proprietăților fizice ale rășinii de bază, menținând, în același timp, capacitatea lor de prelucrare în componente cu pereți subțiri.

Compușii ranforsați cu nanoparticule încorporează nanoplachete ultrafine, care interacționează direct cu structura polimerului, sporindu-i proprietățile de rezistență la încovoiere și îmbunătățind rigiditatea componentelor.

Până în prezent, pentru a asigura dispersia plachetelor ultrafine în matricea polimerică, polimerii de tipul poliamidelor și elastomerii termoplastici posedau o capacitate limitată de încărcare a nanomaterialelor, de obicei de 15%. Compania Foster a dezvoltat modele brevetate de îmbinare, de tip spiralat, capabile de a realiza încărcări de până la 30%, având ca rezultat o creștere a modulului de încovoiere cu până la 300%, la cateterele obținute din elastomeri termoplastici, destinate domeniului medical.

Gama de compuși ranforsați cu nanoparticule, utilizați în producerea dispozitivelor medicale cu pereți subțiri, include poliamidele, elastomerii termoplastici și poliuretanii termoplastici, având un grad de încărcare pentru consolidarea nanoplachetelor cuprins între 1 și 30%.

Tehnologia de nanoranforsare oferă posibilitatea de a modifica proprietățile unui dispozitiv medical, fără înlocuirea polimerului de bază, necesare pentru aplicațiile de coextrudare și lipire.

De exemplu, modulul de încovoiere al unui durometru 72, realizat dintr-un polimer termoplastic, poate fi reglat la valori cuprinse între 690 și 2 758 MPa, folosind nanoranforsări cu o încărcare de până la 30%.

Smart*textiles and nanotechnology, mai 2013, p. 7*

Quality monitoring for wastewater generated by the textile finishing

IOANA CORINA MOGA
FLOAREA PRICOP
MARIUS IORDĂNESCU
RĂZVAN SCARLAT
ANGELA DOROGAN

REZUMAT – ABSTRACT

Monitorizarea calității apelor uzate, generate de industria textilă

Utilizarea tehnologiilor convenționale în scopul epurării apelor uzate, generate de industria textilă, creează probleme din ce în ce mai grave inginerilor de mediu, din cauza restricțiilor din ce în ce mai dure de deversare a efluenților, impuse prin legislația de mediu. În lucrare sunt prezentate rezultatele obţinute în urma cercetărilor derulate pe platforma Parcului Industrial şi Tehnologic Giurgiu Nord, unde îşi desfăşoară activitatea societăţi comerciale din industria textilă şi unde s-a dorit minimizarea impactului negativ asupra mediului, generat de fabricile de textile. Astfel, s-a realizat retehnologizarea staţiei de epurare, precum şi îmbunătăţirea procesului de producţie, prin utilizarea unor coloranţi ecologici şi prin modificarea fluxului tehnologic de vopsire a ţesăturilor, în scopul reducerii încărcării cu poluanţi a apelor uzate. În lucrare este prezentat un nou proces de vopsire ecologic şi modalităţile de proiectare a treptei biologice de epurare.

Cuvinte-cheie: epurare, ape uzate, monitorizare, bazin aerob, modelare, simulare

Quality monitoring for wastewater generated by the textile finishing

The use of conventional textile wastewater treatment processes becomes drastically challenged to environmental engineers with increasing more and more restrictive effluent quality by water authorities. In the present paper are presented the results obtained in two research projects. The paper presents the results obtained as a result of research carried out on the platform of the Technological and Industrial Park Giurgiu North, where textile industry companies are operating and where we wanted to minimize the negative environmental impact generated by the textile factories. We worked on the refurbishment and technologization of the wastewater treatment palnt and the improvement of the production process (using organic dyes and modifying the dyeing process flow of the fabric) in order to reduce the pollutants found in the wastewater. A new environmentally friendly dyeing process is presented in this paper and also ways to design a biological treatment stage.

Key-words: wastewater treatment, monitoring, aerobic basin, modeling, simulation

Modern textile dyes are supposed to have high degree chemical and photolytic stability in order to keep their forms and colors. For that reason the dyes are produced showing resistance to sunlight, detergent, soap and water. These characteristics of the dyes affect the methods of water treatment.

With the accumulation of the dyeing substance in water environment, appears the danger of toxic and carcinogenic products [1]. Releasing colored waste - water into the environment may cause great damages to the human body, functions of kidneys, reproductive system, liver, brain and nervous system [2].

In natural water masses occur aesthetic corruptions due to the existence of color and it hinders the permeability of oxygen. The decrease of the decomposed oxygen in water masses severely affects the life in water environment. For that reason eliminating the dyes from wastewater is the basic environmental problem and it is vital because the dyes are visible even in low concentrations.

Wastewater resulted from dyeing may contain toxic components and heavy metals due to chemicals and dyeing substances [3]. With this structure dying wastewater causes problems in refining facilities. Thus, color removal has become the most important environmental problem that can be faced in the matter of wastewater treatment [4].

SPECIFIC POLLUTANTS GENERATED BY THE TEXTILE INDUSTRY

In textile processing, the industry uses a number of dyes, chemicals, auxiliary chemicals and sizing materials. As a result, contaminated wastewater is generated, which can cause environmental problems unless properly treated before its disposal.

The textile industry is characterized by several pollutants, the most common ones being [5]:

- Presence of color in the wastewater is one of the main problems in textile industry. Colors are easily visible to human eyes even at very low concentration. Hence, color from textile wastes carries significant esthetic importance. Most of the dyes are stable and light or oxidizing agents have no effect onto them. They are also not easily degradable by the conventional treatment methods.

Removal of dyes from the effluent is a major problem in most of textile industry branches.

- Dissolved solids contained in the industry effluents are also a critical parameter. Use of common salt and glauber salt etc. in processes directly increases total dissolved solids (TDS) level in the effluent.
- Wastewater generated by the textile industry is not free from metal contents. There are mainly two sources of metals. Firstly, the metals may come as impurity with the chemicals used during processing, such as caustic soda, sodium carbonate and salts. The metal complex dyes are mostly based on chromium.
- Due to the use of chlorine compounds in textile processing, residual chlorine is found in the waste flow.
- Textile effluents are often contaminated with non-biodegradable organics termed as refractory materials. Detergents are typical examples of such materials. The presence of these chemicals results in high chemical oxygen demand (COD) value of the effluent. Organic pollutants, which originate from organic compounds of dye stuffs, acids, sizing materials, enzymes, tallow etc. are also found in textile effluents.

Some values related to the characterization of wastewater in the dry-house in which different dyes and fibers are dyed are shown in table 1.

Some of the quality parameters that must be monitored are mentioned in table 2 [6], as well as the maximum allowed values for the discharged effluents in natural receptors (rivers, lakes – NTPA 001) [7] or in municipal sewage systems (NTPA 002) [8].

Table 1

THE CHARACTERIZATION OF DYING WASTEWATER

Type of dye	**Fiber variety**	**Color**	**Biological oxygen demand**, mg/l	**Biological oxygen demand**, mg/l	**Total suspended solids**, mg/l	**Dissolved solids**, mg/l	***pH***
Acid	Polyamide	4 000	240	315	14	2 028	5.1
1:2 metal complex	Polyamide	370	570	400	5	3 945	6.8
Alkaline	Acrylic	5 600	210	255	13	1 469	4.5
Direct	Viscose	12 500	15	140	26	2 669	6.6
Reagent, noncontinious	Cotton	3 890	0	150	32	12 500	11.2
Reagent, continious	Cotton	1 390	102	230	9	691	9.1
Vat	Cotton	1 910	294	256	41	3 945	11.8
Dispers, high temperature	Polyester	1 245	198	360	76	1 700	10.2

Table 2

QUALITY INDICATORS FOR DISCHARGED WASTEWATER

Quality indicator	**Unit**	**NTPA 001/2005**	**NTPA 002/2005**
pH	-	6.5 - 8.5	6.5 - 8.5
Suspended matter	mg/dm^3	35	350
Biochemical oxygen demand	mg/dm^3	20	300
Chemical oxygen demand	mg/dm^3	70	500
Ammonium nitrogen	mg/dm^3	2.0	30
Total nitrogen	mg/dm^3	10.0	-
Total phosphorus	mg/dm^3	1.0	5.0
Sulphides and hydrogen sulphide	mg/dm^3	0.5	1.0
Sulphates	mg/dm^3	600	600
Organic solvents extractable substances	mg/dm^3	20	30
Petroleum products	mg/dm^3	5.0	-
Biodegradable synthetic detergents	mg/dm^3	0.5	25

CASE STUDY – WASTEWATER TREATMENT PLANT (WWTP) FROM GIURGIU NORTH INDUSTRIAL AND TECHNOLOGICAL PARK

Experimental research on the finishing biotechnology (pretreatment and dyeing) of the cellulosic textile materials

The classical finishing technologies and biotechnologies for textile finishing were simultaneously experienced at Giurgiu North Industrial and Technological Park, in order to compare both mechanical and physical-chemical properties of the textile materials as well as the results in terms of wastewater pollution. The comparative technological scheme of conventional and organic cellulosic textile materials finishing (fig. 1) and the dyeing process diagram (fig. 2) highlight the advantages of using biotechnology instead of classical technologies.

The comparative results of wastewater quality indicators for classical technologies and biotechnologies, as well as pollution reduction percentage are presented in table 3.

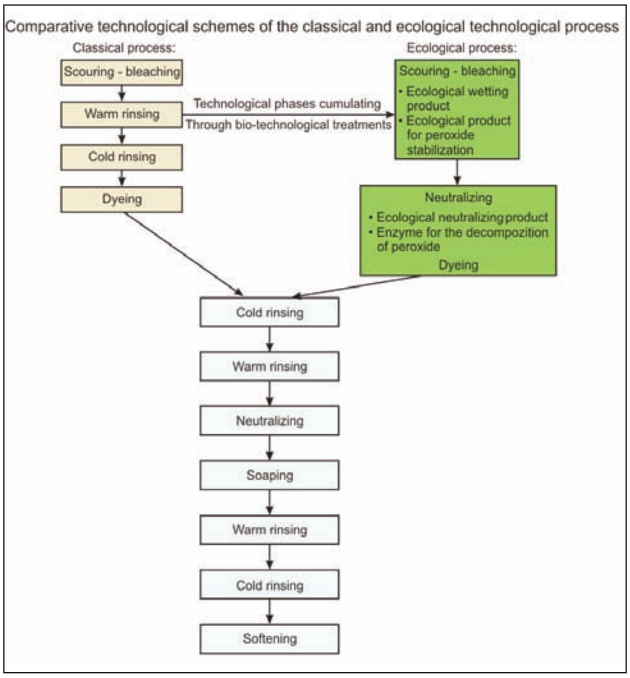

Fig. 1. Comparative scheme of the classical and ecological technological process

The experimental results presented in table 3 are obtained at a Romanian textile factory. Both processes were tested (the classical one and the ecological process) and samples were taken from the wastewater generated. The samples were analyzed and the main quality indicators were determined. The textile factory produces denim cotton fabric. The dyes used for denim fabric are very toxic and in many countries they are forbidden. That is why, this topic is very important and it was studied during several years of research. The results obtained at the Romanian textile company are very good and a significant improvement of the quality indicators can be observed in table 3. The new conceived technology was tested and the following socio-economical effects were obtained [9]:

– reduction of technological phases number (phases cumulating);
– reduction of technological process time by 45 minutes;
– reduction of technological consumptions/kg textile material by: 56 l water, 0.007 kWh power, 1.02 kg steam, 0.05 kg chemical products;
– reduction of total costs/kg textile material (water, power, steam, chemical products) by 0.293 euro/kg textile material;
– dying quality enhancement (dye fastness enhancement);
– value reduction of quality indicators for wastewater (*p*H, COD, BOD, suspended solids, sulphates, detergents), by 30 – 70%;
– cost reduction for wastewaters de-pollution by 2 – 4 euro/l wastewater.

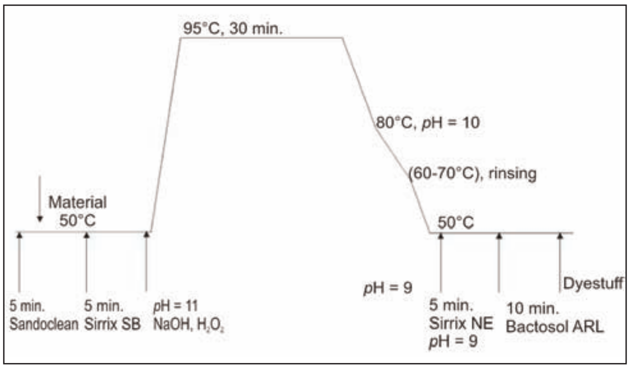

Fig. 2. Ecological process diagramme

Table 3

COMPARATIVE ANALYSES OF WASTEWATER QUALITY INDICATORS							
Test	***p*H**	**COD mgO_2/l**	**BOD mgO_2/l**	**Suspended solids,** mg/l	**Sulphates,** mg/l	**Detergents,** mg/l	**Residuum,** mg/l
P_1 wastewater – classical process	12.3	449.82	807.38	167	184.5	6.3	1 810
P_2 wastewater – ecological process	7.6	201.9	275.8	11	92.9	5.7	1 100
NTPA 002/2005	6.5-8.5	300	500	350	600	25	-
Diminution of P_1/P_2, %	38.2	55.1	65.8	93.4	49.6	9.5	39.2

Wastewater monitoring

The case study presents the wastewater treatment plant in Giurgiu Nord Technological and Industrial Park (GNTIP). The wastewater treatment process is conducted in five circuits (fig. 3), each with its own specificity: wastewater circuit, air circuit, sludge circuit, reagents circuit, wastewater circuit.

Wastewater is sent with pre-pumps in the screen chambers. It is afterwards directed to an underground basin where the flow gets homogenized, still and uniform. A submersible pump directs the wastewater to the reaction chamber of the wastewater treatment plant. The following two stages are for settling solids and removing foam. Wastewater circuit continues with water passing through an underground aerated basin and finally through a settling compartment.

Air circuit consists of a blower, air compressor, systems of pipes and tubes for air transport, system of diffusers and electric and control panel of the 2 pieces of equipment. Air is blown through perforated pipe type diffusers made of polyethylene within the reaction chamber and in the underground basin which follows after the stage 2 – settling. If necessary air is introduced by compressor in the basin situated after the reaction chamber.

Sludge is extracted from the 2 mechanical treatment stages. The coarse suspended solids are also retained by rare screens and removed from the wastewater mass. Sludge is discharged from wastewater treatment using pumps. Reagents circuit consists of chemical treatment plant and solution supply circuit of the reaction chamber.

To discharge wastewater into the public sewerage network an upstream network manhole is provided. This is the place where samples were taken from, in order to be tested, for the determination of water quality and the treatment degree.

Monitoring system will cover the entire process flow taking data from the existing plants and from measurement and control equipment, installed to permanently monitor the water quality.

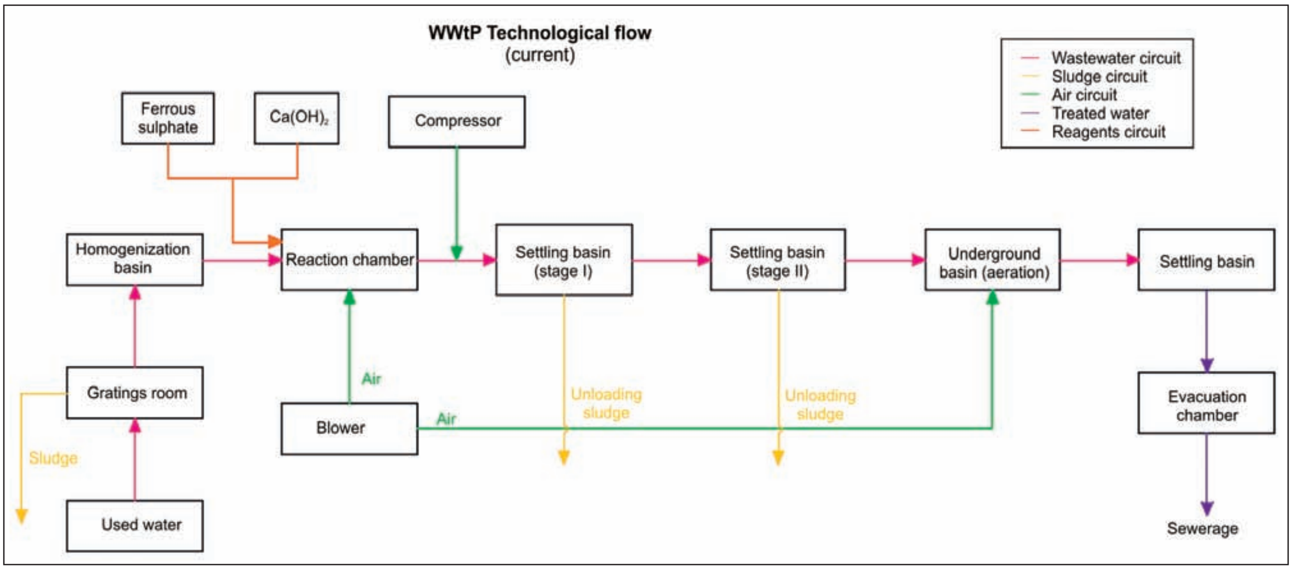

Fig. 3. Existing treatment flow in Giurgiu North Technological and Industrial Park [9]

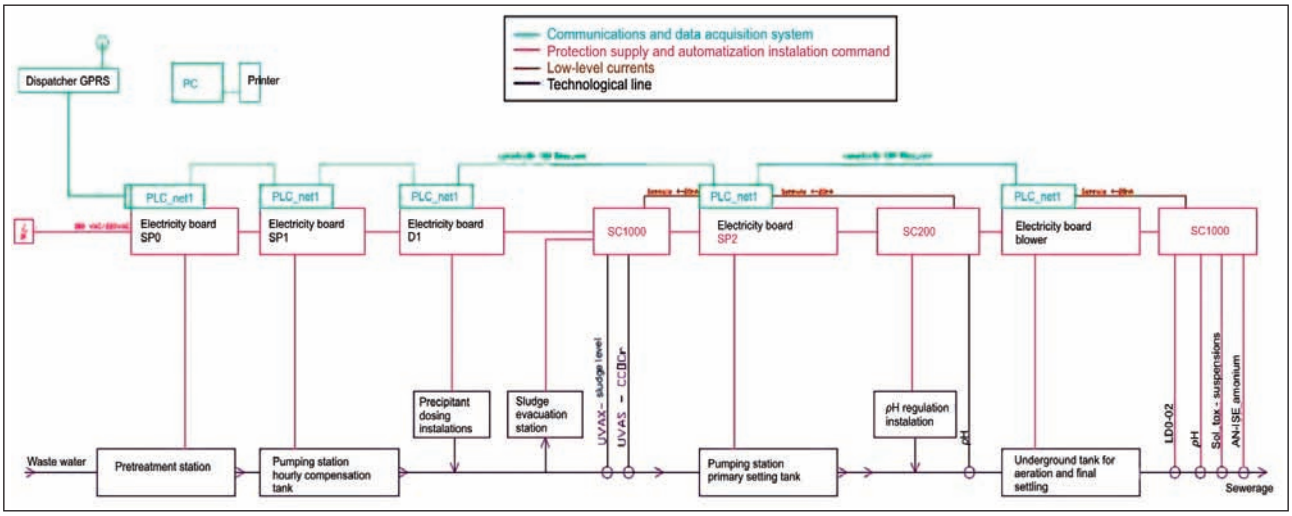

Fig. 4. Overall diagram of monitoring and automation installations

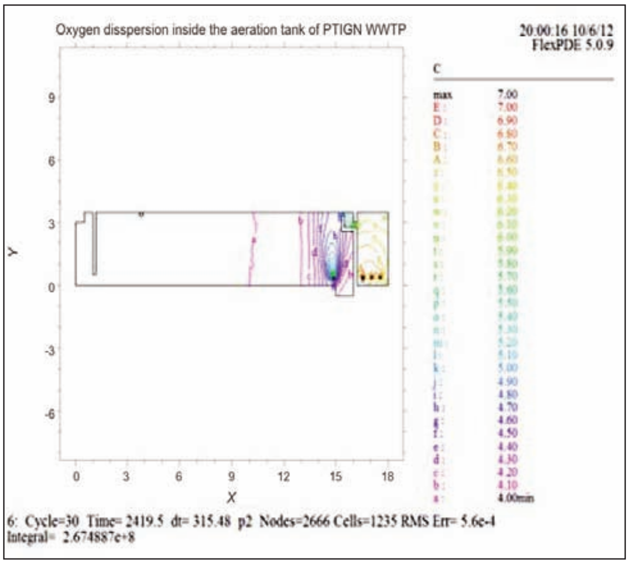

Fig. 5. Dissolved oxygen profiles

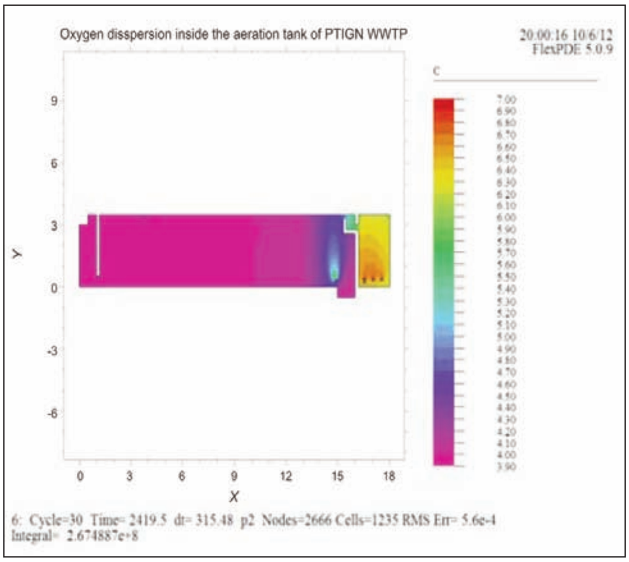

Fig. 6. Dissolved oxygen dispersion

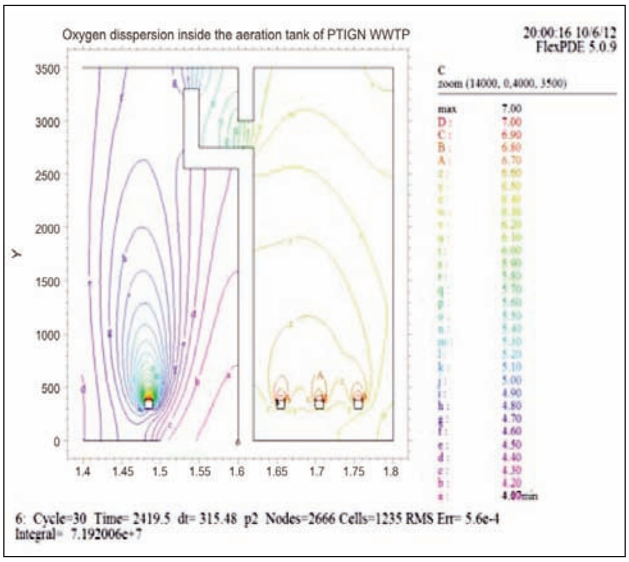

Fig. 7. Dissolved oxygen profiles (zoom)

Monitoring application is a type of SCADA program (Supervisory Control and Data Acquisition) and collects data in the field using a data acquisition system with installed flow PLC for process control and for the online analog signals acquisition.

SCADA system proposed for the automation and monitoring of wastewater treatment plant in Giurgiu Nord Technological and Industrial Park is shown in figure 4. Selection of monitoring points takes into account significant point sources, appropriate quality monitoring points of environmental factors (in our case, monitoring of wastewater before and after treatment) and monitoring of critical process parameters.

Within the water treatment plant of the GNTIP the following sensors can be located: dissolved oxygen sensor, 2 *p*H sensors, turbidity/ suspended solids sensor, ammonium and NO_3 sensor, CCO Cr sensor, sensor for measuring the sludge level.

Mathematical modeling and monitoring of the aeration processes

The second stage is for biological treatment of wastewater loaded with organic matter. Commonly used process is the aerobic process dependent on maintaining the dissolved oxygen concentration to 1–3 mg/l. The oxygen quantity inside the basin should cover both microorganisms breathing and oxidation of organic matter. Considerable savings can be achieved by realizing a correlation between the oxygen demand and the operation of the blowers. In the process of aerobic biological treatment with activated sludge, the following monitoring sensors can be installed [10]:

- in the aerobic basin can be measured the values for organic load, ammonia, total phosphorus (if not measured at the output of the primary clarifier), dissolved oxygen, redox potential, *p*H, ammonium concentration, concentration of suspended solid particles inside the aeration tank and based on these values can be controlled the activated sludge recirculation pump, injected air flow, air pressure injected into the aerobic system;
- in the secondary clarifier can be measured the values for sludge quantity, concentration of suspension solids in recirculating activated sludge, the height of activated sludge layer inside the clarifier, concentration of suspended solids discharged from the clarifier.

Numerical simulations for the aeration processes

The numerical simulations were realized for the reaction chamber, where an aeration system is mounted. Near the reaction basin is placed the first settling basin. Here, air is introduced inside the wastewater mass with the help of an additional compressor.

The dissolved oxygen profiles are presented in figures 5 – 8. The maximum values are obtained near the diffusers. In this area it will be obtained a transfer process of high intensity, because of the renewal contact area between gas and liquid, where the gas bubble are formed and detach from the diffuser. While the gas bubbles are rising inside the water column from the biological reactor, the value of dissolved oxygen is decreasing because of: oxygen consumption needed at organic matters biochemical oxidation, the oxygen concentration from the air bubble is reduced, due to the transfer effect near the diffuser. Inside the reaction chamber the level of the dissolved oxygen is higher than the level obtained inside the clarifier. This situation is normal, because inside the reaction chamber are placed more diffusers and the basin is reduced compared to the clarifier. Because the total length of the 2 basins is very high (18 m) in figures 7 and 8 are presented to sections only for the areas with aeration systems (a zoom is realized). Here, more easily, can be observed the concentration of the oxygen profiles.

As was mentioned before, the air compressor is not always in function. So, for this particular situation, additional numerical simulations are realized and presented in figures 9 and 10. Here, the values for the dissolved oxygen are lower, fact that is explained by using a decreased number of diffusers. Depending on the wastewater characteristic, the air compressor introduces or not air inside the first part of the clarifier. The simplified form for the dispersion equation was considered for the realization of the numerical simulations [11] :

$$\frac{\partial \overline{C}}{\partial t} + \frac{\partial}{\partial x}\left(\overline{u}\,\overline{C}\right) + \frac{\partial}{\partial y}\left(\overline{w}\,\overline{C}\right) = \frac{\partial}{\partial x}\left(\varepsilon_x \frac{\partial \overline{C}}{\partial x}\right) + \frac{\partial}{\partial y}\left(\varepsilon_y \frac{\partial \overline{C}}{\partial y}\right) - kCC \qquad (1)$$

where:

ε_x, ε_y represent the dispersion coefficients, on the two direction of fluid current, because of the turbulent regime are considered the average values for these coefficients;

u, v is velocity components on the two axes taken in consideration;

C – concentration for the dissolved oxygen;

k – oxygen consumption for organic matter degradation and for microorganism breathing process.

CONCLUSIONS

During our research we have developed a continuous versatile dyeing process, with organic sulfur dyes, characterized by minimal water consumption, low amount of waste water, “zero” dye in wastewater.

The continuous dyeing process with sulfur dyes with high exhaustion degree is adaptable also to the semi-continuous process in which the dye is fixed by oxidation/fixation without prewash.

The procedure allows fixing the dye 100%, requiring only a rinsing after the fixing stage.

It is a short procedure, eco-friendly, and by comparison with the classic procedure (padding-laying with reactive vinylsulphonic dyes or padding – vapouring with sulphur dyes), leads to a decrease in water consumption of about 90%.

In order to determine the main quality indicators of wastewater on various technological processes there

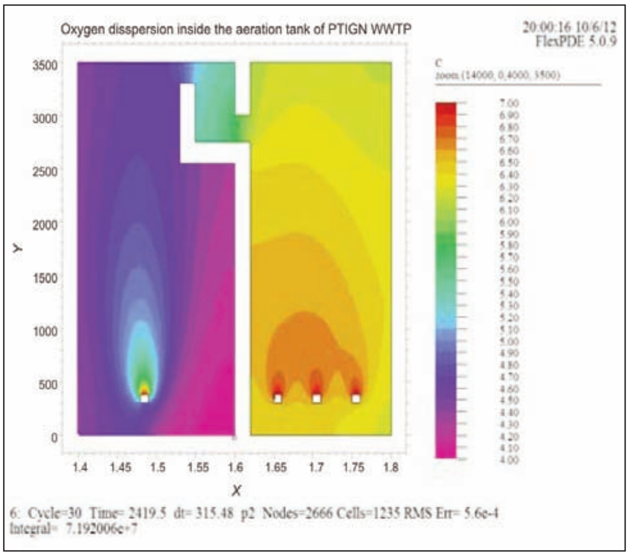

Fig. 8. Dissolved oxygen dispersion (zoom)

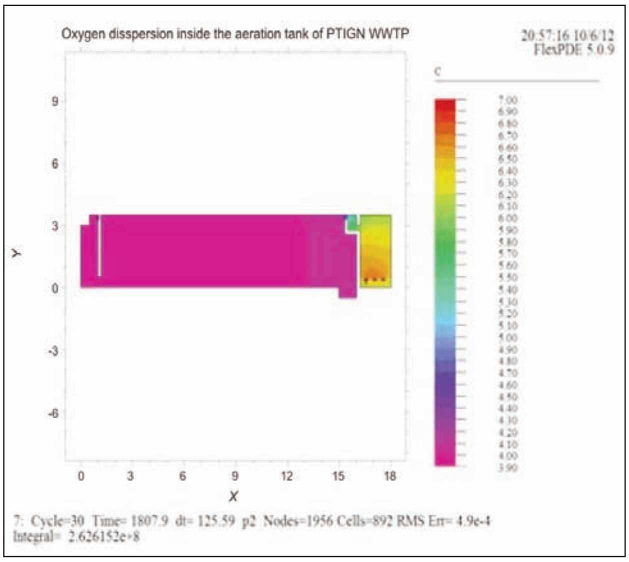

Fig. 9. Dissolved oxygen dispersion (zoom)
(the air compressor is not in operation)

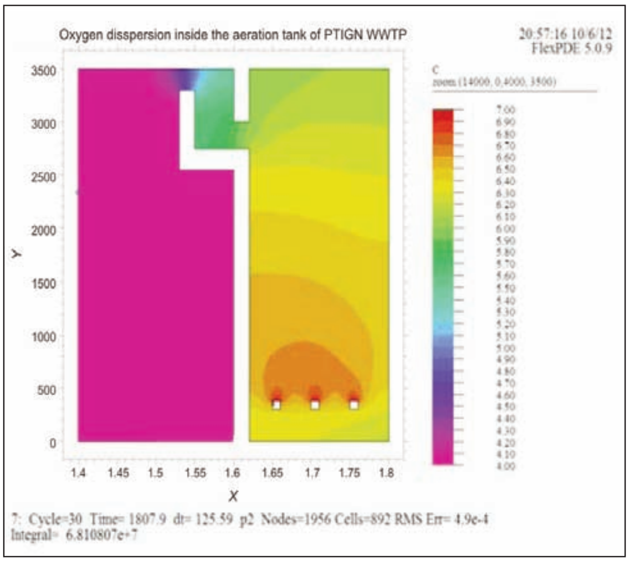

Fig. 10. Dissolved oxygen dispersion (zoom)
(the air compressor is not in operation)

were performed comparative studies. In this regard, we have performed dyeing both with classical dyes and sulfur dyes with a high degree of exhaustion. We have sampled wastewater from both processes and performed analyses within accredite laboratory. Better results were obtained in the case of using the ecological technology with sulphur dyes with high exhaustion degree, and the quality indicators of the wastewater were reduced (by 33–97)% compared to the quality indicators of the wastewater resulted from the classic dyeing technology. The sulphites quantity was diminished significanlty (97%).

The numeric simulations based on mathematical modelling have led to the proper dimensioning of the aeration system within the wastewater treatment plant.

AKNOWLEDGEMENTS

The work has been co-funded by the Sectorial Operational Programme Human Resources Development 2007–2013 of the Romanian Ministry of Labor, Family and Social Protection through the Financial Agreement POS-DRU/89/1.5/S/62557 and by the Romania-Bulgaria Cross-Border Cooperation Programme 2007–2013 (project ENVI-CONTEH no. MIS - ETC cod 129).

BIBLIOGRAPHY

[1] Petropol, G. D. *Surse de apă şi ingineria apelor reziduale*. Note de curs, 2009

[2] Mitchell, M., Stapp, W. *Red river basin water quality monitoring manual*, 2005

[3] Bertea, A. F., Butnaru, R. *Polyamide dyeing wastewater recycling after Fenton-like oxidative treatment.* In: Industria Textilă, 2012, vol. 63, issue 6, pp. 322-326

[4] Odenbach, R. *Standard operating procedures for water quality monitoring.* Minnesota: Red Lake Water District, 2001

[5] Metcalf and Eddy. *Wastewater engineering treatment, disposal, reuse.* 3rd edition, Mcgraw-Hill Book Co., 1991

[6] Supra, L. F. *Overview of wipp effluent monitoring program*, 2005

[7] *NTPA-001/2002 - Normativ din 28 februarie 2002 privind stabilirea limitelor de încărcare cu poluanți a apelor uzate industriale și orășenești la evacuarea în receptorii naturali*

[8] *NTPA-002/2002 - Normativ din 28 februarie 2002 privind condițiile de evacuare a apelor uzate în rețelele de canalizare ale localităților și direct în stațiile de epurare*

[9] Pricop, F. et al. *Integrated systems of monitoring and controlling wastewater quality.* In: Industria Textilă, 2013, vol. 64, issue 1, pp. 40-45

[10] Robescu, D., Lanyi, S., Robescu, D. *Controlul automat al proceselor de epurare a apelor uzate*. Editura Tehnică, 2004

[11] Mandiș, I. C., Robescu, D., Pricop, F. *Mathematical modeling and numerical simulation of ozone mass transfer processes used to treat wastewaters from textile industry.* In: Industria Textilă, 2009, vol. 60, issue 4, pp. 220-227

Authors:

Cerc. şt. gr. III dr. ing. IOANA CORINA MOGA
Universitatea Politehnica București
Str. Splaiul Independenței nr. 313, 060042 Bucureşti
e-mail: corinamoga@yahoo.com

Cerc. şt. gr. III ing. FLOAREA PRICOP
Cerc. şt. gr. III ing. RĂZVAN SCARLAT
MARIUS IORDĂNESCU
Cerc. şt. gr. III dr. ing. ANGELA DOROGAN
Institutul Naţional de Cercetare-Dezvoltare pentru Textile şi Pielărie
Str. Lucreţiu Pătrăşcanu nr. 16, 030508 Bucureşti
e-mail: certex@ns.certex.ro

Materii prime

CERERI MARI PENTRU NANOFIBRELE DE TITAN

Cercetătorii de la ***Universitatea Nanyang***, din Singapore, au creat o nanofibră din dioxid de titan, cu costuri de producție reduse și cu multiple utilizări, cum ar fi: generarea hidrogenului și producerea de apă curată și chiar de energie, desalinizarea apei și recuperarea energiei din apele desalinizate, realizarea de celule solare flexibile, dublarea duratei de viață a bateriilor litiu-ion, producerea unui nou tip de bandaj antibacterian.

Echipa de cercetare coordonată de Darren Sun, prof. asociat la Universitatea Nanyang, a transformat cristalele de dioxid de titan în nanofibre brevetate, din care pot fi fabricate, cu ușurință, membrane filtrante flexibile, obținute dintr-o combinație de carbon, cupru, zinc sau cositor, în funcție de produsul final ce urmează a fi realizat.

Dioxidul de titan este un material ieftin și ușor de procurat. S-a dovedit științific faptul că dioxidul de titan are capacitatea de a accelera reacțiile chimice fotocatalitice și că este hidrofil, cu o afinitate ridicată pentru apă. Datorită acestor avantaje, nanomaterialele obținute din dioxid de titan sunt ușor de produs și au un preț de cost redus, având un potențial imens pentru a face față provocărilor globale continue din domeniul energetic și cel al protecției mediului.

Odată cu creșterea populației (8,3 miliarde de locuitori, în 2013), cererea globală de energie, alimente și apă potabilă este tot mai mare. Legat de aceasta, prof. Sun menționa: “*Deși nu există o soluție rezonabilă pentru rezolvarea celor două mari provocări existente la nivel mondial – energia regenerabilă ieftină și furnizarea unor mari cantități de apă curată – situația poate fi îmbunătățită cu ajutorul membranei multifuncționale, care conține nanoparticule din dioxid de titan, factorul-cheie în descoperirea unor astfel de soluții... Cu acest nanomaterial unic, echipa speră să poată transforma deșeurile de astăzi în resursele de mâine de apa curată și de energie*”.

Dioxidul de titan are o mulțime de aplicații: poate genera, în același timp, hidrogen și apă curată, atunci când este expus la lumina soarelui; poate fi utilizat la confecționarea, cu costuri reduse, a unor membrane filtrante flexibile, cu proprietăți speciale antivegetative; desanilinizează apa în cazul utilizării ca membrană pentru osmoză, ce permite un flux mare; valorifică energia din apa rezultată în urma desalinizării; poate fi folosit la producerea, cu costuri reduse, a celulelor solare flexibile, generatoare de electricitate; dublează durata de viață a bateriilor litiu-ion, atunci când este utilizat ca anod; datorită proprietăților antibacteriene superioare, poate fi utilizat la dezvoltarea unui nou tip de bandaj antibacterian.

Inițial, pentru a realiza membrane antibacteriene destinate filtrării apei și împiedicării dezvoltării bacteriilor care blochează porii membranelor și opresc trecerea fluxului de apă, Sun a folosit dioxid de titan cu oxid de fier. Pe parcursul experimentelor, echipa a descoperit că aceste membrane ar putea acționa ca fotocatalizatori, transformând – sub acțiunea razelor solare – apa uzată în hidrogen și oxigen. Un astfel de efect este obținut, de obicei, cu ajutorul platinei, un metal prețios scump și rar.

“*Cu o astfel de descoperire, este posibil să se realizeze, cu costuri mai mici, tratarea apelor uzate simultan cu stocarea energiei solare sub formă de hidrogen, care să poată fi disponibilă în orice moment din zi sau din noapte, indiferent dacă este sau nu soare, ceea ce o face cu adevărat o sursă de combustibil curat ... Astfel, se obține o producție de hidrogen mult mai ieftină, cu un randament de aproximativ trei ori mai mare decât în cazul folosirii platinei. Concomitent, se poate produce apă curată, cu un cost al energiei aproape de zero, ceea ce ar putea schimba sistemul actual de reciclare a apei, peste tot în lume*” – a declarat Sun.

Hidrogenul este un combustibil curat, care poate fi utilizat pentru pilele de combustie auto sau în centrale electrice, pentru generarea electricității.

Această descoperire, care a fost publicată recent în revista academică *Water Research,* a arătat că o cantitate mică de nanomaterial (0,5 g de nanofibre din dioxid de titan, tratate cu oxid de cupru) poate genera 1,53 ml de hidrogen pe oră, atunci când este introdus într-un litru de apă uzată. Prin această metodă, se produce o cantitate de hidrogen de trei ori mai mare, decât în cazul folosirii platinei. În funcție de tipul de apă uzată, cantitatea de hidrogen generată poate ajunge chiar la 200 ml pe oră.

Particulele de dioxid de titan nu numai că ajută ca apa să fie descompusă, dar ele pot face ca membranelele filtrante să fie mai hidrofile, permițând apei să treacă cu ușurință, în timp ce contaminanții sunt respinși, inclusiv sarea, ceea ce este perfect pentru desalinizarea apei prin osmoză. Pornind de la aceasta, a fost realizată o noua membrană pentru osmoză, care permite un flux mai mare. Această descoperire, publicată recent în revista *Energy and Environmental Science*, reprezintă primul raport privitor la nanofibrele și particulele de TiO_2 utilizate într-un sistem de osmoză, pentru producerea apei curate și generarea de energie.

Datorită proprietăților antimicrobiene și a costurilor reduse, aceste membrane pot fi folosite pentru realizarea bandajelor antibacteriene respirabile, care pot combate infecțiile – în cazul rănilor deschise, și pot grăbi procesul de vindecare, permițând oxigenului să pătrundă în ghips. Proprietățile acestor membrane sunt similare cu cele ale bandajelor de plastic, comercializate în prezent pe piață.

Proiectele de cercetare derulate au arătat că, atunci când este tratat cu alte materiale sau când se regăsește sub o altă formă (cristalină), dioxidul de titan poate avea și alte utilizări, cum ar fi producerea celulelor solare. Prin realizarea unei plăci policristaline din dioxid de titan negru, echipa de cercetare a dezvoltat o celulă solară flexibilă, care permite generarea electricității de la razele solare.
În același timp, o altă echipă a profesorului Sun se preocupă de dezvoltarea nanomaterialelor din dioxid de titan negru, în scopul producerii bateriilor litiu-ion, folosite la dispozitivele electronice. Rezultatele preliminare ale au arătat că, atunci când nanoparticulele din dioxid de titan modificate cu carbon sunt utilizate ca anod, ele pot dubla capacitatea energetică a bateriilor litiu-ion, oferindu-le o durată de viață mult mai lungă.

Sursa: www.ntu.edu.sg

Textile nețesute

NEŢESUTE DIN NANOFIBRE PENTRU REGENERAREA ŢESUTURILOR

Companiile germane ***Biopharm GmbH***, cu sediul în Heidelberg, şi ***Freudenberg*** – cu sediul în Weinheim, lider în sectorul neţesutelor, au elaborat Brevetul internaţional 2012/175611, publicat în 27 decembrie 2012, care tratează neţesutele ce conţin proteina GDF-5.
Materialele sunt special proiectate pentru a accelera procesele de regenerare a ţesuturilor şi de vindecare a leziunilor, iar brevetul elaborat acoperă domeniul de utilizare a acestora ca pansamente şi tampoane pentru leziuni, dar şi ca implanturi.
GDF-5 este o moleculă morfogenă, care susţine proliferarea şi diferenţierea celulelor din ţesuturi, precum și refacerea ţesutului. Se înrudeşte cu GDF-6 şi GDF-7, aceste trei proteine prezentând proprietăţi biologice comparabile şi un grad foarte ridicat al omologiei secvenţei de aminoacizi. S-a demonstrat faptul că aceste proteine îndeplinesc, în primul rând, rolul de inductori şi reglatori importanţi pentru oase şi cartilaje.
Proteinele de tipul GDF-5, ce reprezintă factori de creştere, au fost utilizate cu succes în cercetarea terapeutică şi chirurgia recuperativă, ele susţinând procesele de vindecare naturală a diferitelor ţesuturi vătămate, fie independent, fie în combinaţie cu materiale cu matrice specifică. Deşi au fost dezvoltate câteva compoziţii farmaceutice cu conținut de proteine mature, active biologic, înrudite cu GDF-5, formarea şi manipularea acestora a fost problematică, din cauză că proteina matură tinde să interacţioneze cu câteva materiale solide şi are o solubilitate foarte mică în condiţii fiziologice.
În scopul vindecării leziunilor, au fost dezvoltate pansamente chirurgicale atât sub formă de loţiune, cât şi în formă solidă, realizate cu diferite contururi și dimensiuni şi din diferite tipuri de materiale, pentru a asigura cicatrizarea rănii în condiţii semisterile. Unele pansamente sunt confecţionate din colageni, altele din componente sintetice, cum ar fi polimerii termoplastici amorfi.
Există pansamente de ultimă generaţie, pentru leziuni, care posedă, suplimentar, proprietăţi de administrare a unor medicamente, cum ar fi antibioticele sau citokinele EGF (factor de creştere epidermică) şi PDGF/Becaplermin (factor de creştere derivat din plachete). PDGF modificat genetic este disponibil în comerț sub denumirea de Regranex, ca gel topic pentru vindecarea leziunilor (0,01%). Acesta a primit aprobarea de utilizare în tratarea ulceraţiilor piciorului diabetic, extinse la ţesutul subcutanat şi în profunzime.
Pentru vindecarea leziunilor şi regenerarea altor ţesuturi sunt solicitate, mai ales, materiale care livrează corpului omenesc proteine ce se comportă ca factori de creştere şi de diferenţiere. De aceea, scopul deținătorilor brevetului menționat a fost acela de a îmbunătăţi utilitatea terapeutică a GDF-5 şi a proteinelor înrudite, prin furnizarea unor materiale şi dispozitive noi de vindecare a leziunilor. Noile pansamente pentru leziuni sunt confecţionate din textile neţesute, care conţin cel puţin o substanţă activă biologic, în special substanţe antimicrobiene şi antibiotice.
Pe parcursul studiilor privind îmbunătăţirea utilităţii terapeutice a GDF-5 şi a proteinelor înrudite, inventatorii prezentei aplicaţii au descoperit că astfel de neţesute sunt adecvate, în primul rând, pentru furnizarea de proteine cu factor de creştere şi de diferenţiere. Combinaţia dintre GDF-5 şi neţesutele bioresorbabile a dus la obținerea unor efecte neaşteptate, benefice aplicării proteinei GDF-5.
Neţesutele biodegradabile au furnizat un substrat pentru GDF-5, prezentând o eliberare mai intensă de proteină matură, dar și bune proprietăţi de manipulare. Această combinaţie de administrare a proteinei GDF-5 va fi controlată la locul de aplicare şi, prin urmare, va apărea efectul factorului de creştere în locul vizat de acţiunea farmacologică. Pe lângă acest control spaţial, cantităţi mai mari de GDF-5 activ sunt extrase din neţesutele biodegradabile într-un interval de câteva zile. Datorită încorporării proteinei GDF-5 în materialele neţesute, efectele de precipitare dependente de *p*H sunt depăşite şi, totodată, este micșorată interacţiunea cu materialele solide.

Sursa: www. biopharm.de

Nanotehnologii

NOUL SISTEM 4SPIN CU JET SPOREȘTE PRODUCTIVITATEA

Ca urmare a eforturilor depuse pentru dezvoltarea de noi tehnologii capabile să producă nanofibre din materiale greu filabile, dezvoltatorii de la firma ***Contipro***, din Republica Cehă, au reușit să crească

în mod semnificativ producția de nanofibre, prin elaborarea unui nou sistem cu jet. În funcție de soluția folosită, acest sistem cu jet ar putea fi de șapte ori mai productiv decât tehnologia actuală.
Datorită proprietăților excepționale, nanomaterialele pot fi utilizate în diverse domenii, de la medicină la aplicațiile de mediu. Cu toate acestea, utilizarea lor pe scară largă este împiedicată de prețul ridicat al nanomaterialelor, comparativ cu cel al materialelor clasice. De aceea, nanomaterialele sunt folosite numai atunci când beneficiile proprietăților lor sunt mai mari decât prețul.
În timp ce cea mai utilizată metodă industrială de producție a nanofibrelor se bazează pe formarea acestora din polimeri, prin electrofilare în câmp electrostatic, sistemul brevetat multijet, fără ac, asigură formarea fibrelor cu ajutorul unui flux de aer cald, format în jurul jetului. Acest lucru face posibilă obținerea de nanofibre din soluții foarte vâscoase sau din soluții cu un procent foarte mare de solvent și, de asemenea, crește în mod semnificativ productivitatea jetului, reducând astfel costurile de producție a nanomaterialelor.
Scopul inițial al proiectului l-a constituit elaborarea unui sistem cu jet care să permită dezvoltarea de noi tipuri de materiale pentru medicină. Curând, prin comparațiile testelor de laborator, s-a constatat că metoda elaborată este mult mai eficientă decât metoda clasică de producție a nanofibrelor. Mai mult, noua tehnologie oferă condiții controlate și reglajul cu mare precizie al jetului, permițând atingerea unor valori mult mai stabile ale caracteristicilor nanofibrelor produse în cadrul proceselor de lungă durată. Deoarece nanofibrele sunt de mii de ori mai fine decât un fir de păr uman, orice modificare minoră a caracteristicilor acestora este de mare importanță.
Noul sistem cu jet, brevetat, a fost dezvoltat ca un modul pentru dispozitivul de producție a nanofibrelor 4SPIN, lansat de Contipro, în Japonia, la sfârșitul lunii ianuarie 2013. Acest dispozitiv a fost conceput, în special, pentru îmbunătățirea producției de nanofibre, în condiții de laborator, iar sistemul multijet fără ac s-a dovedit a fi cel mai eficient modul dintre emițătorii furnizați.
Versiunea pilot a dispozitivului a fost concepută de Contipro, în laboratoarele sale, și va fi urmată de o unitate complet operațională pentru producția de nanofibre. În acest sens, numeroase dispozitive Contipro sunt destinate să ofere mijloace ample de transfer al rezultatelor cercetării nanomaterialelor de la stadiul de laborator la practici de producție și clienți. Acest lucru poate fi realizat cu ajutorul echipamentului de laborator existent, cu emițători variind de la un electrod cu ac la un sistem multijet fără ac, precum și cu ajutorul unei viitoare versiuni pilot și, mai ales, prin intermediul versiunii complet operaționale 4SPIN.
Un alt element care diferențiază seria de echipamente de filare 4SPIN de alte dispozitive existente pe piață este posibilitatea de a dezvolta noi aplicații ale biopolimerilor în domeniul medical.

Smarttextiles and nanotechnology, mai 2013, p. 8

Noi tehnologii

NOI PERFORMANȚE ALE CELULELOR SOLARE CU PELICULE SUBȚIRI

Laboratoarele federale elvețiene pentru știința materialelor și tehnologie – ***Empa***, au realizat celule solare cu pelicule subțiri, pe bază de substraturi polimerice flexibile, cu o eficiență record, de 20,4%.
Celulele dezvoltate în cadrul Laboratorului pentru Pelicule Subțiri și Celule Fotovoltaice se bazează pe un material semiconductor din seleniură de cupru, indiu și galiu (CIGS), cunoscut pentru potențialul său de a oferi electricitate solară eficientă și rentabilă. În prezent, se dorește o gamă mai largă de aplicații industriale ale acestei tehnologii. Recordul eficienței energetice de 20,4%, care a fost atins pentru ultima generație de celule solare CIGS cu pelicule subțiri, pe bază de substraturi polimerice flexibile, reprezintă o îmbunătățire semnificativă față de recordul anterior, de 18,7%, obținut de aceeași echipă în mai 2011.
Echipa a optimizat caracteristicile stratului CIGS, obținut la temperaturi scăzute, care absoarbe lumina și contribuie la obținerea curentului fotoelectric din celulele solare. Valoarea eficienței celulelor a fost atestată de către ***Institutul Fraunhover pentru Sistemele Solare*** (ISE) – din Freiburg, Germania.
Noul record Empa în ceea ce privește eficiența celulelor solare flexibile depășește în prezent valoarea record de 20,3% pentru celule solare CIGS aplicate pe substraturi din sticlă și atinge cea mai ridicată eficiență pentru celulele solare pe bază de plăci de siliciu policristalin.
Totodată, a fost eliminată diferența de eficiență dintre celulele solare pe bază de plăci de siliciu policristalin și celulele cu pelicule subțiri CIGS.
Peliculele subțiri și modulele solare flexibile, de înaltă performanță, sunt atractive pentru numeroase aplicații, cum ar fi: fermele solare, acoperișurile și fațadele clădirilor, automobilele și electronicele portabile. Ele pot fi produse utilizând procesele continue “roll-to-roll”, care oferă reduceri ale costurilor ulterioare, în comparație cu tehnologiile standard pe bază de siliciu.
“Seria de eficiențe record ale celulelor solare CIGS, flexibile, dezvoltate la Empa, demonstrează performanța excelentă a celulelor solare cu pelicule subțiri, comparativ cu cea a celulelor de siliciu policristalin ... Acum este momentul pentru următoarea etapă – o tehnologie aplicată la scară largă cu un partener industrial, care să acopere domenii vaste ale unui proces de producție eficient din punct de vedere al costurilor” – a declarat Gian-Luca Bona, directorul Empa.
Empa colaborează în prezent cu Flisom, o companie recent înființată, implicată în industrializarea celulelor solare flexibile CIGS.

Sursa: www. empa.ch

PROF. ING. ARISTIDE DODU LA 90 DE ANI DE VIAȚĂ ȘI 65 DE ANI DE ACTIVITATE

Domnul prof. ing. cercetător științific gradul I Aristide Dodu s-a născut la 9 iunie 1923, în satul Dădăeşti, comuna Vultureni din judeţul Bacău, într-o familie modestă de învăţători.

Excelenta sa devenire personală s-a bazat pe aptitudinile deosebite manifestate încă din fragedă copilărie, dar și pe inițiativă, creativitate, inovare, perseverență etc.

Având o reală înclinaţie spre inginerie, cu toate că mediul socio-economic în perioada de după cel de-al II-lea razboi mondial era nefavorabil, a reuşit să urmeze cu succes cursurile Facultăţii de Textile la Institutul Politehnic din Bucureşti, Secţia Mecanică Textilă, obţinând diploma de inginer. În paralel cu studiile efectuate la Politehnica Bucureşti, a urmat cursurile Academiei de Arte Frumoase (1944–1949) şi ale Seminarului Pedagogic Universitar (1947–1949), din Bucureşti.

Prestigioasa și îndelungata activitate profesională a prof. ing. Aristide Dodu a început ca inginer la S.C. Apollo S.A. – București, unde – în perioada 1949–1954 – a ocupat funcțiile de șef de serviciu și șef de secție. Prof. ing. Dodu Aristide este unul dintre fondatorii cercetării textile din România, activând în calitate de inginer, cercetător ştiinţific principal, şef de laborator şi specialist consultant la Institutul de Cercetări Textile – Bucureşti, încă din primii ani de funcționare a acestei unități și până în anul 1989. Activitatea științifică s-a corelat cu cea educațională, lucrând ca profesor la Grupul Școlar MIU și ca profesor asociat pentru cursurile postuniversitare sau de perfecţionare a inginerilor textilişti, la Institutul Politehnic Bucureşti şi la cel din Iaşi, profesor asociat la Facultatea de Design-Modă şi Creaţie Vestimentară din cadrul Universităţii EUROPA-ECOR, din Bucureşti, consultant în domeniul pregătirii pentru doctorat în cadrul ASE – Bucureşti, Institutului Politehnic din Iaşi şi din Bucureşti şi Academiei Militare Bucureşti.

Activitatea ştiinţifică a prof. ing. Aristide Dodu s-a materializat în participarea la realizarea obiectivelor a peste 250 de proiecte de cercetare ştiinţifică și elaborarea de studii tehnico-economice pentru domeniul textil, finalizate cu tehnologii și produse noi, cu un grad ridicat de performanță tehnică și aplicabilitate industrială. Specializarea multidisciplinară a condus la inițierea și organizarea, pentru prima dată în România, a unei secții de cercetare și producţie a articolelor medicale textile implantabile la om: proteze vasculare, valve biologice pentru inimă, proteze de sinus frontal şi arcade, înlocuitor de meninge, colomelă auditivă, proteze rinoplastice, aţă chirurgicală pentru implantări pe termen lung, petice de plastii, ligamente pentru genunchi etc. și la proiectarea și realizarea primei mașini rectilinii de tricotat cu comenzi electronice pentru realizarea de tricoturi complet conturate și cu structuri jacard, cu rapoarte de desen nelimitate. Gradul ridicat de inovare al rezultatelor proiectelor de cercetare s-a reflectat atât prin obținerea a peste 35 de Brevete de Invenţii şi Certificate de Inovator, cât și prin participarea, în calitate de autor și coautor, la referate susținute la peste 500 de conferințe și publicații, din care 60 de cărți, manuale, tratate și broșuri: *Manualul Inginerului Textilist* (ediţiile I şi a II-a) – care a primit Premiul AGIR în anul 2004, *Dicționarul Explicativ Poliglot pentru Ştiinţă şi Tehnologie* – elaborat sub auspiciile Academiei de Științe Tehnice din România, care a primit Premiul AGIR în anul 2006, *Lexiconul Tehnic Român, Tehnologia tricotajelor* (vol. I şi II) etc.

Recunoașterea prestigioasei activități științifice și didactice a condus la nominalizarea prof. ing. Aristide Dodu ca Membru de onoare al Academiei Oamenilor de Știință și Decan al Colegiului de Etică Profesională din AGIR, alegerea ca Preşedinte de onoare al IFKT – România şi Preşedinte de Onoare al Societăţii Inginerilor Textilişti din România, membru al Comisiei de Terminologie pentru Ştiinţe Exacte a Academiei Române, membru al Colegiului de redacţie al publicaţiei „Univers Ingineresc“ şi al revistei „Industria Textilă“, cotată ISI, membru al New York Academy of Sciences, în anul 1999 etc. Personalitatea remarcabilă a prof. ing. Aristide Dodu, evidențiată prin modestie, abilități de comunicare, capacitate deosebită de sinteză și tenacitate în atingerea obiectivelor propuse au atras atenția unităților de cercetare și învățământ superior, asociațiilor profesionale din țară și străinătate, care i-au acordat peste 50 de premii, diplome și medalii, printre care și Ordinul Național pentru Merit în grad de Cavaler.

Cu ocazia împlinirii a 90 de ani de viață și 65 de ani de activitate profesională, colegii și colaboratorii din Institutul Național de Cercetare-Dezvoltare pentru Textile și Pielărie și membrii SIT–AGIR urează domnului prof. ing. Aristide Dodu un călduros „LA MULȚI ANI“.

Dr. ing. Emilia Visileanu
Editor şef al revistei Industria Textilă